ZINC PROTEOME AND ZINC APOPROTEINS IN ZINC-DEFICIENT YEAST *SACCHAROMYCES CEREVISIAE*

by
Yirong Wang

A dissertation submitted in partial fulfillment of
the requirements for the degree of

Doctor of Philosophy
(Nutritional Sciences)

At the
University of Wisconsin-Madison
2021

Date of final oral examination: 11/30/2021

The dissertation is approved by the following members of the Dissertation Committee:

David Eide, Professor, Nutritional Sciences
Jing Fan, Assistant Professor, Nutritional Sciences
Brian Parks, Assistant Professor, Nutritional Sciences
Joseph Pierre, Assistant Professor, Nutritional Sciences
C.-L. Eric Yen, Associate Professor, Cellular and Molecular Biology

Table of Contents

Acknowledgements

I want to dedicate this thesis to three important people in my academic career: my mother, Dr. Mitsi A Blount, and Dr. David J Eide.

My mother, Dier Bao, is a passionate K12 teacher and the strongest, most hard-working teacher I know. She cares about teaching so much that she went back to her classroom a week after her lung cancer surgery. Getting her master's degree in education and psychology in her 50s, her work ethics and her love for pedagogy had such an impact on me that I want to follow her steps. My mother doesn't speak any English, nor does she know anything about biology research, but she supported me unconditionally whenever I need it. I owe her my life, and all achievements I have ever obtained.

My "science mom", Dr. Mitsi A Blount, is my first science mentor who changed my view on basic biological research. She broke all the stereotypes I have for a scientist and for basic biology research. Knowing that I'm passionate about diabetes and human nutrition, Dr. Blount created a special project for me and later encouraged me to do many things that I never imagined myself doing. I was an awkward international student with language barriers, but Dr. Blount made me feel welcome and accepted. I found a sense of belonging in her lab and in science. Without her, I won't be able to recognize the importance of basic biology research and won't be getting my Ph.D. degree.

I would like to thank my PhD advisor, Dr. David J Eide. Dave is the best PhD advisor one could have asked for. Not only is he one of the most knowledgeable people I have met, but Dave is also humble, calm and is always willing to make time to listen to me despite being the chair of the department with many other responsibilities. Dave pushes me to become a critical scientist, and he is always there to guide me through difficulties in research progress, and to offer me advice in teaching and mentoring. I feel very lucky to be your student.

I would also like to thank my committee members Dr. C.-L. Eric Yen, Dr. Jing Fan, Dr. Brian Parks, Dr. Joseph Pierre and Dr. Roger Sunde for generously offering their time, helpful tips and insightful comments on my research progress. Thank you for always being encouraging to my research projects even when I encounter bottlenecks. Thank you for being role models for me and share your career experience with me.

I would like to thank Dr. C.-L. Eric Yen and Dr. Guy Groblewski for being amazing teaching mentors to me. Thank you for trusting me and giving me countless opportunities to practice my teaching skills in your class and exploring my interests in pedagogy. My teaching philosophy is largely formed by observing how both of you teach, interact with students and design course materials. I don't think I will be where I am today without both of your generous help.

I also owe tremendous debt to our graduate coordinator Katie Butzen, and Erika Anna. Katie always has graduate students' best interests in her heart and will go out of her way to help create opportunities for us. Erika taught me how to stay humble and appreciate the strength of culture and community. Katie and Erika, thank you for always being there, listening to me and always offering comfort. Thank you for celebrating every of my little accomplishments.

I want to thank our lab manager Janet Taggart and everyone in the Eide lab to assist me to become a better scientist. I want to thank the nutritional sciences administration staff: Bill Omdahl, Julie Ewing, Scott Anderson, and Mary Lou Krase for all the support they provided to ensure our department runs smoothly, for helping me professionally and personally. I want to give special thanks to Mary Lou for standing up and fighting landlord for me, and for kindly gifting me so many of her arts, and plants that I will cherish.

I want to thank my friends Kayla, James, Grace, Charles, Juliani for always cheering me up and looking out for me.

I want to thank my husband Tommy for being my best friend, and for making me a better person. I feel insanely lucky to meet you. You are one of the best things that happened to me. Thanks for always laughing at my silly jokes and for learning mandarin to get to know my family. Plus, thanks for the countless hugs you offered, Tommy.

I feel very blessed to become part of a wonderful new family. Laurel, Tom, Maeve, Tony, Judy and Dennis, thank you for always supporting me and Tommy. You are the family I always wanted to have, and I could never ask for better in-laws. Lastly, I want to give a special shoutout to my nephew Conor and niece Kiera, thank you for being so adorable, loving and for making me want to make this world a better place.

Abstract

Zinc has been recognized as indispensable cofactor for many proteins and as a key signaling molecule regulating myriads of cellular activities. In Chapter One of this thesis, I first outline a brief history of research progress in zinc biology. Past research has established zinc quota, the amount of zinc atoms cells requires to grow optimally. While zinc quota is high, "free" cellular zinc concentration is low. Many efforts have been devoted to investigating how cells use homeostatic and adaptive mechanisms to maintain zinc requirement under zinc deficiency. When cells fail to use all these to sustain the zinc requirement of the cells, zinc proteins accumulate in their apo form. Only a handful of *in vivo* zinc apoprotein examples were known before this research. With the advancement in bioinformatic and multi-"omics" technology, zinc biologists started to systematically characterize the zinc proteome thus making this thesis possible.

In Chapter Two, with collaboration with others, I first cataloged the yeast zinc proteome of 582 known or potential zinc-binding proteins using a bioinformatics approach and determined protein abundance of half of these zinc-binding proteins. Two significant findings are that first I discovered widespread zinc sparing, which describes cells down-regulating the abundance of zinc-binding proteins to free up as many zinc atoms as possible. The scale of zinc sparing is estimated to be 4 million zinc atoms or about 40% what the cells need for optimal growth. Another critical finding is that I confirmed the large accumulation of unmetalated zinc apoproteins *in vivo* during zinc deficiency. Two examples of such zinc apoproteins, Fba1

aldolase and Met6 methionine synthetase, are provided to support the conclusions from the bioinformatics and proteomics data.

Zinc is critical in folding so zinc apoproteins that lost their zinc atoms could induce the unfolded protein response. Zinc-deficient cells need mechanisms to stabilize such large quantity of zinc apoproteins to prevent them from aggregating and becoming cytotoxic. Zinc deficiency has also been known for generating oxidative stress. In Chapter Three, I investigated the role of the previously characterized zinc-responsive 2-cys peroxiredoxin Tsa1 in preventing aggregation of unmetalated zinc apoproteins. One previously unknown target of Tsa1, Rpd3, was discovered in this research. Rpd3 is a class I histone deacetylase that forms three distinct complexes to regulate transcription in response to variety of cellular stresses such as heat shock, oxidative stress, and salt stress. Rpd3 was shown in this chapter to be zinc apoproteins in both zinc-replete and deficient cells, with larger accumulation in the zinc-deficient yeast.

Overall, these findings from this thesis contributed to our growing understanding of the zinc proteome and how cells respond to a limited amount of zinc under zinc deficiency.

Chapter 1: General Introduction

Discovery of the essentiality of zinc in plants and animals

Can any organisms live without zinc? After 150 years of research on zinc biology, now we know the answer is no. Every organism needs zinc to live, thrive and reproduce.

Jules Raulin did not know the answer when he started to investigate which specific mixture of minerals would help plants growth. Raulin used a common fungus ("black mold") *Aspergillus niger:* he carefully withdrew one mineral at a time and measured the growth (dry weight) of the fungus. After rounds of trial and error, he established zinc was required for the optimal growth of the fungus[1]. Although at this time Raulin had no technology that made sure his basal medium was without zinc contamination, he was the first to demonstrate the requirement of zinc for organisms to grow optimally. The problem of contamination, though, would go on to produce inconsistent results of whether zinc is an essential nutrient for growth for decades, thus delaying the recognition of essentiality of zinc in life.

In animals, universal and relatively stable distribution of zinc in animal tissues has been observed by many scientists, suggesting that zinc might be a required element for animal health[2]. But attempts to demonstrate the essentiality of zinc failed due to lack of other essential nutrients such as vitamins, and due to traces of zinc contamination in the "purified rations" fed to the animals[2]. Rebecca Hubbell and Lafayette Mendel took extreme cautions in controlling the zinc contamination in animal diets but only observed a mild favorable increase of growth in mice supplemented with zinc[3]. In 1934, right here at the University of Wisconsin-Madison, WR Todd, CA Elvehjem and EB Hart conducted seminal experiments and were the first to show that zinc is

essential for rat growth. The brilliance of the study by Todd et al. was that they added essential vitamins and redistilled the water used for the rats knowing that there might be zinc contamination from the tap water. In this way, they controlled the amount of zinc to make a larger difference in zinc-replete and zinc-deficient rations[4]. They were able to observe a significant difference in growth among the rats while others such as McHargue missed that finding because he failed to remove the trace amount of zinc in the rat rations made from commercial foods[5]. Later, reports that zinc is essential to prevent various animals such as pigs, birds, and dogs from showing growth retardation and other adverse symptoms were established during 1950s to 1970s[2].

Ananda Prasad found zinc is essential for humans in the 1960s: patients from villages of Shiraz, Iran showed severe growth retardation, testicular atrophy, and other symptoms that could not be explained by other mineral deficiencies[6]. Later, Prasad's study in Egypt showed that supplementing zinc to patients alleviated growth retardation and hypogonadism within 3 to 6 months, establishing a causal relationship between human zinc deficiency and these symptoms[7]. It took another one and half decades for zinc to be established with a recommended dietary allowance (RDA) value due to the difficulty in producing consistent results.

While early zinc biologists were busy establishing zinc as an essential nutrient, they also raised the question of what exact role(s) does zinc play in the cell. CA Elvehjem and EB Hart published a follow-up study in 1938 where they tried to investigate the potential role of zinc in pancreatic enzyme activities. They observed less activity of the pancreatic enzymes isolated from zinc-deficient rats but were not able to establish direct relationship with zinc[8].

The first confirmed molecular role of zinc in a living cell was its catalytic role in carbonic anhydrase purified from the ox blood. Carbonic anhydrase converts carbon dioxide and water into carbonic acid. Keilin and Mann found carbonic anhydrase contains a physiologically relevant amount of zinc and showed a linear dose-dependent relationship between carbonic anhydrase activity and zinc content[9]. This critical finding opened the door for zinc biology researchers to explore widely distributed molecular roles of zinc for the next 80 years.

General molecular roles of zinc in cells

The most recognized molecular roles of zinc are as a catalytic or structural cofactor, and as a regulatory agent of proteins. Unlike iron and copper, zinc is redox inert under physiological conditions. This gives zinc a unique advantage to serve as a protein cofactor without producing unwanted reactions and changing coordination preferences. Enzymes that use zinc are found in each of the six enzyme categories and are widely involved in carbohydrate, lipid, protein, nucleic acid metabolism and beyond.

When zinc serves as a catalytic cofactor, the metal is essential for the enzyme activity and is directly involved in catalyzing reactions with the substrate. Zinc is a Lewis acid that accepts a pair of electrons and interacts with substrates with the help from at least one water molecule in addition to its three protein ligands[10,11]. The water molecule allows for an open coordination site that is considered essential for the catalytic role of zinc. Examples of proteins that have a catalytic zinc cofactor include carbonic anhydrase, many proteases and class II fructose 1,6-bisphosphate aldolases.

A second function of zinc in proteins is maintaining protein structure so proteins are properly folded for optimal function. This is usually supported by a stable tetrahedral coordination of histidine and cysteine amino acid ligands and therefore can ensure the proper folding of local and overall structure of the proteins[10,11]. The best characterized structural zinc site is the "zinc finger". The classic C2H2 zinc finger was first discovered in a protein transcription factor IIIA in frog[12]. The finger-like structure coordinated by one or more zinc ions help to stabilize the protein and provide a new DNA recognition principle[13]. Now, the zinc finger motif in some proteins has been assigned functions besides structural role but "zinc finger" remains as a classic example of the metal serving as structural cofactor of proteins.

The third proposed role of zinc is acting as a regulatory agent. Unlike catalytic and structural roles, the role of regulatory zinc is harder to define consistently. Some researchers consider a signaling role of zinc as regulatory, but I will discuss the signaling role separately. Here in this thesis, I define the regulatory role of zinc as follows: when zinc serves as a regulatory agent for a protein or a protein complex, it binds to that protein and regulates its activity, its ability to be modified by other biological processes, its structural integrity and/or the location of the protein or protein complexes. It is distinct from zinc's role as catalytic cofactor because regulatory zinc does not interact with the substrate directly. According to Bert Vallee, it is different from the catalytic role of zinc because the regulatory zinc could either activate or inhibit the enzyme activity while catalytic zinc is essential for enzyme activity[14]. The regulatory zinc responds to a variety of signal cues such as lipids and oxidative stress, and usually regulates the protein via disulfide formation and reduction[15]. I will use a few examples to demonstrate the definition. One example is zinc-binding proteins that use cysteines as ligands and are part of a signaling cascade such as protein

kinase C (PKC). PKC has different isoforms, but all of them have conserved zinc fingers that coordinate two zinc ions. When zinc is bound to PKC, the thiol groups are protected by the presence of zinc and the enzyme is inactive. However, when lipid signals or oxidative stress signals arise, the oxidative microenvironment forces the thiols to form disulfide bond thus releases the zinc from PKC. Subsequently the enzyme PKC unfolds, and is phosphorylated and becomes active[16]. A similar mechanism of zinc functioning as a "switch" or "hinge" of protein activity regulation is the bacterial heat shock protein Hsp33[17]. Another example of regulatory zinc has been observed in the interface of circadian clock protein complex CRY1/PER2 in mammalian cells. Schmalen et al. used mutational studies and radio-active ^{65}Zn and discovered that zinc is critical for the two proteins to interact. The presence of zinc stabilized the protein complex to regulate gene transcription and a series of downstream metabolic activities *in vivo*. When zinc is not present, the thiols of the cysteines of CRY1 form a disulfide bond and CRY1 is unable to interact with PER2[18]. These two examples illustrate my definition of regulatory zinc in protein and protein complexes.

It is worth noting that the role of zinc in proteins is not always black and white. In some proteins, the zinc ions could contribute to regulate the protein, structural stability and/or optimal catalytic activity of the zinc-binding proteins. One prominent example is liver alcohol dehydrogenase which contains two zinc ions in each subunit of the protein. One "active" zinc is shown to be coordinated by two cysteines, one histidine and a water molecule thus are involved directly in catalysis while the other zinc ion is coordinated by four cysteines thus be considered to support structural stability[19]. This structural zinc site is also contributing to the maximal enzyme activity of the whole protein. In other proteins such as the tumor suppressor p53 and class I histone deacetylases, the

one zinc ion serves as both catalytic and structural cofactor. In p53, the cofactor zinc has also been deemed as important in recognizing specific sets of DNA targets, thus is considered to have a regulatory function as well[20]. Now with the emerging technologies and bioinformatic tools, we are able to predict that as much as 10% of eukaryotic genome encodes proteins that are zinc-binding[21] and we are able to assign them to putative catalytic and/or structural roles based on the bioinformatic information available. We refer to the collection of zinc proteins encoded by a genome of an organism as its "zinc proteome" and I will discuss the detailed progress of predicting and characterizing zinc proteomes in the "**The gradual understanding of zinc proteome**" section. But we need to always keep in mind the possibility of zinc playing multiple roles in the same protein even if it is assigned to one specific role based on computational prediction.

Besides being a cofactor of proteins, zinc ions also play a significant role in signaling. As I mentioned above, this is often considered a regulatory role of zinc. Although an exciting area of research, this role of zinc in signaling is not the focus of this thesis. Readers who are interested in zinc signaling can read the second edition of the book "Zinc Signaling" edited by Toshiyuki Fukada and Taiho Kambe (2019)[22]. It has been known that zinc functions as a neuromodulator in so-called "gluzincergic" neurons. Upon stimulus, zinc is released, together with glutamate, and subsequently modulate receptors such as N-methyl-D-aspartate (NMDA) receptors. The released zinc is then removed from the synaptic cleft and recycled[23]. A recent milestone of zinc signaling research is the discovery of the "zinc spark", which refers to the exocytotic release of billions of zinc ions from mammalian eggs upon activation[24,25]. The magnitude of zinc release is also correlated with embryo quality[26]. Another example of zinc signaling is the "zinc wave", during which free zinc is released from the endoplasmic reticulum and acts as a novel intracellular second

messenger. One of the proposed functions of a zinc wave is to inhibit phosphatase activity therefore regulating kinase signaling pathways and subsequently the gene expression of cytokines in mast cells[27]. The zinc wave follows minutes after Ca^{2+} influx, while "zinc spark" seems to concomitantly happen as Ca^{2+} levels change. Recently, Amy Palmer's lab explored the exact mechanism of how physiologically relevant concentration of zinc activates the mitogen-activated protein kinase signaling pathway, although no detectable changes of Ca^{2+} were found[28]. These findings seem to suggest zinc ion can act as either an extracellular or intracellular signaling molecule in many different cell types and in many different sequences of cellular events, dependent or independent of Ca^{2+}.

To conclude this section, zinc plays many important biochemical and molecular roles in the cell. The more characterized role(s) of zinc include its serving as structural or catalytic cofactor of proteins. The emerging role of regulatory zinc includes zinc controlling the activity of protein/protein complexes, its role in signaling cascades, and beyond.

Zinc quota, cellular concentration of zinc and the intracellular "free zinc"

As discussed in the last section, zinc plays critical roles in the cells. But how much zinc do cells need to fulfill these roles? To answer this question, one has to know the concept of "zinc quota", referring to the amount of zinc atoms present in the cells under certain conditions. "Minimum zinc quota", a related concept, refers to the minimal amount of zinc atoms required for optimal growth of the cells[29].

Zinc quotas were previously measured or estimated by several different groups. Outten and O'Halloran measured the zinc quota of *Escherichia coli* to be 10^5 zinc atoms per cell using inductively coupled plasma mass spectrometry (ICP-MS)[29]. Our group estimated the minimum zinc quota of yeast *Saccharomyces cerevisiae* to be 10^7 atoms per cell, based on cell-associated zinc measurements[30]. Minimum zinc quota of different types of mammalian cells were measured to be 10^8 atoms per cell by ICP-MS[31,32]. The minimum zinc quota seems to be proportional to the cell size and the number of zinc-binding proteins. Eukaryotic cells contain more zinc-binding proteins than prokaryotic cells, therefore the minimum zinc quota is also two to three magnitudes higher in absolute value. However, the total cellular zinc concentration is relatively consistent in all organisms.

There are several factors that affect a cell's ability to accumulate zinc. Most cells show similar total cellular concentrations of zinc between 0.1 to 1 mM. The type and function of the cell is one of the factors that affect cellular zinc concentration. For example, zinc-containing "gluzincergic" neurons and prostate cells accumulate much higher concentrations of zinc due to their specialized functions[33,34]. Another factor that influences cellular zinc concentration is the physiological stage of the cell. During maturation, mammalian egg cells can accumulate an astonishingly 0.2M of zinc that is required to activate the oocyte[25]. Disease state(s) also affects how much zinc can accumulate in the cells. Huang et al. measured total cell-associated zinc to show that a cancerous RWPE2 cells accumulate 40-50% less zinc compared to its genetically identical non-cancerous cell line [35]. Ability to concentrate zinc is one of the markers used to gauge the progression of prostate cancer and several other diseases[34]. The difference of zinc accumulation observed in cancerous versus non-cancerous cells might be due to the underlying differences in expressing zinc uptake

transporters or other mechanisms in maintaining zinc levels. The detailed homeostatic mechanisms will be discussed in the "**How zinc homeostasis is maintained"** section.

Although the requirement of total cellular zinc is high, the cytosolic labile "free" zinc level is within a low and tightly controlled range. Various organelles, such as ER and mitochondrion, also have their own labile zinc pool. It is also speculated that labile "free" zinc may not be equally distributed in the same cellular organelle due to the unknown microenvironments of the organelles[36]. Some interesting recent studies showed that other stresses, such as oxidative stress and starvation-induced autophagy, may change the distribution of "free" zinc in different cellular compartments[37–39]. Over the years, researchers have also observed that the concentration of "free" zinc in cell is not static, and fluctuations of zinc ions happen during cell cycle even without any other interventions such as metal chelation or oxidative stress stimuli. Li and Maret used FluoZin-3 AM, a fluorescent Zn^{2+} sensor, to show that cellular "free" zinc peaks twice in one cell cycle of mammalian cells[40]. All these results suggest that cellular "free" zinc concentration is tightly regulated and serve as a foundation for various biological events in cells.

It makes sense that zinc biologists want to understand how much "free" zinc is present in different parts of the cell and in different stages of cell cycle because it helps to further understand the biological functions of zinc in a spatial- and temporal-relevant way. For example, knowing concentration of "free" zinc provides a reference for *in vitro* studies that look at inhibitory effects of zinc on various enzymes. If the inhibitory effect only occurs at a zinc concentration that is so out of the physiological relevant range in any stage(s) or types of the cell, then the results of such

experiments are less meaningful and could potentially create unnecessary conflicts with other studies in the literature.

Numerous attempts to measure the labile "free" zinc pool have been made since the early 1990s. Simons estimated that the free intracellular zinc is around 2.4 x 10^{-11}M (24 pM) in red blood cells[41]. Although he did not differentiate cytosol "free" zinc from those in the organelles, the estimation he gave is well within the picomolar range found in later studies. Adebodun and Post used ^{19}F-NMR to detect ~1 nM of intracellular "free" zinc ions in human leukemia cells[42]. Many other studies used fluorescent dyes such as zinquin in splenocytes, mag-fura-5 in neuronal cells and got a result of micromolar range of "free" zinc in those cells[43,44] . Kleineke and Brand measured an average of 1.3 mM (0.6 – 2.7 uM) zinc ions in primary hepatocytes from rats fed in a zinc-replete diet. Newer studies utilizing zinc sensors showed that cytosolic zinc ion is around tens to the hundreds of picomolar range, although there is a wide disagreement on the exact numbers[45–47]. Based on the various type of studies presented, I think we can generally agree that cellular "free" zinc is in the hundreds of picomolar to low nanomolar range. It is not the focus of this thesis to discuss in detail why these disagreements exist so if the readers are interested in the comparisons of different methods that measure labile zinc, please refer to the excellent reviews and papers from Amy Palmer's lab[46,48].

Level of intracellular "free" zinc can also be estimated by affinity of certain zinc transcriptional factors. Studies of the zinc-responsive transcription factor Zap1 in *Saccharomyces cerevisiae* gives an excellent example of how this estimation works. Zap1 is a direct sensor of zinc and controls gene expression of around 89 genes[49] . There are seven C2H2 zinc fingers in Zap1, five of which

(ZF3 to ZF7) are in the DNA-binding domain and the remaining two zinc fingers (ZF1 and ZF2) are in one of the activation domains (AD2). These zinc fingers have different binding affinities. Compared to ZF3 - ZF7, ZF1 and ZF2 have a relative higher affinity and lower stability for Zn^{2+}, which makes them ideal for sensing the change of cellular zinc level. Metal binding studies of ZF1 and ZF2 showed that the affinity for Zn^{2+} is between 0.3 to 5 nanomolar range[50]. Later studies measured an affinity for zinc at 2.5 pM[51]. This measurement of ZF1 and ZF2's affinity for zinc is in general agreement with the "free" zinc level measured by other direct methods, further demonstrating the range of cytosolic "free" zinc is at picomolar range.

To conclude this section, zinc is quite abundant and highly required by the cells despite being frequently labeled as "trace element". The "free" zinc level in the cell, on the other hand, is extremely low and tightly controlled. Now you may wonder where are all the zinc is required by cells, if zinc ions are not freely roaming in the cells? Evidence has shown that majority of zinc is bound to proteins and the large quantity of zinc is required to make these proteins functional. We will discuss the zinc-binding proteins in the section "**The gradual understanding of zinc proteome**". The mechanisms of maintaining the high zinc quota and low "free" zinc will be discussed in "**How zinc homeostasis is maintained**".

How zinc homeostasis is maintained

Cells require abundant zinc but zinc availability in the environment changes constantly, therefore cells have developed complicated mechanisms to maintain intracellular and intra-organellar zinc to ensure its survival. Tremendous amount of work has been done to investigate how cells sense changes in zinc availability and respond to those changes using transcriptional and post-

transcriptional mechanisms. Our lab has been a pioneer in uncovering mechanisms of zinc homeostasis under zinc deficiency over the past three decades using the model organism yeast *Saccharomyces cerevisiae*. In this section, I will mostly focus on zinc homeostatic mechanisms of yeast *Saccharomyces cerevisiae.* I will also briefly discuss the research progress on zinc homeostasis of mammalian cells for readers who are interested in higher order organisms.

Zinc homeostasis in *Saccharomyces cerevisiae* is mostly maintained by zinc uptake and zinc storage transporters that are regulated by the zinc sensing transcription factor Zap1. Although zinc efflux is also an important homeostatic mechanism for many organisms, yeast *S. cerevisiae* does not seem to have this layer of regulation. As mentioned in the previous section, the two zinc fingers (ZF1 and ZF2) in the activation domain AD2 of Zap1 constantly bind and disassociate with zinc thus serving as direct zinc sensor. When cellular "free" zinc level is low, ZF1 and ZF2 lose their zinc and therefore enabling Zap1 to recruit coactivators to turn on gene transcription of many important genes. Among these genes, *ZRT1* and *ZRT2* are essential parts of the zinc uptake machinery. Zrt1 and Zrt2 are plasma membrane transporters, and they are both members of the ZIP/SLC39 family of zinc transporters that aim to increase cytosolic zinc level, either from extracellular space or organelles. During mild zinc deficiency, transcription of the relative low affinity Zrt2 transporter is activated. However, if cellular zinc level keeps dropping, *ZRT2* transcription is inhibited while *ZRT1* transcription is turned on as Zrt1 is the high affinity zinc uptake transporter. This double uptake transporter system ensures enough time for the yeast cells to prepare for the upcoming severe zinc restriction, and at meantime allows for rapid zinc uptake if zinc becomes available to maintain cellular zinc level[49,52].

Another homeostatic mechanism used to maintain cytosolic zinc levels in yeast is vacuolar storage of excess zinc. When yeast cells are in an environment with abundant zinc, they store the extra zinc atoms in the vacuole and mobilize the zinc atoms when environmental zinc drops to a deficient level. These processed are accomplished by three transporters: Zrc1, Cot1 and Zrt3. Zrc1 and Cot1 belong to the CDF/SLC30 family of metal transporters, which transport zinc out of cytosol. Zrc1 and Cot1 transport zinc into the vacuole for storage. Zrt3 is ZIP family transporter, and it mobilizes zinc out of the vacuole under the regulation of Zap1 during zinc deficiency[53]. There is also a Zap1-regulated transporter Zrg17 that transports zinc into the ER to maintain ER zinc homeostasis[53].

Besides regulating zinc uptake and storage transporters, yeast cells have another mechanism that contribute to maintaining cellular zinc homeostasis. This mechanism is termed "zinc sparing" and refers to when cells down-regulate abundant zinc-binding proteins and redirect these "freed up" zinc atoms to other essential functions. Often cells will replace the down-regulated zinc-binding proteins with non-zinc, or less-zinc requiring proteins that perform similar functions. "Zinc sparing" was previously characterized in bacteria where alternative non-zinc binding ribosomal subunits are used in place of zinc-binding subunits[54,55], and in the marine diatom *Thalassiosira weissfloggi* where cadmium-dependent protein is substituted for the classic zinc-binding enzyme carbonic anhydrase[56]. Several "zinc sparing" examples have been found in yeast *Saccharomyces cerevisiae*. One prominent example is the alcohol dehydrogenase Adh1. Adh1 is one of the most abundant zinc-binding proteins and requires two zinc atoms per monomer to be functional. When zinc is deficient, Zap1 induces an intergenic RNA transcript that efficiently represses *ADH1* gene expression thus down regulates Adh1 protein abundance[57]. At the same time, Zap1 increases the expression of *ADH4*, whose protein product requires only one zinc atom or iron as its cofactor.

This switch from Adh1 to Adh4 during zinc deficiency alone frees up millions of zinc atoms that can be used for other critical proteins that only use zinc as their cofactors. Another zinc-binding alcohol dehydrogenase Adh3 in mitochondria was shown to be regulated in similar manner to Adh1[57]. One additional example of "zinc sparing" in yeast cells is RNA Polymerase I (RNAPI) subunit Rpa190. Zinc bound to Rpa190 is "spared" through increased vacuole degradation[58]. These two examples of "zinc sparing" show that yeast cells can utilize both transcriptional and/or post-transcriptional regulation to control the abundance of zinc-binding proteins, rather than simple degradation. However, there are still lingering questions such as what is the scale of "zinc sparing" across the whole zinc proteome? Are there new mechanisms of "zinc sparing" in yeast cells? One of the goals of the experiments described in **Chapter 2** is to identify more targets, capture the scope and potentially find new mechanisms of "zinc sparing".

In mammalian cells, there are currently no known transcription factors that respond to zinc deficiency. However, there are two transcription factors that sense the increase of cytosolic zinc and respond to control gene expression. One such transcription factor is an ortholog of Zap1, ZNF658, that was identified to be a repressor of zinc transporters including ZnT5 and ZnT10[60]. ZnT5 (SLC30A5) transports zinc into the secretory granule and is thought to facilitate insulin synthesis in pancreatic beta cells[61]. ZnT10 (SLC30A10) is believed to transport zinc into endosomes and may be involve in manganese transport too[62,63] . Upon treatment of Caco-2 cells with 100 mM zinc, ZnT5 and ZnT10 levels were reduced, and this reduction was abrogated when ZNF658 expression was inhibited by siRNA treatment. ZNF658 is also shown to regulate ribosome biogenesis, one of the essential cellular process that requires abundant zinc[60]. Further

research is needed to illustrate the precise functions and mechanisms of ZNF658 and how it regulates zinc homeostasis in mammalian cells.

Metal-response element-binding transcription factor-1 (MTF-1) is another transcription factor and is the main activator that responds to increasing level of cellular zinc. It also responds to many other stress signals such as high levels of other metals, oxidative stress, and hypoxia although sensing these responses might occur indirectly through changing zinc levels in the cytosol. Although binding sequences vary, MTF-1 has been shown to regulate gene expression of many genes in *Drosophila*, mouse, and human models[64]. The best understood gene regulated by MTF-1 encodes metallothionein (MT). MT is a cysteine-rich protein that can bind to many different metals such as zinc, copper, cadmium, mercury, and silver. Technically, the apo form of MT without any metals should be called thionein. Upon elevated zinc levels (or other heavy metals), MTF-1 shuttles into the nucleus and recruits coactivators to increase the gene expression of many different thioneins that can bind and buffer the excessive zinc. Other than MTs, MTF-1 has been shown to induce gene expression of zinc transporters (ZnT-1, ZnT-2, Zip10) in mouse, ferroportin-1 in mouse, hepcidin in human, ferritin in Drosophila and many redox-related genes in mouse and human[64]. The variety of genes that can be induced by MTF-1 is interesting and may illuminate the interconnection between zinc, copper, iron, hypoxia and oxidative stress.

In summary, maintaining cellular zinc level is an important aspect of cells' ability to combat environmental variation of zinc availability. Therefore, cells from different organisms have evolved similar and yet different strategies to maintain zinc homeostasis because too little or too

much zinc are both detrimental to the cells. A lot of progress has been made but much work remains to be done to understand these mechanisms, especially in mammalian cells.

The significance of studying cellular responses to zinc deficiency

It is important to study how cells respond to zinc deficiency because zinc deficiency, especially marginal zinc deficiency, is largely underestimated. Since the discovery of zinc deficiency in humans in 1963, a lot of effort has been made to characterize the clinical symptoms of zinc deficiency in humans. Classic severe zinc deficiency symptoms include growth retardation, hair loss, delayed wound healing, hypogonadism in males, etc[65]. The clinical manifestations of mild deficiency are much harder to characterize; they can range from loss of appetite to suppressed immune system functions. Recently, zinc deficiency, or disrupted zinc homeostasis, has been associated with many chronic diseases such as Type II diabetes, obesity, Alzheimer's disease and certain types of cancer[66]. With the paradigm shift from investigating severe zinc deficiency to associating zinc deficiency with chronic diseases, it becomes especially critical to understand the scope of zinc deficiency and how cells respond to it because we are aiming for optimal health.

The World Health Organization (WHO) estimates that around one-third of the world population, varying from 4-73% across subregions, is at risk of being zinc deficient or burdened with diseases related to zinc deficiency[67]. This estimation used International Zinc Nutrition Consultative Group (IZiNCG)'s method of calculating the presence of zinc in nations' food supply and corrected for factors that affect the bioavailability of zinc in foods. The WHO report uses this estimation to assess global zinc deficiency risk because accurately measuring zinc deficiency in human subjects proved to be difficult and inconsistent.

Currently, the Biomarker of Nutrition for Development (BOND) Zinc Expert Panel recommends using serum zinc as a biomarker to assess individual zinc status. Using serum zinc as a marker, the 2011-2014 National Health and Nutrition Examination Survey (NHANES) data estimated that around 4% of the US children and 8% of the US adults are zinc deficient[68]. Surprisingly, serum zinc has been shown by many groups to be poorly correlated with dietary zinc intake or zinc supplement use[69]. The report by Hennigar et al. also showed that how difficult it is to accurately measure serum zinc because serum zinc is affected by sex, age, and even time of blood draw[68]. This study excluded subjects who had chronic inflammation conditions because serum zinc levels have been shown to be impacted by oxidative stress and inflammation.

Serum zinc is not an accurate indicator of individual whole body zinc status because whole body zinc homeostasis is tightly regulated to maintain serum zinc within a narrow range. This tight regulation of serum zinc is necessary because either too little or too much zinc can be detrimental to its critical roles in signaling, modulating protein activity, and so much more. It is very likely that peripheral tissues and organs that require a lot of zinc, such as skin and prostate, can be zinc deficient even when serum zinc indicates no zinc deficiency. This phenomenon was observed as early as 1938 when EB Hart group looked at zinc status in organs in zinc-deficient rats. What their group found was that there was significantly less zinc in the bones and teeth of the mild zinc-deficient rats, while zinc levels in soft tissues such as blood were comparable to rats that were fed sufficient amounts of zinc[8]. Based on the variety of critical roles zinc plays in cells, marginal zinc deficiency that affects certain organs in the body is not ideal for our current goal of preventing chronic diseases and achieving optimal health.

Thus in my opinion zinc deficiency, and especially marginal zinc deficiency, is one of the most underestimated human nutrient deficiencies worldwide. There is an increasing need to develop more accurate, accessible biomarkers to assess whole body zinc status and to detect marginal zinc deficiency. Therefore, characterizing and quantifying mammalian zinc proteomes, and analyzing the zinc proteome's response to a gradient of zinc is the critical first step because it provides us with a database to find targets for developing and testing new biomarkers. Following the publication of my proteomics analysis in zinc-deficient yeast cells (**Chapter 2**)[59], there have already been efforts to adopt similar "multi-omics" approaches to discover potential targets as biomarkers to assess zinc status in rats, and the authors have validated several of these biomarkers in two human patient populations[70].

Studying zinc deficiency in fungus and bacteria is also critical to understand the virulence of pathogens. Zinc is an essential nutrient for both host and the pathogens, as discussed in the "**General molecular roles of zinc in cells**" section. During the evolution process, both hosts and pathogens have developed a series of mechanisms to win the survival war. The hosts can restrict the essential nutrients in the circulation, especially minerals such as iron and zinc, required by the pathogens as one of the mechanisms to "starve" the pathogens. This phenomenon is termed "nutritional immunity"[71]. On the other hand, pathogenic fungi and bacteria developed their own mechanisms to adapt to such mineral restrictions and therefore increase their virulence, the ability to infect and spread. As human hosts in this "war", we need to understand the pathways that are critical for pathogen virulence to develop drugs that can fight off microbial infections.

With the emerging knowledge of human microbiota, it is also crucial to study how microbes (bacteria, fungi, and viruses) compete for available zinc in the human body and how they adapt to periodic excessive and/or restriction of zinc. Although this area of research exploring the relationship between host zinc status and its microbiota composition is still in its infancy, some studies detected changed microbiota at the phylum level in zinc-deficient chicks, and changed species of microbiota along with changes of certain antibiotic resistance genes in zinc-supplemented piglets[72–74]. Therefore, studying how organisms respond to zinc deficiency at cellular level is critical at many levels.

The gradual understanding of zinc proteome

Before delving into the findings that led to our characterization of the yeast zinc proteome, I want to define the concept of zinc proteome first. Zinc proteome is defined as the group of proteins in a cell or organism that are known or likely to bind zinc ion(s) *in vivo*. It took zinc biologists decades to be able to start capturing the wide scope of zinc-binding proteins since the discovery of the first zinc-binding enzyme carbonic anhydrase, because determining whether a protein binds zinc *in vivo* is difficult.

Early studies of characterizing zinc-binding proteins usually involved the purification of proteins and analysis their zinc content. As mentioned in the first section, D. Keilin and T. Mann purified carbonic anhydrase and determined the zinc in different fractions by the dithizone method, and by analyzing crystalized zinc salt. Correlating the activity of carbonic anhydrase and its zinc content, they showed that carbonic anhydrase in ox blood binds zinc in *vivo*[9]. Two decades passed before the next zinc enzyme carboxypeptidase A was discovered to contain zinc *in vivo* by Bert Vallee in

1954[75]. One of the reasons that this method of discovering zinc-binding proteins was slow and not practical for capturing the zinc proteome is because one must have a basic understanding of the desired protein such as its function and location, which is unknown for many zinc-binding proteins until much later. Another reason is that the presence of zinc in a protein can be transient and lost, or artificially introduced during the purification processes. Overall, purifying proteins and analyzing its zinc content was a good start at the beginning of zinc proteome research and remains to be a useful way to validate the presence and the quantity of zinc in proteins if done with careful procedures.

The next phase of discovering and characterizing zinc proteome was led by Bert Vallee. Vallee applied a method called atomic absorption spectrophotometry that can measure small quantities of zinc in biological fluids. This method is fast, much more sensitive than the dithizone method and is free of the interference of other metals[76]. Bert Vallee and R.J.P. Williams also pioneered metal substitution – mainly use paramagnetic metals such as cobalt – to study the metal-binding sites of zinc-binding proteins. Using quantitative analytical methods, Vallee characterized many important zinc-binding proteins, such as carboxypeptidases, alcohol dehydrogenases, and metallothionein[75,77,78]. He was also able to classify zinc-binding proteins to all six classes of enzymes[14]. Vallee, in collaboration with others, largely pioneered the work on characterizing zinc coordination, function, ligand preferences of zinc-binding proteins and he also compared the structural similarities between different zinc enzymes, thus laying a foundation for future bioinformatic strategies of predicting and cataloging the zinc proteome[10,14,79].

The field of cataloging zinc proteome using bioinformatic tools has been transformed with the completion of genome sequencing and with the increasingly abundant data of solved protein 3D structures. The groundbreaking approach of mining zinc-binding proteins on a genomic scale was developed by Claudia Andreini, Ivano Bertini, Antonio Rosato, and Lucia Banci from the University of Florence. They developed a strategy that combines three approaches: 1) searching known structural metal binding patterns from Protein Data Bank (PDB) and analyzing the proteins encoded by the whole genome, 2) searching in a library of metal-binding domains conserved based on sequence alignments from Pfam database, and 3) referencing known annotations of gene sequences of the particular organism. Using this strategy, the University of Florence group were able to predict zinc-binding proteins and other metalloproteins in many different organisms[21,80,81]. This paradigm-shifting pipeline is a great start to systemically cataloging and predicting zinc-binding proteins, with a few exceptions. The exceptions mostly arise due to the complexity of defining zinc-binding patterns to form known zinc-binding motifs. For example, it is not yet possible to predict zinc binding by a protein complex where zinc is coordinated at the interface of two proteins, with each protein contributing to one or two amino acid ligands. In this scenario, the ligands for zinc ions have fewer discernable patterns without the 3D structure of the protein complex. This is the case for circadian protein CRY1/PER complex mentioned in the "**General molecular roles of zinc in cells**" section. Nonetheless, the strategy developed by Claudia Andreini and colleagues has opened the door to a new era of zinc research.

Other attempts to catalog or quantify zinc proteome have also been made by various groups around the globe. These zinc proteome researchers mainly focus on two perspectives: one perspective focuses on finding all possible zinc-binding proteins and characterizing their properties in different

organisms using bioinformatic approaches, i.e. nature of the zinc-binding protein, number and types of zinc sites, interactors of zinc-binding proteins etc.; the other perspective of zinc proteome research uses advanced proteomics techniques and focuses on identifying and quantifying the proteins whose expression changes in response to zinc deficiency or to elevated zinc in the cells. Readers should be cautioned that the latter type of proteomics research is usually not entirely focusing on quantifying zinc proteome per se because many non-zinc-binding proteins also change in expression in response to cellular zinc levels. It is understandable that researchers focused on either perspective because it is difficult to know which proteins are zinc-binding if the authors haven't used the bioinformatic tools to identify the zinc proteome first in the organism they are studying.

I will briefly examine a few examples of studies that attempted to catalog or quantify the zinc proteome. Claudia Andreini was the first scientist to ever catalog the human zinc proteome[21]. Using the bioinformatic strategy she developed (mentioned above), Andreini estimated that 10% of human genes encode known or likely zinc-binding proteins and this finding is widely recognized and referenced. She also performed a functional classification of the human zinc proteome and showed that zinc-binding proteins were present in all six classes of enzymes with the majority of them being hydrolases.

Sharma et al. used several bioinformatic databases, including 3D structure databases and Metal IPB database developed by the University of Florence group, to systemically characterize the zinc proteome of a plant pathogen *Xanthamonas translucens* pv. *undulosa* (*Xtu)* which causes leaf streak in wheat and barley crops. Zinc availability from the plant host is a limiting factor for the

virulence of *Xtu*[82]. This study by Sharma et al. focused on identification of potential zinc-binding proteins and their putative roles in the host-pathogen interactions and the virulence of the pathogen *Xtu*[83].

Hsieh et al. carried out the first quantified proteome analysis towards zinc deficiency in the single-celled green alga *Chlamydomonas reinhardtii* at the University of California-Los Angeles. Although the authors did not specifically look for zinc-binding proteins in their proteomics analysis, they did find 222 differentially expressed proteins responding to zinc deficiency. Known zinc-binding proteins such as alcohol dehydrogenase (Adh1), carbonic anhydrase (Cah1, Cah8) and two members of COG0523 family of proteins (Zcp1 and Zcp2), were also shown to be differentially expressed. COG0523 family of proteins are hypothesized to be zinc metallochaperones and have significant increased expression in zinc deficiency, which was validated by independent methods, i.e. proteomic analysis and immunoblot analysis, in this work[84].

Another quantitative proteomic analysis that focused on human lung epithelial cells was aiming to identify proteins differentially expressed in response to excessive amount of zinc (up to 400 mM zinc added to the medium). In this study, Zhao et al. used 2D-polyacrylamide gel electrophoresis coupled with mass spectrometry but failed to detect any differentially expressed MTF-1 transcription factor targets, such as ZnT1, which were designed to be the positive control of excessive zinc to mammalian cell cultures. The authors interpreted that this was due to the small abundance and fold changes that were skewed by the 2D-PAGE approach, so they used independent immunoblotting and RT-qPCR to verify their positive control ZnT1 in a time-course experiment. It is very possible that the basal medium concentration Zhao et al. used contains zinc

contamination that the authors are not aware of, therefore not enough of a zinc difference is present between the basal and zinc-supplemented medium to detect a significant change of MTF-1 targets. The most differentially expressed proteins in this epithelial cell study are again not specifically zinc-binding proteins[85].

In a 2016 study, Fukao et al. investigated the proteome response to zinc, calcium, and magnesium deficiency in *Arabidopsis thaliana* roots. The authors took the extra caution to validate the elemental components in their medium using inductively coupled plasma-atomic emission spectroscopy (ICP-AES) and OFFGEL electrophoresis to separate peptides into 24 fractions before LC-MS, in an attempt to detect proteins with low abundance. The number of differentially expressed proteins detected were highly cell specific and only seven proteins were downregulated significantly (> 1.5-fold change) in response to zinc deficiency in the epidermal cells of the plants. Protein expression remained largely unchanged or little changed in the other parts of the Arabidopsis roots. They did identify some zinc-binding proteins in their proteomic analysis such as histone modifiers, copper/zinc superoxide dismutase 1 (Sod1), alcohol dehydrogenase but the scope of the study was limited[86].

To summarize this section, many efforts have been made to catalog zinc proteomes in different organisms and to quantify the whole proteome's response to various zinc concentrations. However, none of these studies combined both approaches to characterize zinc proteome in detail and to specifically quantify the zinc proteome. My work, discussed in **Chapter 2 of this thesis**, combines bioinformatic tools, ICP-AES and the coupled "multi omics" approach to achieve a focused cataloging and quantification of zinc proteome in yeast *Saccharomyces cerevisiae*[59].

Zinc apoproteins and its importance in the cells

The accumulation of zinc apoproteins in zinc-deficient cells is an exciting discovery in the zinc biology field. In this thesis, zinc apoproteins refer to zinc-binding proteins that are in the unmetalated, or apo, form and are not functional or have lost their optimal structures, depending on the role(s) of zinc in the specific proteins. Before the tools of bioinformatics and proteomics became widely used, there were only a handful of documented examples of zinc apoproteins accumulating *in vivo*. I will discuss a few of these zinc apoprotein examples and candidates in the following paragraphs.

One of the most extensively studied and thus best characterized zinc apoproteins is the tumor suppressor p53. It is a transcription factor that uses zinc as its cofactor. Zinc is required by p53 for proper protein folding, specific DNA sequence recognition, and certain protein-protein interactions[87–90]. p53 is often referred to as the "guardian of the genome" due to its function to maintain genome stability and prevent tumorigenesis[91]. p53 responds to a wide range of cellular stress signals such as DNA damage, oxidative stress, and hypoxia[92–94]. Under these stress conditions, p53 binds to specific DNA sequences and activates transcription of genes involved in cell-cycle arrest and/or apoptosis to either repair the cellular damage or stop the cells from proliferating. Recent findings also suggest that p53 is involved in cellular senescence and other important cellular programs such as autophagy[95,96]. Despite its critical cellular roles, p53 has been found to be prone to form aggregates, lose its function as a transcription factor, and even serve as a "seed" of coaggregation with its paralogs p63 and p73. These aggregates have been observed to form in cultured cells, and in tissue samples from animals and human patients[97–102].

From the perspective of zinc, the aggregation of p53 in cancers and other diseases can be explained by two reasons: 1) intrinsic structure instability of p53 at physiological temperatures and mutations that accelerate zinc loss, and 2) disrupted cellular zinc homeostasis that favors the formation of p53 apoprotein. The first explanation is well studied by *in vitro*, *in vivo,* and computational simulation studies. p53 structure has three well-defined regions: a transactivation domain at its N-terminus, the DNA-binding domain (DBD), and the oligomerization domain at the C-terminal end. In this thesis, I will emphasize the p53 DBD because that is where the zinc-binding site is located. The p53 DBD uses two loops, L1 and L3, and the loop-sheet-helix motif to bind DNA[88]. Zinc is tetrahedrally coordinated by three cysteines and one histidine: Cys176 and His179 of Loop L2, and Cys238 and Cys242 of loop L3. The L3 loop binds to the DNA minor groove. A number of protein structure and stability studies and computer simulations show that zinc is critical for holding the L3 loop in a proper orientation for DNA minor groove binding[20,87]. The Loh group from SUNY Upstate Medical University has performed a series of elegant experiments to demonstrate that zinc site of p53 is unstable at physiological temperature (37°C) due to its low thermodynamic and kinetic stability. p53 is prone to lose zinc if cellular zinc levels are slightly disturbed by even one order of magnitude from the picomolar and low nanomolar range[103]. p53 is also the most frequently mutated gene in many difficult-to-treat human cancers and other abnormalities, with over 20,000 mutations documented by the International Agency for Research on Cancer p53 database (http://p53.iarc.fr). Seventy five percent of cancer-associated p53 mutations are missense mutations, where a single base pair substitution changes one amino acid in the protein to another. Among these mutations, over half have been found near the zinc site in the core DBD of p53. For example, R175H, R248Q, R249S and G245S are a few of the best studied

examples of p53 mutants that have lost zinc binding capacity even when zinc is abundant in the cells[104,105].

The connection between disrupted zinc homeostasis and p53 apoproteins is less established. Due to the universal molecular roles of zinc in cells, there could potentially be multiple mechanisms that link zinc deficiency to accumulation of p53 apoproteins. The first mechanism is direct loss of zinc bound to p53 in zinc-deficient tissues. Many tissues have been shown to have significantly lower zinc content when they turn cancerous, such as in prostate cancer cells[106]. The second mechanism is that zinc deficiency disrupts the availability of zinc to p53. There could be a metalation machinery, such as metallochaperones, or some ATP-dependent machinery that deliver metals to proteins, whose function is impaired in zinc-deficient cells. Studies have shown that reactivating p53 after TPEN (N,N,N',N'-tetrakis(2-pyridinylmethyl 0-1,2-ethanediamine, a zinc chelator) treatment does not require protein synthesis, but requires ATP and other facilitating factors such as Hsp70 and thiol-reducing agents[107–112]. The third mechanism that links zinc deficiency to p53 forming apoprotein is through oxidative stress, or local oxidizing environment around p53. This mechanism is highly possible because zinc deficiency has been shown to induce oxidative stress in yeast, mammalian cell cultures, and animals[113–116]. The oxidative stress could also induce the formation of disulfide bond between the cysteines in the zinc site of p53, which "forces out" zinc and renders p53 apoprotein. It has also been shown in vitro that oxidizing environment abolishes DNA-binding activity of p53 while reducing agent restores it[108].The fourth possible mechanism involves other pathways that regulate p53 abundance and post-translational modifications. p53 is known to be tagged for degradation by the zinc-binding E3 ubiquitin-protein ligase Mdm2. When cells are zinc deficient, it has been shown that the interaction between p53

and Mdm2 is impaired and there is an accumulation of p53 due to decreased degradation. The accumulating p53 lack the DNA-binding ability to function as transcription factors and are very likely in apo form. This have been shown in culture cells and in mice[114,117]. Based on the above evidence and proposed mechanisms, I think it is very likely that p53 is constantly switching between the metalated and misfolded apoprotein form, with the natural fluctuations of zinc during different cell cycles to maintain genome stability and regulate gene expressions. However, when zinc homeostasis is disrupted by zinc deficiency resulting from different stresses, or diseases states, this metalation/de-metalation cycle is disrupted and p53 could become "trapped" in its apoprotein state, forming aggregates and unable to be "cleared".

Another zinc protein proposed to accumulate as the apoprotein *in vivo* is superoxide dismutase 1 (Sod1). Sod1 uses zinc as its structural cofactor and uses copper to catalyze the reaction converting superoxide anion into hydrogen peroxide and O_2. Misfolding and protein aggregation of Sod1 has been associated with both sporadic and familial amyotrophic lateral sclerosis (ALS), or Lou Gehrig's disease[118,119]. There are over 140 mutants of Sod1 linked to ALS and some of them cannot bind metals efficiently. Due to the role of zinc in proper folding of Sod1, it is natural for scientists to hypothesize that zinc-deficient Sod1 apoprotein plays a role in misfolding and protein aggregation, and the onset of ALS. Many *in vitro* studies have shown that different zinc-deficient mutant and wild-type forms of Sod1 are misfolded and likely to become aggregated at physiological temperature[120–123]. One X-ray crystallography study provided a potential explanation for how unmetalated Sod1 undergoes oligomerization: Sod1 apoprotein is disordered and exposes free cysteines that would otherwise be buried in the metalated protein[124]. In a transgenic mouse model that express the G93A mutant of SOD1 gene, depletion of zinc in the mouse diet accelerated

the disease progression while supplementing the diet with moderate zinc helped attenuate mice longevity[125]. Although there were no direct *in vivo* experiments that showed wild-type Sod1 accumulates as the apoprotein and there is much debate about the role of zinc-deficient Sod1 in initiating and progressing ALS, Sod1 remains to be an interesting zinc apoprotein candidate[118,126].

There are some other known zinc apoproteins and candidates for zinc apoproteins in different organisms. One such candidate is FolE of the bacteria *Bacillus subtilis*. FolE, also named GTP cyclohydrolase I (GCYH-I), is a zinc-binding protein that is essential. It catalyzes the first step of de novo folate biosynthesis in bacteria and plants. Bacterial cells that had been treated with EDTA displayed impaired folate biosynthesis that only supplementing inosine can reverse the growth defect. A fluorescent-based activity assay showed that bacteria cells lost 50% of FolE activity after 80 minutes of EDTA treatment. This strongly suggests that zinc-dependent FolE loses its specific activity due to loss of zinc when bacterial cells are zinc deficient[127]. In the fission yeast *Schizosaccharomyces pombe*, Pho8 is a phosphatase that requires zinc. Hu et al used an alkaline phosphatase activity assay and discovered that Pho8 is inactive in zinc-deficient cells even though the cells are producing plenty of Pho8 mRNA and protein. More surprisingly, Pho8 activity can be rapidly restored when zinc is re-supplied to the medium even with the presence of cycloheximide, indicating that there is a pool of Pho8 zinc apoproteins accumulating in zinc-deficient fission yeast[128]. Another candidate for zinc apoprotein is animal δ-aminolevulinic acid dehydratase (ALAD). It uses zinc as a catalytic cofactor and catalyzes the second step of heme synthesis, synthesizing porphobilinogen from two molecules of aminolevulinic acid[129]. When adult rat hepatocytes were cultured in zinc-free medium for 24 hours, more than 95% of ALAD lost its activity and the loss of activity is associated with zinc loss[130]. In human cells, the breast

cancer tumor suppressor *BRCA1* gene encodes a protein that has a zinc-dependent RING finger motif. Mutations, such as C61G, of the BRCA1 protein could cause its inability to bind zinc, thus trapping the protein in its apo form[131]. Lastly, the human metallothionein (MT) is an example of partially saturated zinc apoprotein. MT can bind up to seven divalent metal ions, including zinc. There is evidence suggesting that MT is naturally a mixture of partially metalated proteins in physiological conditions and this allows buffering of "free" zinc ions in the cell[47,132].

Above are summarized examples of known zinc apoproteins or zinc apoprotein candidates. Although important in many aspects of biological functions under normal and disease conditions, the accumulation of zinc apoproteins has never been systemically investigated. Common methods to determine whether a zinc-binding protein is in its apo form generally involve activity assays – enzymatic or DNA binding assays – if zinc acts as a catalytic cofactor or facilitate enzyme activity in any extent. For known proteins that use zinc as a structural cofactor, structural changes of proteins resulted from loss of zinc can be detected by a number of spectroscopic techniques[133]. One way to detect zinc apoprotein regardless of zinc's function in the protein is N-Ethylmaleimide - maleimide PEG (NEM/PEG-maleimide) analysis. NEM/PEG-maleimide analysis is based on solvent accessibility to cysteine ligands of the zinc-binding proteins. When cells were treated with NEM *in vivo*, cysteine ligands that have zinc occupied are protected from reacting with NEM while the apo form is not. After protein extraction and subsequent reaction of protected cysteines with mPEG in vitro, fully metalated zinc-binding proteins will show an increase of molecular weight on immunoblots, thus differentiating themselves from the apoproteins. Reducing reagents can also be applied to differentiate zinc occupancy and disulfide bonds. This method not only applies to zinc proteins that use cysteines as direct ligands, but it also applies to the zinc-binding proteins

that have changed structure and cysteine reactivity to NEM due to zinc loss. This method has been proven useful for detecting both types of zinc-binding proteins mentioned above. For example, we confirmed Met6 methionine synthase, which has cysteines as zinc ligands, as an apoprotein. We also confirmed Fba1 aldolase as zinc apoprotein use NEM/PEG-maleimide analysis coupled with enzyme assay even Fba1 does not use cysteines as its direct zinc ligands[59]. With the advancement in proteomics, NEM/PEG-maleimide analysis can be applied to a proteome level and become a powerful tool to "fish out" more zinc apoprotein candidates.

Prior to our lab's work, many questions about the zinc proteome and the accumulation of zinc apoproteins had not been addressed. For example, when do zinc apoproteins accumulate? What is the scope of apoprotein accumulation in various organisms? How do we verify the status of metalation since zinc could be catalytic and/or structural cofactor of the proteins? Can we re-metalate apoproteins *in vivo*? What mechanisms are present in the cells to stabilize or degrade apoproteins to prevent unfolded protein stress? I will address these questions in **Chapter 2** and **Chapter 3** of this thesis. An interesting observation of zinc apoproteins is its interconnection with disulfide bonds formation induced by oxidative stress or oxidizing microenvironment in the cells. For example, the zinc sites of ALAD are oxidized when zinc is lost, and the activity of ALAD is only recovered in a reducing environment[130]. There are also other examples of zinc-binding proteins "releasing" zinc when encountered with oxidative stress even when cellular zinc is abundant. This leads to another set of questions: what is the signal of inducing apoprotein accumulation? And what is (are) the purpose(s) of apoprotein accumulation? Future studies that address these questions are desperately needed.

References

1. Jules Raulin. Etudes Chimiques Sur La Vegetation. *Ann des Sci Nat Bot*. 1869;5:93.
2. Nielsen FH. History of zinc in agriculture. *Adv Nutr*. 2012;3(6):783-789. doi:10.3945/an.112.002881
3. Hubbell RB, Mendel LB. Zinc and Normal Nutrition. *J Biol Chem*. 1927;75(2):567-586. doi:10.1016/s0021-9258(18)84166-7
4. W.R.Todd, C.A. Elvehjem EBH. Zinc in the nutrition of the rat. *Am J Physiol*. 1934;107:146-156. doi:10.1111/j.1753-4887.1980.tb05879.x
5. McHARGUE JS. Further evidence that small quantities of copper manganese and zinc are factors in the metablism of animals. *Am J Physiol*. 1979;77(2):887-894. doi:10.1152/ajplegacy.1926.77.2.245
6. Prasad AS, Schulert AR, Miale A, Farid Z, Sandstead HH. Zinc and Iron Deficiencies in Male Subjects with Dwarfism and Hypogonadism but Without Ancylostomiasis,Schistosomiasis or Severe Anemia. *Am J Clin Nutr*. 1963;12(6):437-444. doi:10.1093/ajcn/12.6.437
7. Sandstead HH, Prasad AS, Schulert AR, et al. Human zinc deficiency, endocrine manifestations and response to treatment. *Am J Clin Nutr*. 1967;20(5):422-442. doi:10.1093/ajcn/20.5.422
8. Hove E, Elvehjem CA, Hart EB. Further studies on zinc deficiency in rats. *Am J Physiol*. 1938;124(3):750-758. doi:10.1152/ajplegacy.1938.124.3.750
9. D. K, T. M. Zinc is required by Carbonic Anhydrase. *Nature*. 1939;144(3644):442. doi:10.1038/144442a0
10. Vallee BL, Auld DS. Zinc: Biological Functions and Coordination Motifs. *Acc Chem Res*. 1993;26(10):543-551. doi:10.1021/ar00034a005

11. McCall K, Huang C, Fierke C. Function and Mechanism of Zinc Metalloenzymes. *J Nutr*. 2000;130(5):1437s-1446s. doi:10.1093/jn/130.5.1437S

12. Miller J, McLachlan AD, Klug A. Repetitive zinc-binding domains in the protein transcription factor IIIA from Xenopus oocytes. *EMBO J*. 1985;4(6):1609-1614. doi:10.1002/j.1460-2075.1985.tb03825.x

13. Klug A. The discovery of zinc fingers and their development for practical applications in gene regulation and genome manipulation. *Q Rev Biophys*. 2010;43(1):1-21. doi:10.1017/S0033583510000089

14. Vallee BL, Galdes A. The Metallobiochemistry of Zinc Enzymes. In: Meister A, ed. *Advances in Enzymology and Related Areas of Molecular Biology*. ; 1984:283-430. doi:10.1002/9780470123027.ch5

15. Pace NJ, Weerapana E. Zinc-binding cysteines: diverse functions and structural motifs. *Biomolecules*. 2014;4(2):419-434. doi:10.3390/biom4020419

16. Korichneva I, Hoyos B, Chua R, Levi E, Hammerling U. Zinc release from protein kinase C as the common event during activation by lipid second messenger or reactive oxygen. *J Biol Chem*. 2002;277(46):44327-44331. doi:10.1074/jbc.M205634200

17. Jakob U, Muse W, Eser M, Bardwell JCA. Chaperone activity with a redox switch. *Cell*. 1999;96(3):341-352. doi:10.1016/S0092-8674(00)80547-4

18. Schmalen I, Reischl S, Wallach T, et al. Interaction of circadian clock proteins CRY1 and PER2 is modulated by zinc binding and disulfide bond formation. *Cell*. 2014;157(5):1203-1215. doi:10.1016/j.cell.2014.03.057

19. Riordan JF. The role of metals in enzyme activity. *Ann Clin Lab Sci*. 1977;7(2):119-129.

20. Duan J, Nilsson L. Effect of Zn2+ on DNA recognition and stability of the p53 DNA-

binding domain. *Biochemistry*. 2006;45(24):7483-7492. doi:10.1021/bi0603165

21. Andreini C, Banci L, Bertini I, Rosato A. Counting the zinc-proteins encoded in the human genome. *J Proteome Res*. 2006;5(1):196-201. doi:10.1021/pr050361j
22. Toshiyuki Fukada TK. *Zinc Signaling*. Springer; 2019. doi:10.1007/978-981-15-0557-7_9
23. Huang EP. Metal ions and synaptic transmission: Think zinc. *Proc Natl Acad Sci U S A*. 1997;94(25):13386-13387. doi:10.1073/pnas.94.25.13386
24. Kim AM, Bernhardt ML, Kong BY, et al. Zinc sparks are triggered by fertilization and facilitate cell cycle resumption in mammalian eggs. *ACS Chem Biol*. 2011;6(7):716-723. doi:10.1021/cb200084y.Zinc
25. Que EL, Bleher R, Duncan FE, et al. Quantitative mapping of zinc fluxes in the mammalian egg reveals the origin of fertilization-induced zinc sparks. *Nat Chem istry*. 2015;7(2):130-139. doi:10.1038/nchem.2133.Quantitative
26. Zhang N, Duncan FE, Que EL, O'Halloran T V., Woodruff TK. The fertilization-induced zinc spark is a novel biomarker of mouse embryo quality and early development. *Sci Rep*. 2016;6(October 2015):1-9. doi:10.1038/srep22772
27. Yamasaki S, Sakata-Sogawa K, Hasegawa A, et al. Zinc is a novel intracellular second messenger. *J Cell Biol*. 2007;177(4):637-645. doi:10.1083/jcb.200702081
28. Anson KJ, Corbet GA, Palmer AE. Zn2+ influx activates ERK and Akt signaling pathways. *Proc Natl Acad Sci U S A*. 2021;118(11):1-10. doi:10.1073/PNAS.2015786118
29. Outten CE, O'Halloran T V. Femtomolar sensitivity of metalloregulatory proteins controlling zinc homeostasis. *Science (80-)*. 2001;292(5526):2488-2492. doi:10.1126/science.1060331
30. MacDiarmid CW. Zinc transporters that regulate vacuolar zinc storage in Saccharomyces

cerevisiae. *EMBO J*. 2000;19(12):2845-2855. doi:10.1093/emboj/19.12.2845

31. Palmiter RD, Findley SD. Cloning and functional characterization of a mammalian zinc transporter that confers resistance to zinc. *EMBO J*. 1995;14(4):639-649. doi:10.1002/j.1460-2075.1995.tb07042.x

32. Suhy DA, Simon KD, Linzer DIH, O'Halloran T V. Metallothionein is part of a zinc-scavenging mechanism for cell survival under conditions of extreme zinc deprivation. *J Biol Chem*. 1999;274(14):9183-9192. doi:10.1074/jbc.274.14.9183

33. Frederickson CJ, Suh SW, Silva D, Frederickson CJ, Thompson RB. Importance of Zinc in the Central Nervous System: The Zinc-Containing Neuron. *J Nutr*. 2000;130(5):1471S-1483S. doi:10.1093/jn/130.5.1471S

34. Kolenko V, Teper E, Kutikov A, Uzzo R. Zinc and zinc transporters in prostate carcinogenesis. *Nat Rev Urol*. 2013;10(4):219-226. doi:10.1038/jid.2014.371

35. Huang L, Kirschke CP, Zhang Y. Decreased intracellular zinc in human tumorigenic prostate epithelial cells: A possible role in prostate cancer progression. *Cancer Cell Int*. 2006;6:1-13. doi:10.1186/1475-2867-6-10

36. Maret W. Metals on the move: Zinc ions in cellular regulation and in the coordination dynamics of zinc proteins. *BioMetals*. 2011;24(3):411-418. doi:10.1007/s10534-010-9406-1

37. Fang H, Geng S, Hao M, et al. Simultaneous Zn2+ tracking in multiple organelles using super-resolution morphology-correlated organelle identification in living cells. *Nat Commun*. 2021;12(109):1-5. doi:10.1038/s41467-020-20309-7

38. Abiria SA, Krapivinsky G, Sah R, et al. TRPM7 senses oxidative stress to release Zn2+ from unique intracellular vesicles. *Proc Natl Acad Sci U S A*. 2017;114(30):E6079-E6088.

doi:10.1073/pnas.1707380114

39. Miki T, Awa M, Nishikawa Y, et al. A conditional proteomics approach to identify proteins involved in zinc homeostasis. *Nat Methods*. 2016;13(11):931-937. doi:10.1038/nmeth.3998

40. Li Y, Maret W. Transient fluctuations of intracellular zinc ions in cell proliferation. *Exp Cell Res*. 2009;315(14):2463-2470. doi:10.1016/j.yexcr.2009.05.016

41. Simons TJB. Intracellular free zinc and zinc buffering in human red blood cells. *J Membr Biol*. 1991;123(1):63-71. doi:10.1007/BF01993964

42. Adebodun F, Post JFM. Role of intracellular free Ca(II) and Zn(II) in dexamethasone-induced apoptosis and dexamethasone resistance in human leukemic CEM cell lines. *J Cell Physiol*. 1995;163(1):80-86. doi:10.1002/jcp.1041630109

43. Zalewski PD, Forbes IJ, Seamark RF, et al. Flux of intracellular labile zinc during apoptosis (gene-directed cell death) revealed by a specific chemical probe, Zinquin. *Chem Biol*. 1994;1(3):153-161. doi:10.1016/1074-5521(94)90005-1

44. Sensi SL, Canzoniero LMT, Yu SP, et al. Measurement of intracellular free zinc in living cortical neurons: Routes of entry. *J Neurosci*. 1997;17(24):9554-9564. doi:10.1523/jneurosci.17-24-09554.1997

45. Vinkenborg JL, Nicolson TJ, Bellomo EA, Koay MS, Rutter GA, Merkx M. Imaging of intracellular free Zn2+ in real time using genetically-encoded FRET sensors. *Nat Methods*. 2009;6(10):737-740. doi:10.1038/nmeth.1368

46. Qin Y, Miranda JG, Stoddard CI, Dean KM, Galati DF, Palmer AE. Direct comparison of a genetically encoded sensor and small molecule indicator: implications for quantification of cytosolic Zn2+. *ACS Chem Biol*. 2013;8(11):2366-2371. doi:10.1021/cb4003859

47. Krężel A, Maret W. Dual nanomolar and picomolar Zn(II) binding properties of

metallothionein. *J Am Chem Soc*. 2007;129(35):10911-10921. doi:10.1021/ja071979s

48. Carpenter MC, Lo MN, Palmer AE. Techniques for Measuring Cellular Zinc. *Arch Biochem Biophys*. 2016;611:20-29. doi:10.1016/j.abb.2016.08.018

49. Eide DJ. Transcription factors and transporters in zinc homeostasis: lessons learned from fungi. *Crit Rev Biochem Mol Biol*. 2020;55(1):88-110. doi:10.1080/10409238.2020.1742092

50. Bird AJ, McCall K, Kramer M, Blankman E, Winge DR, Eide DJ. Zinc fingers can act as Zn2+ sensors to regulate transcriptional activation domain function. *EMBO J*. 2003;22(19):5137-5146. doi:10.1093/emboj/cdg484

51. Qin Y, Dittmer PJ, Park JG, Jansen KB, Palmer AE. Measuring steady-state and dynamic endoplasmic reticulum and Golgi Zn 2+ with genetically encoded sensors. *Proc Natl Acad Sci U S A*. 2011;108(18):7351-7356. doi:10.1073/pnas.1015686108

52. Levy S, Kafri M, Carmi M, Barkai N. The Competitive Advantage of a Dual-transporter System. *Science (80-)*. 2011;334(6061):1408-1412. doi:10.1126/science.1207154

53. Eide DJ. Homeostatic and adaptive responses to zinc deficiency in saccharomyces cerevisiae. *J Biol Chem*. 2009;284(28):18565-18568. doi:10.1074/jbc.R900014200

54. Nanamiya H, Akanuma G, Natori Y, et al. Zinc is a key factor in controlling alternation of two types of L31 protein in the Bacillus subtilis ribosome. *Mol Microbiol*. 2004;52(1):273-283. doi:10.1111/j.1365-2958.2003.03972.x

55. Sankaran B, Bonnett SA, Shah K, et al. Zinc-independent folate biosynthesis: Genetic, biochemical, and structural investigations reveal new metal dependence for GTP cyclohydrolase IB. *J Bacteriol*. 2009;191(22):6936-6949. doi:10.1128/JB.00287-09

56. Alterio V, Langella E, De Simone G, Monti SM. Cadmium-containing carbonic anhydrase

CDCA1 in marine diatom Thalassiosira weissflogii. *Mar Drugs*. 2015;13(4):1688-1697. doi:10.3390/md13041688

57. Bird AJ, Gordon M, Eide DJ, Winge DR. Repression of ADH1 and ADH3 during zinc deficiency by Zap1-induced intergenic RNA transcripts. *EMBO J*. 2006;25(24):5726-5734. doi:10.1038/sj.emboj.7601453

58. Lee YJ, Lee CY, Grzechnik A, et al. RNA polymerase I stability couples cellular growth to metal availability. *Mol Cell*. 2013;51(1):105-115. doi:10.1016/j.molcel.2013.05.005

59. Wang Y, Weisenhorn E, Macdiarmid CW, et al. The cellular economy of the Saccharomyces cerevisiae zinc proteome. *Metallomics*. 2018;10(12):1755-1776. doi:10.1039/c8mt00269j

60. Ogo OA, Tyson J, Cockell SJ, Howard A, Valentine RA, Ford D. The Zinc Finger Protein ZNF658 Regulates the Transcription of Genes Involved in Zinc Homeostasis and Affects Ribosome Biogenesis through the Zinc Transcriptional Regulatory Element. *Mol Cell Biol*. 2015;35(6):977-987. doi:10.1128/mcb.01298-14

61. Kambe T, Narita H, Yamaguchi-Iwai Y, et al. Cloning and characterization of a novel mammalian zinc transporter, zinc transporter 5, abundantly expressed in pancreatic β cells. *J Biol Chem*. 2002;277(21):19049-19055. doi:10.1074/jbc.M200910200

62. Bosomworth HJ, Thornton JK, Coneyworth LJ, Ford D, Valentine RA. Efflux function, tissue-specific expression and intracellular trafficking of the Zn transporter ZnT10 indicate roles in adult Zn homeostasis. *Metallomics*. 2012;4(8):771-779. doi:10.1039/c2mt20088k

63. Leyva-Illades D, Chen P, Zogzas CE, et al. SLC30A10 is a cell surface-localized manganese efflux transporter, And parkinsonism-causing mutations block its intracellular trafficking and efflux activity. *J Neurosci*. 2014;34(42):14079-14095.

doi:10.1523/JNEUROSCI.2329-14.2014

64. Günther V, Lindert U, Schaffner W. The taste of heavy metals: Gene regulation by MTF-1. *Biochim Biophys Acta*. 2012;1823(9):1416-1425. doi:10.1016/j.bbamcr.2012.01.005

65. Livingstone C. Zinc: Physiology, deficiency, and parenteral nutrition. *Nutr Clin Pract*. 2015;30(3):371-382. doi:10.1177/0884533615570376

66. Maret W. Zinc and human disease. *Met Ions Life Sci*. 2013;13:389-414. doi:10.1007/978-94-007-7500-8_12

67. Caulfield LE, Black RE. Zinc deficiency in Comparative Quantification of Health Risks. In: *Comparative Quantification of Health Risks*. Vol 1. ; 2004:257-280. https://www.who.int/publications/cra/chapters/volume1/0257-0280.pdf.

68. Hennigar SR, Lieberman HR, Fulgoni VL, McClung JP. Serum zinc concentrations in the US population are related to sex, age, and time of blood draw but not dietary or supplemental zinc. *J Nutr*. 2018;148(8):1341-1351. doi:10.1093/jn/nxy105

69. King JC. Yet again, serum zinc concentrations are unrelated to zinc intakes. *J Nutr*. 2018;148(9):1399-1401. doi:10.1093/jn/nxy190

70. Wang M, Fan L, Wei W, et al. Integrated multi-omics uncovers reliable potential biomarkers and adverse effects of zinc deficiency. *Clin Nutr*. 2021;40(5):2683-2696. doi:10.1016/j.clnu.2021.03.019

71. Hood Indriati M, Skaar EP. Nutritional immunity: transition metals at the pathogen-host interface. *Nat Rev Microbiol*. 2012;10(8):525-537. doi:10.1038/nrmicro2836.

72. Usama U, Jaffar Khan M, Fatima S, Fatima S. Role of Zinc in Shaping the Gut Microbiome; Proposed Mechanisms and Evidence from the Literature. *J Gastrointest Dig Syst*. 2018;08(01):8-11. doi:10.4172/2161-069x.1000548

73. Reed S, Neuman H, Moscovich S, Glahn RP, Koren O, Tako E. Chronic zinc deficiency alters chick gut microbiota composition and function. *Nutrients*. 2015;7(12):9768-9784. doi:10.3390/nu7125497

74. Pieper R, Dadi TH, Pieper L, et al. Concentration and chemical form of dietary zinc shape the porcine colon microbiome, its functional capacity and antibiotic resistance gene repertoire. *ISME J*. 2020;14(11):2783-2793. doi:10.1038/s41396-020-0730-3

75. Vallee BL, Neurath H. Carboxypeptidase, A Zinc Metalloprotein. *J Am Chem Soc*. 1954;76(19):5006-5007. doi:10.1021/ja01648a088

76. Fuwa K, Pulido P, McKay R, Vallee BL. Determination of Zinc in biological materials by atomic absorption spectrophotometry. *Anal Chem*. 1964;36(13):2407-2411. doi:10.1021/ac60219a009

77. Vallee BL, Hoch FL. Zinc, A Component of Yeast Alcohol Dehydrogenase. *Proc Natl Acad Sci U S A*. 1955;41(6):327-338. doi:10.1073/pnas.41.6.327

78. Margoshes M, Vallee BL. A Cadmium Protein From Equine Kidney Cortex. *J Am Chem Soc*. 1957;79(17):4813-4814. doi:10.32388/17n326

79. Vallee BL, Auld DS. Zinc Coordination, Function, and Structure of Zinc Enzymes and Other Proteins. *Am Chem Soc*. 1990;29(24):5647-5659. doi:10.1021/bi00476a001

80. Andreini C, Cavallaro G, Lorenzini S, Rosato A. MetalPDB: A database of metal sites in biological macromolecular structures. *Nucleic Acids Res*. 2013;41(D1):312-319. doi:10.1093/nar/gks1063

81. Putignano V, Rosato A, Banci L, Andreini C. MetalPDB in 2018: A database of metal sites in biological macromolecular structures. *Nucleic Acids Res*. 2018;46(D1):D459-D464. doi:10.1093/nar/gkx989

82. Palmer LD, Skaar EP. Transition Metals and Virulence in Bacteria. *Annu Rev Genet*. 2016;50:67-91. doi:10.1146/annurev-genet-120215-035146

83. Sharma A, Sharma D, Verma SK. Zinc binding proteome of a phytopathogen Xanthomonas translucens pv. Undulosa. *R Soc Open Sci*. 2019;6(9). doi:10.1098/rsos.190369

84. Hsieh SI, Castruita M, Malasarn D, et al. The proteome of copper, iron, zinc, and manganese micronutrient deficiency in Chlamydomonas reinhardtii. *Mol Cell Proteomics*. 2013;12(1):65-86. doi:10.1074/mcp.M112.021840

85. Zhao WJ, Song Q, Wang YH, et al. Zn-responsive proteome profiling and time-dependent expression of proteins regulated by MTF-1 in A549 cells. *PLoS One*. 2014;9(8). doi:10.1371/journal.pone.0105797

86. Fukao Y, Kobayashi M, Zargar SM, et al. Quantitative proteomic analysis of the response to zinc, magnesium, and calcium deficiency in specific cell types of Arabidopsis roots. *Proteomes*. 2016;4(1):1-13. doi:10.3390/proteomes4010001

87. Butler JS, Loh SN. Structure, function, and aggregation of the zinc-free form of the p53 DNA binding domain. *Biochemistry*. 2003;42(8):2396-2403. doi:10.1021/bi026635n

88. Cho Y, Gorina S, Jeffrey PD, Pavletich NP. Crystal structure of a p53 tumor suppressor-DNA complex: Understanding tumorigenic mutations. *Science (80-)*. 1994;265(5170):346-355. doi:10.1126/science.8023157

89. Méplan C, Richard MJ, Hainaut P. Redox signalling and transition metals in the control of the p53 pathway. *Biochem Pharmacol*. 2000;59(1):25-33. doi:10.1016/S0006-2952(99)00297-X

90. Méplan C, Richard MJ, Hainaut P. Metalloregulation of the tumor suppressor protein p53: Zinc mediates the renaturation of p53 after exposure to metal chelators in vitro and in intact

cells. *Oncogene*. 2000;19(46):5227-5236. doi:10.1038/sj.onc.1203907

91. Lane DP. The Guardian of the Genome: p53. *Nature*. 1992;385:15-16. doi:10.1038/358015a0

92. Zhang C, Liu J, Wang J, et al. The Interplay Between Tumor Suppressor p53 and Hypoxia Signaling Pathways in Cancer. *Front Cell Dev Biol*. 2021;9(February). doi:10.3389/fcell.2021.648808

93. Harris SL, Levine AJ. The p53 pathway: Positive and negative feedback loops. *Oncogene*. 2005;24(17):2899-2908. doi:10.1038/sj.onc.1208615

94. Shi T, Dansen TB. Reactive Oxygen Species Induced p53 Activation: DNA Damage, Redox Signaling, or Both? *Antioxidants Redox Signal*. 2020;33(12):839-859. doi:10.1089/ars.2020.8074

95. Rufini A, Tucci P, Celardo I, Melino G. Senescence and aging: The critical roles of p53. *Oncogene*. 2013;32(43):5129-5143. doi:10.1038/onc.2012.640

96. Levine B, Abrams J. p53: The Janus of autophagy? *Nat Cell Biol*. 2008;10(6):637-639. doi:10.1038/ncb0608-637.p53

97. Bullock AN, Henckel J, Dedecker BS, et al. Thermodynamic stability of wild-type and mutant p53 core domain. *Proc Natl Acad Sci U S A*. 1997;94(26):14338-14342. doi:10.1073/pnas.94.26.14338

98. Ishimaru D, Lima LMTR, Maia LF, et al. Reversible aggregation plays a crucial role on the folding landscape of p53 core domain. *Biophys J*. 2004;87(4):2691-2700. doi:10.1529/biophysj.104.044685

99. Ano Bom APD, Freitas MS, Moreira FS, et al. The p53 core domain is a molten globule at low pH: Functional implications of a partially unfolded structure. *J Biol Chem*.

2010;285(4):2857-2866. doi:10.1074/jbc.M109.075861

100. Ano Bom APD, Rangel LP, Costa DCF, et al. Mutant p53 aggregates into prion-like amyloid oligomers and fibrils: Implications for cancer. *J Biol Chem*. 2012;287(33):28152-28162. doi:10.1074/jbc.M112.340638

101. Costa DCF, de Oliveira GAP, Cino EA, Soares IN, Rangel LP, Silva JL. Aggregation and prion-like properties of misfolded tumor suppressors: Is cancer a prion disease? *Cold Spring Harb Perspect Biol*. 2016;8(10):1-21. doi:10.1101/cshperspect.a023614

102. Wilcken R, Wang GZ, Boeckler FM, Fersht AR. Kinetic mechanism of p53 oncogenic mutant aggregation and its inhibition. *Proc Natl Acad Sci U S A*. 2012;109(34):13584-13589. doi:10.1073/pnas.1211550109

103. Blanden AR, Yu X, Blayney AJ, et al. Zinc shapes the folding landscape of p53 and establishes a pathway for reactivating structurally diverse cancer mutants. *Elife*. 2020;9:1-26. doi:10.7554/eLife.61487

104. Kato S, Han SY, Liu W, et al. Understanding the function-structure and function-mutation relationships of p53 tumor suppressor protein by high-resolution missense mutation analysis. *Proc Natl Acad Sci U S A*. 2003;100(14):8424-8429. doi:10.1073/pnas.1431692100

105. Navalkar A, Ghosh S, Pandey S, Paul A, Datta D, Maji SK. Prion-like p53 Amyloids in Cancer. 2019. doi:10.1021/acs.biochem.9b00796

106. Costello LC, Franklin RB. The clinical relevance of the metabolism of prostate cancer; zinc and tumor suppression: Connecting the dots. *Mol Cancer*. 2006;5:1-13. doi:10.1186/1476-4598-5-17

107. Hainaut P, Milner J. Interaction of heat-shock protein 70 with p53 translated in vitro: Evidence for interaction with dimeric p53 and for a role in the regulation of p53

conformation. *EMBO J*. 1992;11(10):3513-3520. doi:10.1002/j.1460-2075.1992.tb05434.x

108. Hainaut P, Milner J. Redox Modulation of p53 Conformation and Sequence-specific DNA Binding in Vitro. *Cancer Res*. 1993;53(19):4469-4473.

109. Hainaut P, Milner J. A Structural Role for Metal Ions in the "Wild-type" Conformation of the Tumor Suppressor Protein p53. *Cancer Res*. 1993;53(8):1739-1742.

110. Hansen S, Midgley CA, Lane DP, Freeman BC, Morimoto RI, Hupp TR. Modification of two distinct COOH-terminal domains is required for murine p53 activation by bacterial Hsp70. *J Biol Chem*. 1996;271(48):30922-30928. doi:10.1074/jbc.271.48.30922

111. Rainwater R, Parks D, Anderson ME, Tegtmeyer P, Mann K. Role of cysteine residues in regulation of p53 function. *Mol Cell Biol*. 1995;15(7):3892-3903. doi:10.1128/mcb.15.7.3892

112. Verhaegh GW, Parat MO, Richard MJ, Hainaut P. Modulation of p53 protein conformation and DNA-binding activity by intracellular chelation of zinc. *Mol Carcinog*. 1998;21(3):205-214. doi:10.1002/(SICI)1098-2744(199803)21:3<205::AID-MC8>3.0.CO;2-K

113. Ho E, Ames BN. Low intracellular zinc induces oxidative DNA damage, disrupts p53, NFκB, and AP1 DNA binding, and affects DNA repair in a rat glioma cell line. *Proc Natl Acad Sci U S A*. 2002;99(26):16770-16775. doi:10.1073/pnas.222679399

114. Ho E, Courtemanche C, Ames BN. Zinc deficiency induces oxidative DNA damage and increases P53 expression in human lung fibroblasts. *J Nutr*. 2003;133(8):2543-2548. doi:10.1093/jn/133.8.2543

115. Song Y, Leonard SW, Traber MG, Ho E. Zinc deficiency affects DNA damage, oxidative stress, antioxidant defenses, and DNA repair in rats. *J Nutr*. 2009;139(9):1626-1631. doi:10.3945/jn.109.106369

116. Eide DJ. The oxidative stress of zinc deficiency. *Metallomics*. 2011;3(11):1124-1129. doi:10.1039/c1mt00064k

117. Li H, Zhang J, Niswander L. Zinc deficiency causes neural tube defects through attenuation of p53 ubiquitylation. *Dev*. 2018;145(24):1-27. doi:10.1242/dev.169797

118. Cleveland DW, Liu J. Oxidation versus aggregation - How do SOD1 mutants cause ALS? *Nat Med*. 2000;6(12):1320-1321. doi:10.1038/82122

119. Trumbull KA, Beckman JS. A role for copper in the toxicity of zinc-deficient superoxide dismutase to motor neurons in amyotrophic lateral sclerosis. *Antioxidants Redox Signal*. 2009;11(7):1627-1639. doi:10.1089/ars.2009.2574

120. Sannigrahi A, Chowdhury S, Das B, et al. The metal cofactor zinc and interacting membranes modulate sod1 conformation-aggregation landscape in an in vitro als model. *Elife*. 2021;10:1-29. doi:10.7554/ELIFE.61453

121. Li Q, Velde C Vande, Israelson A, et al. ALS-linked mutant superoxide dismutase 1 (SOD1) alters mitochondrial protein composition and decreases protein import. *Proc Natl Acad Sci U S A*. 2010;107(49):21146-21151. doi:10.1073/pnas.1014862107

122. Nordlund A, Leinartaite L, Saraboji K, et al. Functional features cause misfolding of the ALS-provoking enzyme SOD1. *Proc Natl Acad Sci U S A*. 2009;106(24):9667-9672. doi:10.1073/pnas.0812046106

123. Banci L, Bertini I, Durazo A, et al. Metal-free superoxide dismutase forms soluble oligomers under physiological conditions: A possible general mechanism for familial ALS. *Proc Natl Acad Sci U S A*. 2007;104(27):11263-11267. doi:10.1073/pnas.0704307104

124. Banci L, Bertini I, Boca M, et al. Structural and dynamic aspects related to oligomerization of apo SOD1 and its mutants. *Proc Natl Acad Sci U S A*. 2009;106(17):6980-6985.

doi:10.1073/pnas.0809845106

125. Ermilova IP, Ermilov VB, Levy M, Ho E, Pereira C, Beckman JS. Protection by dietary zinc in ALS mutant G93A SOD transgenic mice. *Neurosci Lett*. 2005;379(1):42-46. doi:10.1016/j.neulet.2004.12.045

126. Hilton JB, White AR, Crouch PJ. Metal-deficient SOD1 in amyotrophic lateral sclerosis. *J Mol Med*. 2015;93(5):481-487. doi:10.1007/s00109-015-1273-3

127. Chandrangsu P, Huang X, Gaballa A, Helmann JD. Bacillus subtilis FolE is sustained by the ZagA zinc metallochaperone and the alarmone ZTP under conditions of zinc deficiency. *Mol Microbiol*. 2019;112(June):751-765. doi:10.1111/mmi.14314

128. Hu YM, Boehm DM, Chung H, Wilson S, Bird AJ. Zinc-dependent activation of the Pho8 alkaline phosphatase in Schizosaccharomyces pombe. *J Biol Chem*. 2019;294(33):12392-12404. doi:10.1074/jbc.RA119.007371

129. Ikuyo T, Takeo Y, Seiyo S. Zinc and cysteine residues in the active site of bovine liver 5-aminolevulinic acid dehydratase. *Int J Biochem*. 1980;12(5-6):751-756. doi:10.1016/0020-711X(80)90157-3

130. Bevan DR, Bodlaender P, Shemin D. Mechanism of porphobilinogen synthase. Requirement of Zn2+ for enzyme activity. *J Biol Chem*. 1980;255(5):2030-2035. doi:10.1016/s0021-9258(19)85987-2

131. Brzovic PS, Meza J, King MC, Klevit RE. The cancer-predisposing mutation C61G disrupts homodimer formation in the NH2-terminal BRCA1 RING finger domain. *J Biol Chem*. 1998;273(14):7795-7799. doi:10.1074/jbc.273.14.7795

132. Kluska K, Adamczyk J, Krężel A. Metal binding properties, stability and reactivity of zinc fingers. *Coord Chem Rev*. 2018;367:18-64. doi:10.1016/j.ccr.2018.04.009

133. Witkowska D, Rowińska-Żyrek M. Biophysical approaches for the study of metal-protein interactions. *J Inorg Biochem*. 2019;199(6):110783. doi:10.1016/j.jinorgbio.2019.110783

Chapter 2: The cellular economy of the Saccharomyces cerevisiae zinc proteome

ABSTRACT

Zinc is an essential cofactor for many proteins. A key mechanism of zinc homeostasis during deficiency is "zinc sparing" in which specific zinc-binding proteins are repressed to reduce the cellular requirement. In this report, we evaluated zinc sparing across the zinc proteome of *Saccharomyces cerevisiae*. The yeast zinc proteome of 582 known or potential zinc-binding proteins was identified using a bioinformatics analysis that combined global domain searches with local motif searches. Protein abundance was determined by mass spectrometry. In zinc-replete cells, we detected over 2500 proteins among which 229 were zinc proteins. Based on copy number estimates and binding stoichiometries, a replete cell contains ~9 million zinc-binding sites on proteins. During zinc deficiency, many zinc proteins decreased in abundance and the zinc-binding requirement decreased to ~5 million zinc atoms per cell. Many of these effects were due at least in part to changes in mRNA levels rather than simply protein degradation. Measurements of cellular zinc content showed that the level of zinc atoms per cell dropped from over 20 million in replete cells to only 1.7 million in deficient cells. These results confirmed the ability of replete cells to store excess zinc and suggested that the majority of zinc-binding sites on proteins in deficient cells are either unmetalated or mismetalated. Our analysis of two abundant zinc proteins, Fba1 aldolase and Met6 methionine synthetase, supported that hypothesis. Thus, we have discovered widespread zinc sparing mechanisms and obtained evidence of a high accumulation of zinc proteins that lack their cofactor during deficiency.

INTRODUCTION

Zinc is an essential catalytic and/or structural cofactor for many proteins. Approximately 9% of genes in eukaryotic organisms and ~5% of prokaryotic genes encode proteins that bind zinc to become functional (1). The abundance and importance of zinc-dependent proteins is reflected in the concept of the "zinc quota". The zinc quota is defined as the amount of zinc in a cell grown under a given condition (2). The "minimum zinc quota" is the lowest amount of zinc per cell that allows for optimal growth. The minimum zinc quota varies widely for different organisms and has been experimentally determined to be ~10^5 atoms of zinc per cell in *E. coli*, ~10^7 atoms in yeast, and ~10^8 atoms in mammalian cells (2-5). Many studies have indicated that the level of labile or exchangeable zinc in cells is very low and the great majority is tightly bound by the proteins that require this metal for function (6-8). Therefore, the minimum zinc quota is likely dictated by the number of zinc-binding sites on proteins that require the metal for optimal cellular physiology.

Organisms have evolved with many mechanisms of zinc homeostasis. During times of excess zinc exposure, these mechanisms limit uptake and promote efflux to maintain the intracellular metal content at tolerable levels (9, 10). They also control the generation of intracellular zinc stores in the form of either organellar or buffered cytosolic (e.g. metallothionein) pools that are available for later use (3, 11). During zinc deficiency, homeostatic mechanisms work to maintain zinc levels at the minimum zinc quota (12). These mechanisms increase zinc uptake, decrease zinc efflux, and mobilize the release of zinc from intracellular storage sites. An additional mechanism of zinc homeostasis during deficiency has been called "zinc sparing", i.e. reducing the levels of specific zinc-binding proteins to decrease the cellular zinc requirement (13). In some cases, reduced production of a zinc-dependent protein is compensated by increased synthesis of a zinc-independent paralog. In many bacterial species, for example, several zinc-dependent ribosomal

subunits are repressed during deficiency and corresponding zinc-independent subunits are upregulated to take their place (14-16). In this way, cells can reduce their total requirement for zinc and prioritize the distribution of the limited supply of this nutrient to more critical sites and functions.

In *Saccharomyces cerevisiae*, the Zap1 transcription factor is the central regulator of zinc homeostasis (12, 17). Zap1 is a transcriptional activator protein whose activity is low in zinc-replete cells and high in deficient cells. Zap1 increases the expression of many genes including those that encode zinc uptake transporters in the plasma membrane. In addition, Zap1 increases expression of organellar transporters that control the levels of zinc in intracellular compartments such as the vacuole and the endoplasmic reticulum. In addition to maintaining zinc homeostasis, Zap1 also regulates genes involved in adapting cellular processes to the challenges of zinc deficiency. For example, the *CKI1* and *EKI1* genes are induced by Zap1 to maintain phospholipid synthesis (18, 19). The *CTT1* catalase gene is also induced by Zap1 and this response is likely to eliminate the oxidative stress that arises during zinc deficiency (20, 21).

Among the adaptive responses to zinc deficiency, Zap1 induces expression of the *TSA1* gene. Tsa1 is a dual function protein that acts as a peroxidase and as a “holdase”-type protein chaperone (22). Tsa1 function is essential for growth of zinc-deficient cells. Our initial studies indicated a role of the Tsa1 peroxidase activity in protecting zinc-deficient cells against an elevated level of reactive oxygen species (21). Subsequently, we found that the Tsa1 protein chaperone activity was more important than the peroxidase function for zinc-deficient growth (23). Zinc-deficient cells lacking Tsa1 chaperone activity accumulated elevated levels of stress-responsive protein chaperones,

suggesting elevated unfolded protein accumulation and a corresponding heat shock response. Also consistent with this hypothesis, zinc-deficient *tsa1Δ* cells accumulated distinct cytoplasmic foci marked by the Hsp104 disaggregase chaperone. These foci resembled the "IPOD" compartment that accumulates in cells accumulating abundant unfolded proteins (24). Our findings for Tsa1 suggested that zinc-deficient cells accumulate unfolded zinc-dependent proteins because they lack their metal cofactor needed for folding and stability. Under these conditions, the holdase function of the Tsa1 chaperone may stabilize zinc apoproteins and shield them from misfolding and aggregation until zinc supplies increase.

Zap1 also controls an important zinc sparing mechanism involving the abundant zinc-binding alcohol dehydrogenases Adh1 and Adh3 (25). Under zinc-replete conditions, the *ADH1* gene is expressed, and its protein product accumulates to high levels. Under deficient conditions, the *ADH1* promoter is repressed by an intergenic noncoding regulatory RNA under the control of Zap1. This mechanism allows for a transcriptional activator to repress expression of a target gene. The less abundant Adh3 alcohol dehydrogenase is regulated in a similar manner. At the same time, Zap1 induces expression of the *ADH4* gene. *ADH4* encodes an alternative alcohol dehydrogenase that accumulates to lower levels than Adh1 and whose activity is dependent on zinc or possibly iron (26, 27). While Adh1 and Adh3 require two zinc atoms per monomer for function, Adh4 requires only one metal ion and is not as highly expressed as Adh1, thereby providing for a net reduction in the zinc requirement of the cell during deficiency regardless of which metal it uses.

Zap1-independent mechanisms of zinc sparing in *S. cerevisiae* have also been discovered. For example, RNA polymerase I (RNAPI) is targeted for degradation in zinc-deficient cells (28). In

replete cells, RNAPI large subunit Rpa190 is ubiquitinated and retained in the nucleus and nucleolus where it transcribes ribosomal RNA genes. Under zinc-deficient conditions, Rpa190 becomes deubiquitinated, RNAPI is exported from the nucleus and taken up into the vacuole where it is degraded by vacuolar proteases. Similarly, the zinc-binding vacuolar alkaline phosphatase Pho8 is also targeted for degradation in zinc-deficient cells through a mechanism that is independent of Zap1 (29). The zinc released into the vacuole by these mechanisms is likely transported back to the cytosol where it is used by other proteins for their function.

In this study, we performed an analysis of the yeast proteome in replete cells and cells transitioning to conditions of severe zinc deficiency. A major goal of this study was to identify additional examples of zinc sparing in the yeast zinc proteome. A second goal was to test the hypothesis raised by our studies of Tsa1 that zinc-deficient cells accumulate high levels of zinc apoproteins that require protein chaperones for their stability in the absence of their metal cofactor. We describe an extensive catalog of predicted zinc proteins in the yeast proteome and their abundance and distribution in zinc-replete conditions. During the transition to deficiency, we found that decreased accumulation of zinc-binding proteins is widespread and many effects are mediated at least in part by changes in mRNA levels rather than simply degradation of apoproteins. In addition, we present evidence that the accumulation of apoproteins is high during deficiency and that the majority of zinc sites in a cell are not occupied by zinc under these conditions. Thus, we provide unique insights into the economy of zinc in a eukaryotic cell.

RESULTS

Cataloging the zinc proteome of S. cerevisiae.

To determine the effects of zinc status on the abundance of zinc-binding proteins, we first cataloged the proteins that coordinate that ion. Proteins encoded by the yeast genome that are predicted to bind zinc were identified by a bioinformatics analysis that combined global domain searches with local motif searches. Based on this analysis, we identified 571 known or likely zinc-binding proteins in yeast (**Table S1**). To this group, we added several transporter proteins (Zrt1, Zrt2, Fet4, Pho84, Zrt3, Zrc1, Cot1, Zrg17, Msc2) that have been implicated to transport zinc either exclusively or among known substrates. Also included was Zps1, an accessory protein for zinc uptake that is the *S. cerevisiae* ortholog of *C. albicans* "zincophore" Pra1 (30). The yeast genome also encodes two metallothioneins, Cup1 and Crs5, that confer copper resistance. While both also bind zinc in vitro, only Crs5 contributes to zinc resistance when metal levels are high (31, 32). Therefore, Crs5 was included in the zinc proteome and Cup1 was not. These additions raised the total number of predicted zinc-binding proteins in yeast to 582. We refer to this catalog of known or likely zinc-binding proteins as the "zinc proteome". Their number represents ~10% of the total yeast proteome and this is similar to the prevalence of zinc-binding proteins encoded by other eukaryotic genomes (1). In addition, 45 other proteins were identified that may bind zinc based on structural data but these proteins lacked published references to support that zinc is the native metal ion. Therefore, we were unable to assess the functional relevance of zinc binding by members of this group. While not included in the analysis of the zinc proteome described in this study, this list of additional potential zinc-binding proteins is included in **Table S2**.

The catalog of yeast zinc proteins is a useful tool to study the role of zinc in a eukaryotic cell. We examined the zinc proteome of yeast from a number of perspectives to characterize the diverse

functions, types of zinc binding, and subcellular distributions of these proteins. **Figure 1A-D** summarizes classifications of the predicted zinc proteome based on the number of genes in each category that encode those proteins. When classified by the general function of the zinc cofactor, the most abundant group of these genes encode proteins with structural zinc sites (70%) followed by proteins that bind zinc as a catalytic cofactor (18%) (**Fig. 1A**). Some genes, specifically members of the alcohol dehydrogenase family, encode proteins that bind two zincs with one serving a structural role and the other acting in catalysis; these comprise 2% of the total. The remainder encode zinc transport proteins (2%) and genes whose protein products met our search criteria but the function of their metal cofactor has not yet been determined (8%).

Focusing on the 116 genes encoding proteins for which zinc plays a catalytic role (including those having both catalytic and structural zinc sites), enzymes in all six general enzyme classes were found (**Fig. 1B**). The majority of these genes encode hydrolases with smaller numbers of the other classes represented. Similar distributions of genes in these enzyme classes has been found for the predicted zinc proteomes of other organisms (33). For proteins in which zinc plays structural roles, several commonly shared motifs were observed (**Fig. 1C**). These included the C_2H_2-like zinc fingers and Zn_2Cys_6 zinc fingers most often found in DNA-binding transcription factors (34). Additional structural zinc-binding motifs observed included zinc ribbons, treble clef motifs, and zinc necklace domains (35). Some proteins bind multiple zinc atoms and have more than one type of site.

While it has been long recognized that zinc-binding proteins are present in many different compartments, the distribution of specific proteins has not been determined for an entire zinc

proteome. Because previous studies have determined the subcellular distribution of the majority of yeast proteins (36, 37), we could assign subcellular locations to all but 8% of the predicted zinc proteome. The majority of zinc proteome genes (74%) encode nuclear and/or cytosolic proteins (**Fig. 1D**). Less common were genes encoding proteins found in the secretory pathway (ER, Golgi, endosome), mitochondria, vacuole, peroxisomes, plasma membrane, and cell wall.

Mass spectrometry analysis of the predicted zinc proteome in replete cells.

To estimate the absolute abundance of zinc-binding proteins in replete cells, quantitative label-free mass spectrometry was performed on total protein samples from cells grown to exponential phase under zinc-replete conditions (i.e. LZM supplemented with 100 μM $ZnCl_2$) (38, 39). The resulting peak intensities were converted to protein copy number per cell using the "Proteomic Ruler" method (40). Of the ~6000 total genes in yeast, we obtained copy number estimates of 2582 gene products in zinc-replete cells. The median coefficient of variation was 12% for each set of replicates demonstrating the high quality of the mass spectrometry data (**Fig. S1**). From these data, we estimated the total number of proteins per cell to be ~9.2 x 10^7, which is similar to estimates made using other methods (41, 42). Of the 582 proteins in the predicted zinc proteome, we estimated the copy number of 229 (39%). These proteins added up to 7.6 x 10^6 zinc-binding proteins per cell or ~8% of the total protein number. Those zinc proteins not detected in this analysis likely represent proteins of low abundance and therefore would not contribute greatly to this estimate of total zinc protein number. Abundance data for the full proteome are provided in **Table S3**.

In zinc-replete cells, the abundance of zinc proteins delineated by general functional classifications (**Fig. 1E**) was roughly similar to the distribution based on gene number. The majority of zinc protein molecules in a cell had structural sites followed by enzymes that use zinc for catalysis. The proteins with both catalytic and structural sites made up a much larger fraction of the total zinc protein abundance (17%) than reflected by their gene number (2%) due to the high level of alcohol dehydrogenases (Adh1, Adh3, etc.). An impact of the high abundance of alcohol dehydrogenases was also observed when grouping by enzyme class (**Fig. 1F**) with oxidoreductases (including the alcohol dehydrogenases) making up a much larger proportion of protein copy number (41%) than was observed based on gene number (11%). Similarly, lyase protein copy number was more abundant (38%) than their gene number (9%) largely due to the high abundance of the glycolytic enzyme aldolase (Fba1). While hydrolases are very numerous at the gene level, they were consistently of low abundance and accounted for only 9% of detectable proteins that use zinc as a catalytic cofactor.

Considering structural motifs, zinc ribbons were a large fraction primarily due to the high number of ribosomal subunits with this motif (**Fig. 1G**). The high abundance of alcohol dehydrogenases also had a large impact on the fraction of proteins with zinc necklace motifs. Also indicated by the data is the low relative abundance at the protein level of many other classes of zinc motifs. For example, many of the DNA-binding C_2H_2 and Zn_2Cys_6 zinc finger proteins were not detected by mass spectrometry suggesting their abundance is very low. Finally, when considering the subcellular distribution of zinc-binding proteins, the vast majority are found in the cytosol (**Fig. 1H**). While cytosolic zinc proteins represent only 17% of genes, 89% of zinc protein abundance is

cytosolic (not including the 2% of proteins with both nuclear and cytosolic distributions). The nucleus, mitochondria, and other compartments contain far lower levels of zinc-binding proteins.

The detectable zinc-binding proteins ranged from fewer than 10 to over 10^6 copies per cell. Most of these proteins were of relatively low abundance (<10,000 copies per cell) and only a few were of very high abundance (>100,000 copies per cell) (**Fig. 2A**). When these protein copy numbers were translated into number of zinc-binding sites based on their predicted stoichiometries of metal binding, it was clear that a small number of highly abundant proteins dominate the total zinc requirement of a replete cell (**Fig. 2B**). In fact, the twenty most abundant zinc proteins accounted for almost 90% of the total zinc requirement of the cell (**Fig. 2C**). These included Adh1 alcohol dehydrogenase, Fba1 aldolase, several zinc-binding ribosomal subunits, Sod1 superoxide dismutase, and Met6 methionine synthetase. Based on our analysis, the total number of zinc-binding sites in a replete cell was calculated to be 9×10^6. Notably, this number is very close to the experimentally determined minimum zinc quota of a yeast cell (3). Note that transporter proteins were not included in this estimate of zinc-binding sites because they only transiently interact with zinc. Unsurprisingly, neither Crs5 nor Cup1 metallothioneins were detected; these proteins are induced by copper treatment and are expressed at very low levels in untreated cells (43).

The response of the yeast proteome to zinc deficiency.

To determine the effects of zinc deficiency on the total proteome and specifically the zinc proteome of yeast, label-free quantitative proteomics was performed on total protein samples from cells transitioning from growth in zinc-replete to deficient conditions. Cells grown to exponential phase

in a zinc-replete medium (LZM + 100 μM $ZnCl_2$, i.e. the same cells sampled above) were transferred to a zinc-deficient medium (LZM + 1 μM $ZnCl_2$) and cells were harvested after 4, 8, 12, and 16 hours after that transition. These times correspond to approximately 2, 3, 4 and 5 generations of growth. LC-MS peak intensities were converted to protein copy number using the Proteomics Ruler method.

The time course data are also provided in **Table S3** and the effect of zinc deficiency on the total proteome is plotted in **Figure 3**. Cluster analysis was performed to identify cohorts of similarly affected proteins and four clusters were identified. Proteins not included in these four clusters did not share significantly enriched gene ontology (GO) terms. Clusters 1 and 2 consisted of proteins that decreased in abundance during zinc deficiency with cluster 1 showing a larger fold decrease. Cluster 3 increased during zinc deficiency while cluster 4 showed a small increase or no change. **Figure 3** displays some of the significant GO terms that were found for these clusters. A complete list of GO terms is available in **Table S4**. In cluster 1, down-regulated proteins were related to ribosomal proteins, ribosome biogenesis, and cytoplasmic translation. Cluster 2 included many terms found in cluster 1 including protein biosynthesis, ribosome biogenesis, translation, and also unfolded protein binding and chaperone proteins. These results suggest that zinc deficiency causes a systemic decrease in protein synthesis and protein chaperone capacity. Cluster 3 contains up-regulated proteins related to oxidation-reduction processes, mitochondrial function, and vesicle-mediated transport. Up-regulated proteins in cluster 4 are related to proteasome activity, actin binding, and glycolysis. Many of these changes may help mitigate the deficit of zinc.

Many of the effects of zinc deficiency on the total proteome are likely due to indirect consequences of metal status. To focus on responses that are directly controlled by zinc status, we examined the abundance of proteins known or hypothesized to be regulated by the Zap1 transcription factor. Based on several published studies, Zap1 is thought to regulate transcription of 87 genes in response to zinc deficiency (20, 44-49). For the majority of those genes, including the zinc transporters *ZRT1*, *ZRT3*, and *FET4*, Zap1 activation increases gene expression and protein abundance during zinc deficiency. For a small number of other target genes, Zap1 represses gene expression and thereby reduces protein accumulation during deficiency. Of the 87 known or predicted Zap1-regulated genes, protein abundance was measurable for 39 of their encoded proteins and the effect of zinc deficiency on their levels is depicted in **Figure 4**. For most Zap1 target genes, the abundance of their protein products increased in zinc deficiency, consistent with the action of Zap1 as a transcriptional activator. For some proteins, e.g. Ald3, Ctt1, Hsp26, and Adh4, the response to deficiency was immediate and strong. For other proteins, the response was much slower and/or of less dynamic range (e.g. Pep4 and Zrc1). In contrast, four proteins (Adh1, Adh3, Rad27, Hnt1) showed decreased protein abundance during the transition to deficiency. Adh1 and Adh3 were previously shown to be controlled by Zap1-regulated non-coding RNAs that repress promoter function (25). The mechanisms controlling Rad27 and Hnt1 are currently being studied. These varied results demonstrate the diversity of responses of the proteins encoded by genes regulated by Zap1.

The response of the predicted zinc proteome to zinc deficiency.

Of the 229 zinc-binding proteins that were measured in replete cells, 199 of those had sufficient data (measurements at T_0 and at least two subsequent time points) to assess the effects of zinc

deficiency on their abundance (**Table S3**). In addition, there were 13 zinc-binding proteins that were not detected at T_0 but were detected at two or more subsequent timepoints. Similarly, there were 30 zinc-binding proteins detectable at T_0 that were not detected at later time points suggesting a marked loss of protein abundance. As shown in **Figure 5**, of the proteins in the predicted zinc proteome that were detected by mass spectrometry, many more proteins decreased in abundance during the transition from zinc-replete to deficient conditions than increased. Using a fold change of 1.5 or greater and a false discovery rate of 0.05, we found 31 proteins that increased in abundance and more than twice that number of proteins (68) that decreased in response to zinc deficiency. Among those proteins that increased in abundance were several zinc transport proteins (Zrt1, Fet4, Zrt3, Zrc1, Zps1) that are regulated by Zap1. The level of the Msc2 zinc transporter of the endoplasmic reticulum, while not Zap1 regulated (50), also increased in zinc-deficient cells. Also among the increasing proteins was the Adh4 alcohol dehydrogenase, which is activated by Zap1 to likely replace the lost activity of the repressed Adh1 and Adh3 proteins. In addition, many proteins involved in chromatin modification (e.g. Rpd3, Hda1, Hst2, Set3, Gis1, Rsc3), components of the basal transcription machinery (e.g. Sua7, Brf1, Tfa1, Rpb9), and numerous proteases (e.g. Ape2, Ape3, Dpp3, Rpn11) increased in abundance in response to zinc deficiency. Furthermore, the gag-pol fusion proteins of transposable elements Ty1 and Ty2 increased. Increased levels of these Ty-encoded proteins have been observed under other stress conditions (51-53).

Many more zinc-binding proteins that we detected decreased in abundance during deficiency. These included zinc-binding ribosomal subunits and several ribosome biogenesis proteins (e.g. Bud20, Nmd3, Reh1), general translation factors (e.g. Tif5, Tif35, Sui3), tRNA synthetases and

tRNA modifying proteins (e.g. Ths1, Mes1, Dus3), several RNA polymerase subunits and general transcription factors (e.g. Rpa12, Rpa135, Rpa190, Pri1, Taf1) and six alcohol dehydrogenases (Adh1, Adh3, Adh5, Adh6, Bdh1, Sfa1). The effect of zinc deficiency on the abundance of several specific examples is shown in **Figure 6**. To determine if any of the observed changes in protein abundance were the result, at least in part, of altered transcription, we performed quantitative RT-PCR analysis of mRNA levels of 28 of the affected proteins in replete cells and in cells after 8 and 16 h of zinc deficiency. Those data are shown for specific examples in **Figure 6** and the full results are reported in **Table 1**. For 16 of the tested proteins, their decreased abundance during deficiency had some element of transcriptional control ($p < 0.05$). For example, the effect of Zap1 on *ADH1* and *ADH3* expression in zinc deficiency were observed in the RT-PCR results (**Fig. 6**). Our analysis also suggested that the decreases of Adh5, Adh6, and Bdh1 alcohol dehydrogenases also occur at least in part at the transcriptional level.

In contrast, the mRNA encoding 12 of the proteins that decrease in zinc-deficient cells did not decrease during this transition. For example, *RPA190* mRNA was not reduced despite a large decrease in protein (**Fig. 6**). This result is consistent with previous studies showing that Rpa190 is targeted for degradation specifically under zinc-deficient conditions (28). Other examples of post-transcriptional effects newly identified in this analysis are Map1, Bud20, and Ydj1. These data indicated that there is a transcriptional component to the decreased accumulation of many, but not all, zinc proteins during the transition to zinc deficiency.

Estimates of in vivo zinc-binding site number and zinc content suggest significant deficits in zinc metalation during deficiency.

One purpose of the widespread decrease in zinc-binding proteins during deficiency may be zinc sparing, i.e. the regulated decrease in the zinc requirement of the cell. **Figure 7A** shows the relative zinc-sparing effects for zinc-binding proteins grouped by their general function. Decreases in ribosome subunits and ribosomal biogenesis factors and decreases in alcohol dehydrogenase abundance reduce the zinc requirement to the greatest degree while other functional groups contribute to a lesser extent. The hypothesis of targeted zinc sparing suggested that the decrease in zinc proteins is significantly greater than the effects observed for the total proteome. During the transition to zinc deficiency, the total proteome decreased 24% from 9.2 x 10^7 copies per cell to 7.0 x 10^7 copies (**Fig. 7B**). Similarly, the copy number of non-zinc proteins also decreased 24% from 8.4 x 10^7 copies per cell to 6.5 x 10^7. These decreases may reflect the decreased translation capacity of zinc-deficient cells (**Fig. 3**) and/or the results of autophagic degradation, which was previously shown to be induced by zinc deficiency (54-56). In contrast, the effect of zinc deficiency on the zinc proteome was even more striking with protein copy number dropping from 7.5 x 10^6 to 4.5 x 10^6 copies per cell (39%). While regulation of specific zinc proteins during the transition to deficiency may occur for many reasons, these data suggest that widespread zinc-sparing mechanisms are at work to specifically decrease the zinc demand of a cell during deficiency.

Factoring in their predicted stoichiometries of zinc binding, the abundance of zinc proteins in replete cells translates into 9 x 10^6 zinc-binding sites on proteins per cell (**Fig. 7C**). By 16 h after the transition to zinc deficiency, the number of zinc sites decreased to 4.7 x 10^6 sites. Thus, the zinc requirement was found to drop after 16 h of zinc deficiency by over 4 x 10^6 zinc sites per cell

or ~45% of the sites found in replete cells. To determine the amount of zinc available in deficient cells to meet this demand, zinc abundance was determined using ICP-AES. Total zinc in replete cells grown under these conditions was measured to be 2.3 x 10^7 atoms per cell (**Fig. 7C**). This value is approximately twice the estimated number of zinc-binding sites on proteins. By 16 h of zinc deficiency, zinc levels dropped to only 1.7 x 10^6 atoms per cell, i.e. ~30% of the estimated number of zinc-binding sites on proteins. These results suggested that despite the large decrease in zinc protein number described above, a zinc-deficient cell grown under these conditions accumulates a very high level of apoproteins or, alternatively, zinc proteins that are mismetalated with some other cation.

Analyses of zinc-binding proteins indicate reduced zinc metalation during deficiency.

To assess to what degree zinc metalation is disrupted during deficiency, we focused our analysis on the Fba1 aldolase protein. This glycolytic enzyme is the second most abundant protein in the zinc proteome of replete cells (**Fig. 2**) and the most abundant zinc protein in deficient cells. Fba1 levels were similar in replete and deficient cells with approximately 1.1 x 10^6 copies per cell. Thus, the zinc requirement of this enzyme alone is over half of the entire zinc content of a deficient cell. Given these factors, we hypothesized that most Fba1 molecules are either unmetalated or mismetalated during zinc deficiency. To test this hypothesis, we used an enzymatic assay of aldolase activity in permeabilized cells. We confirmed the specificity of the assay for Fba1 aldolase activity using zinc-replete wild-type cells and *fba1*^{DAmP} mutant cells that have lower *FBA1* expression (57). Immunoblots indicated that the *fba1*^{DAmP} strain accumulated ~25% of the wild-type level of protein and the measured enzyme activity showed a similar decrease (**Fig. 8A**). *FBA1* is essential for viability so a null allele could not be used for this experiment.

To determine the effect of zinc status on Fba1 function, aldolase specific activity normalized to Fba1 protein levels as determined by immunoblotting, was measured in cells after growth in zinc-replete and deficient conditions (**Fig. 8B**). Aldolase specific activity was high in zinc-replete cells and greatly reduced in deficient cells. These results were consistent with our hypothesis of reduced zinc metalation during deficiency. To further test this hypothesis, we determined whether zinc added back in vitro restored aldolase activity. EDTA treatment of permeabilized zinc-replete cells reduced aldolase activity and zinc subsequently added back restored activity to the full activity of untreated cells (**Fig. 8C**). In contrast, zinc addition to EDTA-stripped deficient cells for 5, 15, or 30 minutes did not restore activity to replete levels. These data suggest that zinc-deficient cells contain a pool of inactive aldolase that cannot be metalated efficiently with zinc. This conclusion was further supported by analysis of Fba1 activity following zinc addition in vivo. When zinc-deficient cells were supplemented with zinc in vivo prior to permeabilization, much of the missing Fba1-normalized activity was recovered after 1 h of zinc treatment and ~80% of full activity was observed after 8 h (**Fig. 8D**). However, this restoration of activity was completely blocked when the translation inhibitor cycloheximide was added prior to zinc addition. These results suggested that the inactive Fba1 aldolase in zinc-deficient cells cannot be activated with zinc supplementation and new protein synthesis is required to restore full aldolase activity.

To assess the metalation state of aldolase in vivo, we adapted a method previously used to probe zinc binding by proteins in vitro (58-60). N-ethylmaleimide (NEM) is a cell-permeable reagent that alkylates free cysteine thiol groups in proteins. Reactivity of thiols with NEM is greatly reduced by metal binding to those residues or, for non-ligand cysteines, when the thiol group is

inaccessible to solvent. Thus, reactivity to NEM can be used to assess both zinc binding to cysteine ligands and zinc-dependent conformation changes that affect the accessibility of non-ligand cysteines. In our modified procedure, cells growing in culture are treated with NEM to modify reactive cysteine thiols in vivo, lysed, proteins denatured, and then treated with PEG-maleimide, which modifies unreacted thiols that had been protected from in vivo NEM modification. Thiols alkylated by NEM are no longer reactive to PEG-maleimide whereas sites that were not alkylated become modified with the PEG reagent. While NEM modification only slightly alters protein molecular mass and is not detectable by immunoblotting, PEG-maleimide modification increases the apparent molecular mass on SDS-PAGE by ~15 kDa per moiety and is therefore readily detected by immunoblotting. Thiols that are oxidized in vivo are also not modified by NEM; these can be identified as being protected from NEM modification in vivo, reactive to PEG-maleimide in vitro following DTT treatment, but not reactive with PEG-maleimide without pre-treatment with reductant.

Fba1 contains five cysteine residues. While none of these are directly involved in zinc binding, we found that their accessibility to modification by NEM is altered by zinc status. Without modification, Fba1 tagged with the hemagglutinin antigen epitope (Fba1-3xHA) migrates at ~40 kDa on SDS-PAGE (**Fig. 9A**). When treated with PEG-maleimide alone following denaturation, the Fba1-HA protein shifts in mobility to ~115 kDa, corresponding to the addition of five PEG moieties. When zinc-replete cells were treated with NEM in vivo prior to PEG-maleimide treatment in vitro, 1-4 cysteines were protected from NEM reaction to varying degrees with most copies having two NEM-resistant cysteines. In zinc-deficient cells, NEM sensitivity increased as indicated by the decreased abundance of 2-4 x PEG-modified forms and increased abundance of

proteins with 0-1 x PEG moieties added. This result indicates a zinc-dependent conformational change in vivo that changes the sensitivity of one or more cysteines to NEM. The effect on NEM sensitivity was observed both with and without DTT treatment confirming that protection in vivo was not due to thiol oxidation. To quantify these effects, band intensities were measured and the ratio of 0-1 x PEG-modified forms vs. 2-4 x PEG-modified forms was determined (**Fig. 9B**). This analysis demonstrated higher levels of PEG modification (i.e. NEM resistance) in replete cells and lower levels (i.e. NEM sensitivity) in deficient cells. In contrast, no effect of zinc was observed on the NEM sensitivity of the single cysteine in Pgk1; this cysteine is protected from NEM modification in vivo due to solvent inaccessibility but is modified with PEG-maleimide following protein denaturation (**Fig. 9A**). Modification of Pgk1 with PEG-maleimide is highly efficient and provides a positive control for this reaction.

To assess whether the observed conformational change observed for the wild-type Fba1-3xHA protein was due to zinc binding in vivo, we mutated the histidine zinc ligand at position 111 to alanine (H111A). No zinc-responsive changes in NEM reactivity were then observed (**Fig. 9C**). A similar analysis of a mutation in glutamate 183 (E183A) supported this conclusion. The E183A mutation disrupts enzyme activity without affecting metal binding. Despite its lack of activity, the same zinc-dependent conformational change observed for the wild type protein was seen with this mutant **Fig. 9D**). To further confirm that the observed conformational changes were due to the presence or absence of zinc binding, we performed the experiment in permeabilized replete cells using stripped and re-metalated Fba1-3xHA. Without EDTA stripping, PEG-maleimide reactivity was high indicating NEM resistance (**Fig. 9E**). When Fba1-3xHA was stripped of metal with EDTA treatment, NEM resistance was reduced and re-addition of zinc restored protection from

NEM modification. These effects are quantitated in **Figure 9F** and the reciprocal effect of EDTA and zinc on Fba1 enzyme activity is shown. Again, no effect of EDTA or zinc treatment was observed on the PEG sensitivity of Pgk1. These results support the conclusion that the change in NEM sensitivity is directly due to zinc binding in the Fba1 active site.

To test whether the in vivo dependence of Fba1 reactivation on protein synthesis (**Fig. 8**) was due to slow re-metalation with zinc, we used the NEM/PEG-maleimide method. Cells were grown in zinc-replete and deficient conditions. The deficient cells were then resupplied with zinc for 1 or 8 h in the presence or absence of cycloheximide. In vivo NEM treatment was carried out prior to zinc addition and at subsequent timepoints and the cells were then processed for PEG-maleimide modification. In the absence of cycloheximide, full re-metalation was apparent after 1 h of zinc treatment (**Fig. 9G**). Surprisingly, apparent re-metalation was also detected in cycloheximide-treated cells after 1 h and 8 h despite the absence of increased activity. These results suggest that while a substantial fraction of Fba1 protein is not metalated in zinc-deficient cells, it is re-metalated rapidly in vivo and some other factor limits its activity. We hypothesize that the protein may be damaged or modified in some way.

Our analysis of Fba1 identified a zinc-responsive conformational change that affects the accessibility of non-ligand cysteines to NEM modification. To test for effects of zinc status specifically on zinc-binding cysteine ligands in a protein, we tested the in vivo NEM sensitivity of Met6 methionine synthetase. Met6 accumulates to ~145,000 molecules per cell in zinc-replete cells and ~87,000 in deficient cells. Fungal methionine synthetases contain three cysteine residues, two of which (C657 and C737) are homologous to the highly conserved residues Cys659 and

Cys739 shown to bind zinc in the *C. albicans* Met6 protein (61). NEM treatment of zinc-replete cells followed by in vitro treatment with PEG-maleimide demonstrated protection of 1, 2, or 3 cysteines, with most Met6 proteins having three protected cysteines (**Fig. 10A**). Under zinc-deficient conditions, most proteins had only one protected cysteine. This result is consistent with zinc binding protecting the two cysteine ligands while the third thiol is constitutively protected in vivo. Omitting the in vitro DTT reduction step had little effect on the pattern of bands detected indicating that the protective effect of zinc was not conferred by Met6 cysteine oxidation.

This conclusion was supported by the analysis of a mutation that disrupts one of the non-cysteine zinc ligands in the metal site. *S. cerevisiae* His 655 is homologous to H657 of the *C. albicans* and *S. pombe* Met6 proteins, which was identified as zinc binding by structural analysis (62, 63). An H655A mutation resulted in constitutive NEM sensitivity (**Fig. 10B**). In contrast, a mutation in Asp 612 (D612A, homologous to Asp614 in *S. pombe*), which inactivates Met6 by disrupting homocysteine binding (63) had no effect on cysteine sensitivity to NEM in replete conditions, indicating unaltered zinc binding. In deficient conditions, the D612A mutant showed increased NEM protection when compared with the wild-type, suggesting that substrate binding affects zinc lability. Overall however, these observations indicate that the effect of the zinc ligand mutation on NEM sensitivity was not due simply to loss of enzyme activity but reflected a loss of zinc from the active site. Our results are consistent with Met6 accumulating in a zinc-metalated form in replete cells and is only partially metalated in deficient cells.

DISCUSSION

In this report, we cataloged the zinc proteome of yeast, and determined the abundance of many of its proteins, their response to zinc deficiency, and estimated the metalation state of those proteins in zinc-replete and deficient cells. This analysis has provided unprecedented insights into the cellular economy of zinc under replete and deficient conditions. The majority of zinc proteins in yeast bind zinc as a structural cofactor and includes proteins with C_2H_2 zinc fingers, Zn_2C_6 zinc fingers, zinc ribbon domains, and other motifs. These proteins play key roles in gene regulation, transcription, translation, protein degradation, and many other functions. The zinc proteome also plays many catalytic roles and includes enzymes in all six general classes of enzymes. The catalog of the yeast zinc proteome we generated illustrates the diversity of function of this essential cofactor within a eukaryotic cell. We recognize, however, that this is likely not a perfect list of all zinc proteins in yeast. Zinc may play regulatory roles as a second messenger to control different aspects of cell physiology (64, 65). Given that such regulatory sites are probably of lower affinity and greater lability, they may not have been identified in our analysis of stable motifs and domains. Second, some enzymes (i.e. "cambialistic" proteins) are functional with different metal cofactors and the specific metals that metalate those enzymes likely depend on the cellular conditions of metal homeostasis and other factors (66). Thus, to refer to such proteins as "zinc proteins" may not accurately reflect their cofactor requirements. Despite these caveats, however, the catalog of predicted zinc-binding proteins in yeast provides an essential tool for future studies of zinc function, trafficking, and homeostasis.

Using mass spectrometry we measured the abundance of almost half of the entire yeast proteome. Focusing on the zinc proteome, this analysis indicated the existence of 9×10^6 total zinc sites in replete cells. This proteomics-based estimate is remarkably similar to our experimentally

determined measurement of the vacuolar and non-vacuolar pools of zinc under these same growth conditions (3). Cells grown in LZM supplemented with 100 μM $ZnCl_2$ contain 2.3 x 10^7 zinc atoms per cell. When the Zrc1 and Cot1 vacuolar zinc transporters were mutated so that zinc could no longer be stored in the vacuole, the accumulation of zinc in the cell dropped to ~1 x 10^7 zinc atoms per cell. This result indicated that ~60% of the total zinc in a replete cell grown under these conditions is stored in the vacuole. Because labile zinc levels in cells are known to be very low, it is likely that the non-vacuolar zinc atoms are bound by proteins and this conclusion is very consistent with the number of zinc sites we found in these cells using proteomics. Our previous studies also established that the minimum zinc quota of a yeast cell was ~1 x 10^7 zinc atoms per cell. This comparison suggests that the zinc proteome abundance of a replete cell is tuned for optimal growth and even slight deficits that decrease full metalation inhibits cell growth. One caveat to this analysis is that we were only able to measure the abundance of about half of the proteins that comprise the zinc proteome. The proteins missing from our analysis are likely to be of very low abundance and therefore may contribute little to our calculations of the cellular zinc requirement. A result very different from ours was obtained from a similar study of the Gram-negative bacterium *Cupriavidus metallodurans* where it was found that replete cells contain a large excess of zinc-binding sites relative to the minimum zinc quota (67). A high number of zinc sites may add to zinc resistance of this bacterium by serving as a sink for excess metal. Organisms such as *S. cerevisiae* are not adapted to high zinc levels and we suspect it is more indicative of what occurs in most other organisms. A viable alternative hypothesis is that *C. metallodurans* has an excess of zinc sites to serve as a storage pool of the metal in the absence of intracellular organelles.

The total proteome and the zinc proteome of replete cells changes markedly during the transition to deficient conditions. Among the zinc proteins that increased in abundance were several transporter proteins induced by Zap1 to maintain zinc homeostasis. We also observed increased levels of several proteins involved in transcription and chromatin modification. These changes may represent compensatory regulatory responses to loss of these activities due to reduced metalation. The increased abundance of these zinc proteins was more than offset by the decreased abundance of many other zinc proteins such that the net effect was a decrease in the total zinc requirement of the cell by ~45%. We had anticipated that proteasome-mediated degradation of apoproteins may be a common effect during the transition to zinc deficiency and there are some potential cases of this in our results. For example, Map1 aminopeptidase levels drop dramatically in zinc-deficient cells with no detectable change in mRNA abundance. In addition, macroautophagy is induced during zinc deficiency and this process may decrease protein abundance more generally (54-56). However, it is clear that changes in mRNA levels play at least some role in the down-regulation of numerous zinc proteins. While these regulatory effects may occur for many reasons, we hypothesize that a common purpose is to reduce the zinc requirement of the cell, i.e. zinc sparing.

One specific group of proteins that had a great impact on the cellular zinc requirement are the alcohol dehydrogenases. There are 13 different zinc-dependent alcohol dehydrogenases in yeast and we could measure the abundance of seven, Adh1, Adh3, Adh4, Adh5, Adh6, Bdh1, and Sfa1. All but Adh4 decrease in zinc-deficient cells for a net decrease in the zinc requirement of ~9 x 10^5 zinc atoms per cell. As mentioned above, Adh4 is induced and Adh1 and Adh3 are repressed by Zap1 (25). How are the other four Adh enzymes shut off in response to zinc deficiency? A clue

for how Adh6 is regulated comes from our recent analysis of transcription start sites in the yeast genome. Loss of *ADH6* gene expression coincides with the induction of an antisense transcript that initiates downstream of the *ADH6* open reading frame (50). While we have not mapped the 3' end of this antisense transcript, it may pass through the open reading frame and *ADH6* promoter and thereby interfere with *ADH6* transcription. This antisense transcript is likely to be Zap1-dependent because there is a consensus Zap1 binding site, 5'-ACCTTAAAGGT-3', located ~130 bp upstream of where the antisense RNA initiates transcription. Notably, a similar mechanism of antisense regulation was discovered controlling the *ADH1* gene of *S. pombe* in response to zinc (68). While *ADH5* and *BDH1* also show decreased mRNA abundance, we have no clues as yet of how that occurs. While we have not directly examined *SFA1* mRNA levels, it was not detected as zinc regulated in previous transcriptome studies (20, 44). These observations suggest that Sfa1 protein levels decrease due to a post-transcriptional mechanism.

The broad effect of zinc deficiency on the abundance of proteins that comprise the translational machinery of the cell is also striking. Several zinc-dependent ribosomal subunits are decreased in expression. In addition, zinc-binding proteins of the ribosome biogenesis (RiBi) regulon, including ribosome biogenesis factors, translation initiation factors, and tRNA synthetases and modifying enzymes, also decrease (69). Summing all of these proteins, the estimated number of zinc-binding sites drops in deficiency by ~2.2 x 10^6 zinc atoms per cell. This collectively represents about half of the zinc sparing that we observed across the entire zinc proteome. This effect extends far beyond the zinc-dependent proteins and includes a large number of zinc-independent translation machinery proteins as well (**Fig. 3**). It has been previously shown that expression of ribosomal proteins and the RiBi regulon is controlled in response to growth rate such that slower growing

cells have reduced levels of these proteins than do faster growing cells (69, 70). Given that zinc deficiency results in slower growth, the underlying mechanisms linking growth rate to gene expression likely plays some role in their decreased abundance we observed in our studies.

An additional mechanism regulating the translational machinery in response to zinc deficiency is suggested by the studies from Chanfreau and colleagues who showed that RNAPI is specifically targeted for degradation during zinc deficiency (28). Decreased RNAPI levels decrease 5.8S, 18S, and 25S rRNA synthesis, which would then trigger decreased ribosomal protein and RiBi regulon expression. It was previously suggested that targeted degradation of RNAPI was a zinc sparing response because of the zinc no longer required for this specific RNA polymerase complex. Based on our results, we estimate that the number of zinc atoms that are directly spared by degrading the five zinc-binding RNAPI subunits would be ~30,000 total. While not an insignificant amount, it represents only about 1% of the total zinc sparing that we observed. Mutant cells defective for RNAPI degradation are hypersensitive to EDTA, suggesting a greater disruption in zinc homeostasis than is expected from the level of zinc sparing provided by degrading this protein complex alone. Therefore, we suggest that the effect of RNAPI degradation on zinc sparing may be much more extensive because of the resulting effects on the expression of ribosomal subunits and the RiBi regulon. In other words, zinc-responsive RNAPI degradation may be the master switch that controls the bulk of the zinc sparing response in zinc-deficient cells.

Despite the massive decrease in the number of zinc proteins that occurs during deficiency, we found that the number of zinc atoms that cells accumulated under these conditions was not sufficient to metalate even the reduced zinc requirement. In fact, we estimated that 70% of the zinc

sites on proteins in a zinc-deficient cell were either not metalated (i.e. apoproteins) or mismetalated with a different cation. There is some question about how many potential zinc-binding ribosomal subunits in eukaryotes actually bind zinc in vivo (71). Nonetheless, if those proteins are removed from our calculations, the level of zinc atoms per cell are still insufficient for full metalation. Our previous studies of Tsa1 suggested that this protein's chaperone function was critical to tolerate this stress and that zinc apoproteins are the likely clients of Tsa1 (23). We tested the hypothesis of accumulated apoproteins for two abundant zinc proteins, Fba1 and Met6. Despite little change in protein levels, Fba1 enzyme activity was greatly reduced in zinc-deficient cells compared to replete cells. In addition, using a novel application of thiol-reactive agents to study in vivo metalation, we found that Fba1 in cells underwent a conformational change that was dependent on zinc availability and zinc ligands. These results suggested that Fba1 is not fully metalated in zinc-deficient cells. It was therefore surprising that reintroduction of zinc appeared to rapidly metalate the protein but did not restore enzyme activity to replete levels and new protein synthesis was required to restore full activity. It is conceivable that the Fba1 protein is somehow damaged or modified (e.g. by phosphorylation) in zinc-deficient cells such that new Fba1 protein is required to restore activity. One possible mechanism of damage is glycation which has been previously observed for yeast Fba1 (72). Our studies of Met6 also indicated the accumulation of apoproteins during zinc deficiency. For Met6, we could probe reactivity of the cysteine ligands involved in direct zinc binding. These studies suggested that the many Met6 molecules in a cell are also unmetalated. It is conceivable that Fba1 and/or Met6 are mismetalated but if so, binding of that other cation fails to produce the same conformational change as zinc does for Fba1 and fails to protect the bound ligand from reaction with NEM in Met6. It was also surprising that many chaperones, co-chaperones, and chaperonin proteins (e.g. Ssa2, Ydj1, Scj1, Cct2) decreased in

abundance during zinc deficiency (**Fig. 3**, cluster 2) when our other results indicated an increase in apoprotein accumulation and unfolded protein stress. We note that many of the proteins that decreased in abundance during deficiency are "foldase"-type chaperones while Tsa1 is a "holdase"-type protein. These results make biological sense because apoproteins cannot be fully folded without resupply of their metal cofactor and foldase chaperones would not suffice.

CONCLUSIONS

In this report, we have cataloged the zinc proteome of yeast and determined the effects of zinc deficiency on the abundance of these proteins. This analysis highlighted the diverse functions of zinc proteins and mapped in detail the subcellular requirement of this essential metal nutrient. Our studies demonstrated that the majority of zinc proteins detected decrease in abundance during deficiency and this apparent zinc-sparing response is due at least in part to transcriptional regulation of many of their respective genes. Our results also indicated that a surprisingly high number of zinc sites are not metalated with zinc during deficiency. Future studies will address the role of Tsa1 as a chaperone of these abundant zinc apoproteins. Future studies will also address the prevalence of zinc apoproteins more broadly and determine whether all proteins are similarly affected by zinc deficiency or whether some proteins can compete for zinc better than others. It will be exciting to learn whether prioritization of zinc distribution occurs in zinc trafficking among apoproteins.

EXPERIMENTAL METHODS

Strains and growth conditions- Yeast were grown in rich (YPD), synthetic defined (SD), or low zinc medium (LZM), as previously described (73). LZM contains 20 mM citrate and 1 mM EDTA to buffer pH and zinc availability. Glucose (2%) was the carbon source for all experiments. LZM + 1 μM ZnCl2 was routinely used as the zinc-deficient condition, and LZM + 100 μM ZnCl2 as the replete condition. The yeast strains used in this work were BY4743 (MATa/MATα his3/his3 leu2/leu2 ura3/ura3 lys2/LYS2 met15/MET15), BY4742 (MATa his3 leu2 ura3 lys2), BY4741 (MATα his3 leu2 ura3 met15), and BY4741 fba1DAmP (Thermo Fisher Scientific) (57).

Cataloging the zinc proteome of yeast- Using the approach described in Valasatava et al. (74), we created two libraries of Hidden Markov Model profiles (75): a library of zinc-binding Pfam domains (76), and a library of zinc-binding structural motifs. The Pfam domain library was created by merging two lists: first, a list of Pfam domains with known 3D structure that contain a zinc-binding site extracted from MetalPDB (77) in which each of these domains could be associated with the residues responsible for zinc binding and with their positions within the domain sequence and second, a list of Pfam domains without a known 3D structure but annotated as zinc-binding obtained by text mining of the annotations in the Pfam database. The procedure resulted in a set of 573 Pfam domains: 541 with an associated zinc-containing 3D structure, and an additional 32 annotated as zinc-binding domains. The library of zinc-binding structural motifs was created by splitting into fragments the zinc-binding sites stored in MetalPDB as of June 2017, as described in Rosato et al. (35). Only one representative was kept for zinc-binding sites that, though found in different PDB structures, fall in the same position of the same protein domain. Sites that are not physiologically relevant based on literature inspection (e.g., zinc-substituted structures, spurious sites) were manually removed from the dataset. This procedure resulted in a library of 6450 zinc-

binding motifs derived from 2651 zinc-binding sites. An additional library of 339 zinc-binding motifs was compiled separately because the native metal ion of their corresponding proteins is still under investigation.

The zinc proteome of yeast was obtained by using the hmmscan tool (75) to search each yeast sequence for the profiles contained in the two libraries. A yeast sequence was identified as a potential zinc-binding site if at least one of the following conditions was verified: A) The profiles of all the fragments of a given site matched the sequence with an e-value lower than 10−3 and the corresponding ligands are conserved in the sequence. B) The profile of a domain with associated ligands matched the sequence with an e-value lower than 10−5 and the ligands are conserved in the sequence. C) The profile of a domain with no associated ligands matched the sequence with an e-value lower than 10−7. These predictions were integrated by adding the proteins annotated as zinc-binding in the UniProt database (78). In total, 571 yeast proteins were identified as zinc binding using the 6450 motifs (Table S1). An additional set of 45 potential zinc-binding proteins were identified with the 339 input sites as able to bind zinc but for which the identity of the native metal ion is still unknown (Table S2). For each of these proteins, the subcellular location and enzyme EC number were retrieved from UniProt. For each site contained in these proteins, the information on zinc function, number of zinc ions per monomer, and structural zinc-site classification (34) was imported from the site in the library that yielded the best match in the search, and then manually checked.

Mass spectrometry analysis and protein copy number estimations- Mass spectrometry for proteomics analysis was performed on four biological replicates each for times 0, 4, 8, and 12 h of

zinc deficiency and three biological replicates for 16 h of deficiency. Frozen cell pellets of various cell counts were lysed in 300 µl cold methanol. Precipitated proteins were separated by centrifugation for 10 minutes at 13,400 x g and 4°C. The protein pellet was resuspended in 200 µl lysis buffer (8 M urea, 20 mM TCEP, 80 mM chloroacetamide, 100 mM Tris pH 8) and diluted with 1 ml 100 mM Tris pH 8. Protein digestion was performed overnight with trypsin (4 µg) before centrifuging for 5 minutes at 10,000 x g. The resulting supernatant was de-salted with Strata C18 solid phase extraction cartridges and quantified using Pierce Quantitative Colorimetric Peptide Assay (Thermo Fisher Scientific). Peptides were then dried in a vacuum centrifuge before resuspension in 0.2% formic acid.

Samples were analyzed using a LC/MS instrument comprising an Orbitrap Fusion Lumos tribrid mass spectrometer (Thermo Fisher Scientific). Mobile phase A consisted of 0.2% formic acid in water and mobile phase B consisted of 0.2% formic acid in acetonitrile. A 75-minute gradient ranging from 0% to 50% B was used spanning a total runtime of 90 minutes. Analytes were injected onto a 1.7-micron C18 column packed in-house to a length of 35 cm and heated to 60°C. Survey scans of peptide precursors were collected from 350-1350 Th with an AGC target of 1,000,000 and a resolution of 60,000 in the orbitrap followed by HCD MS/MS turbo scans taken in the ion trap.

The resulting LC-MS proteomic data were processed using Maxquant software version 1.5.2.8 and searched against a Saccharomyces cerevisiae database downloaded from Uniprot on 8/10/16. The digestion enzyme was set to trypsin with up to two missed cleavages, carbamidomethylation of cysteines as a fixed modification, and oxidation of methionines and protein N-terminal acetylation

as variable modifications. The match between runs feature was utilized to decrease missing data values within the data set. Precursor mass tolerance was 20 ppm and product ions were searched at 4.5 ppm tolerances. Peptides were filtered to a 1% FDR and combined to protein groups based on the rules of parsimony. Protein copy number calculations were performed in Perseus using the Proteomic Ruler plugin (40). This method uses the peak intensities of histone proteins, which are proportional to DNA content, to estimate protein abundance on a per cell basis. Statistically significant effects were defined as those proteins with 1.5-fold or greater changes and a p-value of <0.05 after Benjamini-Hochberg correction. The proteomics data was deposited in CHORUS (https://chorusproject.org) under Project ID number 1530. Hierarchical cluster was performed using Euclidean distance with Perseus (79). Gene Ontology analysis of four clusters produced from hierarchical clustering was performed using DAVID (80).

Quantitative RT-PCR analysis- Quantitative analysis of gene expression by RT-PCR was performed as previously described (81). Assays were performed on three biological replicates. The sequences of the primer pairs used are provided in Table S5. Gene expression was calculated relative to the average Ct values for three control genes (TAF10, ACT1 and CMD1) selected from multiple candidate genes tested for their highly stable expression under the conditions used in our experiments (data not shown).

ICP-AES analysis- Culture aliquots were washed three times in cold water, pelleted, and frozen in liquid nitrogen. Total zinc was determined using inductively-coupled plasma atomic emission spectrometry (ICP-AES) on six biological replicates for each timepoint. Cell pellets were desiccated by incubation at 60°C for 12-18 h and subsequent dry weights recorded. The dried yeast

pellets were acid digested in 250 µl OmniTrace 70% HNO3 (EMD Chemicals) at 60°C for 12-18 h with 150-200 rpm orbital shaking. The acid lysates were then diluted to 5% HNO3 with OmniTrace water (EMD Chemicals) and analyzed by ICP-AES (5100 SVDV, Agilent Technologies). The ICP-AES instrument was calibrated using National Institute of Standards and Technology (NIST)-traceable elemental standards and validated using NIST-traceable 1577b bovine liver reference material. The detection range for zinc was 0.005-5 parts per million with inter-assay precision <10%. Cesium (50 ppm) was used for ionization suppression and yttrium (5 ppm) was used as an internal standard for all samples. All reagents and plasticware were certified or routinely tested for trace metal work. Zinc content was determined using native software (ICPExpert) and normalized to the cell number in each sample.

Protein extraction and immunoblotting- Yeast protein extracts were prepared for immunoblotting with a TCA extraction protocol as previously described (82). SDS-PAGE and immunoblotting was conducted using a Li-Cor Odyssey infrared dye detection system as previously described (82). Antibodies used were anti-HA (12CA5, Roche product 11583816001), anti-Fba1 (a gift from Dr. Magdalena Boguta) (83), and anti-Pgk1 (Abcam product 22C5D8, lot # GR166098). IR 680 dye-labeled secondary anti-mouse antibody (product 680LT, lot # C30605-02) was obtained from Li-Cor.

Assay of Fba1 aldolase activity- Fba1 enzyme activity was determined using either permeabilized yeast cells or cell lysates. An assay developed by Freire was modified for use with 96-well plates (84). After harvest, cells were washed once with equal volume of ice-cold deionized water containing 1 mM EDTA, twice with ice-cold deionized water, and resuspended in 0.1 M MES-

NaOH pH 6.5 buffer. Cell densities of each sample were normalized to A595 = 1.5, and 0.01% digitonin (w/v) was added to permeabilize the cells. After incubating at 30°C in a shaking water bath for 10 minutes, cells were placed on ice and then washed twice, resuspended with ice-cold 25 mM KH2PO4/K2HPO4 pH 7.4 buffer to a density of A595 = 0.5. A standard assay of aldolase activity contained 10 units of triose-phosphate isomerase (TPI), 4 units of glyceraldehyde 3-phosphate dehydrogenase (GAPDH) in a 25 mM KH2PO4/K2HPO4 pH 7.4 buffer containing 5 mM sodium arsenate, and 5 mM of NAD+ and 20 µl of permeabilized cells. The assay was started by adding 5 mM of the substrate, fructose 1,6-bisphosphate (FBP), and incubated at 30°C in a temperature-controlled plate reader. The absorbance at 340 mm of NADH generated by the assay was recorded at 1-minute intervals for up to 20 minutes. The recorded A340 values were graphed and the linear portion of the graph was used to calculate the rates of Fba1 aldolase activity using an NADH standard curve following normalization to the cell density (A600) in each reaction. Alternatively, some assays were conducted using 1-10 µg of protein lysate per reaction and activity was normalized to total protein level. Cell pellets were resuspended in 0.5 ml of 25 mM KH2PO4/K2HPO4 pH 7.4 buffer containing 1 mM PMSF and 1 x EDTA-free protease inhibitor mix (Roche) and transferred to 1.5 ml tubes. A 0.2 ml volume of glass beads was added and the cells disrupted by vortexing for 5 minutes at 4°C. The homogenate was centrifuged at 16,000 x g for 10 minutes at 4°C and the supernatant stored on ice. The protein concentration was determined using a Bio-Rad DC kit against a BSA standard. To determine specific activity of Fba1 (in nmol NADH/minute/µg Fba1 protein), A340 absorbance values were converted to NADH concentration using a standard curve and resulting activity values (nmol NADH/minute/µg total protein) were normalized to Fba1-HA protein level as determined by immunoblotting, taking into account the value for Fba1 abundance in zinc replete cells that we determined by mass spectrometry (i.e. 1%

of total protein). This normalization was not performed in cases where Fba1 abundance was known to be stable during the experiment (e.g. Figure 9F). For some experiments, zinc was stripped from Fba1 by treating permeabilized cells with 50 mM EDTA and 5 mM FBP in a 30°C shaking water bath for 30 minutes. The cells were then washed five times with ice-cold 25 mM KH2PO4/K2HPO4 buffer containing 1 μM EDTA to prevent any zinc remetalation. Zinc was added back to aliquots of stripped cells by treating with 20 μM ZnCl2 in 30°C shaking water bath for 5, 15, and 30 minutes. The cells were then washed three times with ice-cold 25 mM KH2PO4/K2HPO4 buffer containing 1 μM EDTA and resuspended at A595 = 0.5 for the assay.

Plasmid constructions- All plasmids were constructed by homologous recombination in yeast. Plasmids expressing Fba1 with a triple repeat of the hemagglutinin antigen (HA) epitope fused to the C-terminus were constructed by PCR-amplification of wild-type or mutant FBA1 promoter and coding sequence and fused to the HA tags and terminator of the low copy episomal plasmid YCp-ZRC1-HA digested with BamHI and EcoRI. To generate a wild-type tagged plasmid, a fragment was amplified with the oligonucleotides Fbacds-ha (5'-TAGCCCGCATAGTCAGGAACATCGTATGGGTATAAAGTGTTAGTGGTACGGAAAGT-3') and Fba1pr5' (5'-CACGACGTTGTAAAACGACGGCCAGTGAATTCTGACGCAAGCCCTAAGAA-3') and used to gap repair YCp-ZRC1-HA. To introduce the H265A mutation, a 5'-most fragment was generated using the oligonucleotides H-Arev (5'-TGGAATTCTTGGACAGTAGAACCGGAACCACCGGCGAAGACCAAGA-3') and Fba1pr5', and a 3' -most fragment with H-Acomp (5'- GGTGGTTCCGGTTCTACTGT-3') and Fbacds-ha. The two fragments were combined with gapped YCp-ZRC1-HA for yeast transformation. To

construct the H111A and E183A mutants, a PCR fragment was amplified from the corresponding mutant versions of pFL44L-FBA1 using the oligonucleotides Fba1pr5' and Fbacds-ha prior to gap repair. All plasmids were fully sequenced to verify the mutations. Functionality of the wild-type epitope-tagged plasmid was verified by complementation of aldolase enzyme activity when expressed in an fba1DAmP mutant strain (data not shown). Fba1-3xHA accumulated to a similar level as untagged Fba1 when both forms were coexpressed and detected with anti-Fba1, and the tagged protein had similar specific activity to untagged (data not shown), indicating that the epitope tags had no major effect on stability or function. The Met6-HA construct and inactivated mutant versions were constructed similarly to Fba1-HA using gap repair. The wild-type Met6 plasmid (YCpMet6-HA) was constructed by amplifying Met6 from BY4742 genomic DNA using met6cds3' (5'-CACGACGTTGTAAAACGACGGCCAGTGAATTCcacagccattcaactcag-3') and Met6cds3' (5-TAGCCCGCATAGTCAGGAACATCGTATGGGTAattcttgtattgttcacgga-3') primers, followed by gap repair of YCp-ZRC1-HA digested with EcoRI and BamHI. To construct the H655A mutant, a fragment containing the mutation was generated by PCR amplification of YCpMet6-HA using the oligonucleotides met65'-1 (5'-GGCTGACAAGGATTCTCT-3') and met6H-A3' (5'-CATCAGCATCCAAAGCCTTGATATGGTTTGGATCCAAGTCAGAGTAACAGAAAgcAG AGTGTATTTGAGTCTTGTT3'). This fragment was used to gap repair YCpMet6-HA digested with SacI and BamHI. To construct the D612A mutant, a fragment was amplified from YCpMet6-HA with the met65'-1 and met6DA3' (CTTCTCTTAAAGCTGGTTCAgCAACTTGGATAACCTTGATACCGGCAGCT) oligonucleotides, and a second fragment was amplified with the met6da5' (TATCCAAGTTGcTGAACCAGCTTTAAGAGAAGGTTTACCATTGAGAGAAGGTA) and

met6cds3' oligonucleotides. The two fragments were combined and used to gap repair YCpMet6-HA digested with SacI and BamHI. Wild-type and mutant plasmids were fully sequenced, and the effect of the mutations on activity was verified by complementation of the methionine auxotrophy of a met6 deletion mutant.

NEM/PEG maleimide analysis- To identify cysteine residues showing zinc-dependent reactivity with N-ethylmaleimide (NEM) in vivo, 5 ml cultures of yeast were grown in zinc-replete (LZM + 100 μM ZnCl2) or deficient (LZM + 1 μM ZnCl2) medium to log phase (A595 0.3-0.4) and harvested by centrifugation. Cells were washed twice with ice-cold 1 x PBS + 1 mM EDTA and resuspended in 5 ml PBS + 1 mM EDTA. A solution of 1 M NEM in 100% ethanol was added to 5 ml of cells to give a final concentration of 5 mM NEM. For a negative control, the same volume of 100% ethanol was added to an identical aliquot of cells. After 30 min incubation at 30° with shaking, the cultures were harvested by centrifugation and washed twice with 1 x PBS. Protein was extracted using the TCA method (23) and redissolved in buffer A (200 mM Tris base, 1% SDS, 1 mM EDTA). After measurement of protein concentration (DC protein assay, Bio-Rad), aliquots of protein were processed to modify cysteines with mPEG-5kDa (Sigma) as previously described (23). Briefly, aliquots of 500 μg protein were treated with 20 mM DTT for 10 min at 65°C to reduce disulfide bonds, then reprecipitated by adding 1/10 volume 100% TCA. Precipitated samples were centrifuged and washed twice with acetone to remove TCA, then redissolved in buffer B (100 mM Tris-Cl pH 7.4, 2% SDS, 1 mM EDTA) + 5 mM PEG-maleimide (mPEG). After overnight incubation at 30°C, 10-30 μg of each protein sample was analyzed by SDS-PAGE and immunoblotting to determine the degree of mPEG modification of cysteine residues. To determine the degree to which cysteines were normally oxidized in vivo (and thus

unavailable for reaction with NEM), some control samples were not treated with DTT prior to mPEG treatment.

REFERENCES

1. Andreini C, Banci L, Bertini I, Rosato A. Zinc through the three domains of life. J Proteome Res. 2006;5(11):3173-8.

2. Outten CE, O'Halloran TV. Femtomolar sensitivity of metalloregulatory proteins controlling zinc homeostasis. Science. 2001;292(5526):2488-92.

3. MacDiarmid CW, Gaither LA, Eide D. Zinc transporters that regulate vacuolar zinc storage in *Saccharomyces cerevisiae*. EMBO J. 2000;19(12):2845-55.

4. Palmiter RD, Findley SD. Cloning and functional characterization of a mammalian zinc transporter that confers resistance to zinc. EMBO J. 1995;14(4):639-49.

5. Suhy DA, Simon KD, Linzer DI, O'Halloran TV. Metallothionein is part of a zinc-scavenging mechanism for cell survival under conditions of extreme zinc deprivation. J Biol Chem. 1999;274(14):9183-92.

6. Dittmer PJ, Miranda JG, Gorski JA, Palmer AE. Genetically encoded sensors to elucidate spatial distribution of cellular zinc. J Biol Chem. 2009;284(24):16289-97.

7. Fierke CA, Thompson RB. Fluorescence-based biosensing of zinc using carbonic anhydrase. Biometals. 2001;14(3-4):205-22.

8. Vinkenborg JL, Koay MS, Merkx M. Fluorescent imaging of transition metal homeostasis using genetically encoded sensors. Curr Opin Chem Biol. 2010;14(2):231-7.

9. Chandrangsu P, Rensing C, Helmann JD. Metal homeostasis and resistance in bacteria. Nat Rev Microbiol. 2017;15(6):338-50.

10. Kambe T, Tsuji T, Hashimoto A, Itsumura N. the physiological, biochemical, and molecular roles of zinc transporters in zinc homeostasis and metabolism. Physiol Rev. 2015;95(3):749-84.

11. Krezel A, Maret W. The functions of metamorphic metallothioneins in zinc and copper metabolism. Int J Mol Sci. 2017;18(6).

12. Eide DJ. Homeostatic and adaptive responses to zinc deficiency in *Saccharomyces cerevisiae*. J Biol Chem. 2009;284(28):18565-9.

13. Merchant SS, Helmann JD. Elemental economy: microbial strategies for optimizing growth in the face of nutrient limitation. Adv Microbial Physiol. 2012;60:91-210.

14. Panina EM, Mironov AA, Gelfand MS. Comparative genomics of bacterial zinc regulons: enhanced ion transport, pathogenesis, and rearrangement of ribosomal proteins. Proc Natl Acad Sci USA. 2003;100(17):9912-7.

15. Nanamiya H, Akanuma G, Natori Y, Murayama R, Kosono S, Kudo T, et al. Zinc is a key factor in controlling alternation of two types of L31 protein in the *Bacillus subtilis* ribosome. Mol Microbiol. 2004;52(1):273-83.

16. Gabriel SE, Helmann JD. Contributions of Zur-controlled ribosomal proteins to growth under zinc starvation conditions. J Bact. 2009;191(19):6116-22.

17. Choi S, Bird AJ. Zinc'ing sensibly: controlling zinc homeostasis at the transcriptional level. Metallomics. 2014;6(7):1198-215.

18. Kersting MC, Carman GM. Regulation of the *Saccharomyces cerevisiae* eki1-encoded ethanolamine kinase by zinc depletion. J Biol Chem. 2006;281(19):13110-6.

19. Soto A, Carman GM. Regulation of the *Saccharomyces cerevisiae* CKI1-encoded choline kinase by zinc depletion. J Biol Chem. 2008;283(15):10079-88.

20. Wu CY, Bird AJ, Chung LM, Newton MA, Winge DR, Eide DJ. Differential control of Zap1-regulated genes in response to zinc deficiency in *Saccharomyces cerevisiae*. BMC Genomics. 2008;9:370.

21. Wu CY, Bird AJ, Winge DR, Eide DJ. Regulation of the yeast TSA1 peroxiredoxin by ZAP1 is an adaptive response to the oxidative stress of zinc deficiency. J Biol Chem. 2007;282(4):2184-95.

22. Jang HH, Lee KO, Chi YH, Jung BG, Park SK, Park JH, et al. Two enzymes in one; two yeast peroxiredoxins display oxidative stress-dependent switching from a peroxidase to a molecular chaperone function. Cell. 2004;117(5):625-35.

23. Macdiarmid CW, Taggart J, Kerdsomboon K, Kubisiak M, Panascharoen S, Schelble K, et al. Peroxiredoxin chaperone activity is critical for protein homeostasis in zinc-deficient yeast. J Biol Chem. 2013;188:31313-27.

24. Kaganovich D, Kopito R, Frydman J. Misfolded proteins partition between two distinct quality control compartments. Nature. 2008;454(7208):1088-95.

25. Bird AJ, Gordon M, Eide DJ, Winge DR. Repression of ADH1 and ADH3 during zinc deficiency by Zap1-induced intergenic RNA transcripts. EMBO J. 2006;25(24):5726-34.

26. Williamson VM, Paquin CE. Homology of *Saccharomyces cerevisiae* ADH4 to an iron-activated alcohol dehydrogenase from *Zymomonas mobilis*. Mol Gen Genet. 1987;209(2):374-81.

27. Drewke C, Ciriacy M. Overexpression, purification and properties of alcohol dehydrogenase IV from *Saccharomyces cerevisiae*. Biochim Biophys Acta. 1988;950(1):54-60.

28. Lee YJ, Lee CY, Grzechnik A, Gonzales-Zubiate F, Vashisht AA, Lee A, et al. RNA polymerase I stability couples cellular growth to metal availability. Mol Cell. 2013;51(1):105-15.

29. Qiao W, Ellis C, Steffen J, Wu CY, Eide DJ. Zinc status and vacuolar zinc transporters control alkaline phosphatase accumulation and activity in *Saccharomyces cerevisiae*. Mol Microbiol. 2009;72(2):320-34.

30. Citiulo F, Jacobsen ID, Miramon P, Schild L, Brunke S, Zipfel P, et al. *Candida albicans* scavenges host zinc via Pra1 during endothelial invasion. PLoS Pathog. 2012;8(6):e1002777.

31. Pagani A, Villarreal L, Capdevila M, Atrian S. The *Saccharomyces cerevisiae* Crs5 Metallothionein metal-binding abilities and its role in the response to zinc overload. Mol Microbiol. 2007;63(1):256-69.

32. Palacios O, Atrian S, Capdevila M. Zn- and Cu-thioneins: a functional classification for metallothioneins? J Biol Inorg Chem. 2011;16(7):991-1009.

33. Andreini C, Bertini I. A bioinformatics view of zinc enzymes. J Inorg Biochem. 2012;111:150-6.

34. Andreini C, Bertini I, Cavallaro G. Minimal functional sites allow a classification of zinc sites in proteins. PloS One. 2011;6(10):e26325.

35. Rosato A, Valasatava Y, Andreini C. Minimal functional sites in metalloproteins and their usage in structural bioinformatics. Int J Mol Sci. 2016;17(5).

36. Huh WK, Falvo JV, Gerke LC, Carroll AS, Howson RW, Weissman JS, et al. Global analysis of protein localization in budding yeast. Nature. 2003;425(6959):686-91.

37. Koh JL, Chong YT, Friesen H, Moses A, Boone C, Andrews BJ, et al. CYCLoPs: A comprehensive database constructed from automated analysis of protein abundance and subcellular localization patterns in *Saccharomyces cerevisiae*. G3. 2015;5(6):1223-32.

38. Richards AL, Hebert AS, Ulbrich A, Bailey DJ, Coughlin EE, Westphall MS, et al. One-hour proteome analysis in yeast. Nat Prot. 2015;10(5):701-14.

39. Stefely JA, Kwiecien NW, Freiberger EC, Richards AL, Jochem A, Rush MJP, et al. Mitochondrial protein functions elucidated by multi-omic mass spectrometry profiling. Nat Biotechnol. 2016;34(11):1191-7.

40. Wisniewski JR, Hein MY, Cox J, Mann M. A "proteomic ruler" for protein copy number and concentration estimation without spike-in standards. Mol Cell Proteom. 2014;13(12):3497-506.

41. Ghaemmaghami S, Huh WK, Bower K, Howson RW, Belle A, Dephoure N, et al. Global analysis of protein expression in yeast. Nature. 2003;425(6959):737-41.

42. Milo R. What is the total number of protein molecules per cell volume? A call to rethink some published values. Bioessays. 2013;35(12):1050-5.

43. Jensen LT, Howard WR, Strain JJ, Winge DR, Culotta VC. Enhanced effectiveness of copper ion buffering by CUP1 compared with CRS5 metallothionein in *Saccharomyces cerevisiae*. J Biol Chem. 1996;271:18514-9.

44. Lyons TJ, Gasch AP, Gaither LA, Botstein D, Brown PO, Eide DJ. Genome-wide characterization of the Zap1p zinc-responsive regulon in yeast. Proc Natl Acad Sci USA. 2000;97(14):7957-62.

45. Han SH, Han GS, Iwanyshyn WM, Carman GM. Regulation of the PIS1-encoded phosphatidylinositol synthase in *Saccharomyces cerevisiae* by zinc. J Biol Chem. 2005;280(32):29017-24.

46. De Nicola R, Hazelwood LA, De Hulster EA, Walsh MC, Knijnenburg TA, Reinders MJ, et al. Physiological and transcriptional responses of *Saccharomyces cerevisiae* to zinc limitation in chemostat cultures. Appl Environ Microbiol. 2007;73(23):7680-92.

47. Wu CY, Roje S, Sandoval FJ, Bird AJ, Winge DR, Eide DJ. Repression of sulfate assimilation is an adaptive response of yeast to the oxidative stress of zinc deficiency. J Biol Chem. 2009;284(40):27544-56.

48. Singh N, Yadav KK, Rajasekharan R. ZAP1-mediated modulation of triacylglycerol levels in yeast by transcriptional control of mitochondrial fatty acid biosynthesis. Mol Microbiol. 2016;100(1):55-75.

49. Soto-Cardalda A, Fakas S, Pascual F, Choi HS, Carman GM. Phosphatidate phosphatase plays role in zinc-mediated regulation of phospholipid synthesis in yeast. J Biol Chem. 2012;287(2):968-77.

50. Wu YH, Taggart J, Song PX, MacDiarmid C, Eide DJ. An MSC2 promoter-lacz fusion gene reveals zinc-responsive changes in sites of transcription initiation that occur across the yeast genome. PloS One. 2016;11(9):e0163256.

51. Stanley D, Fraser S, Stanley GA, Chambers PJ. Retrotransposon expression in ethanol-stressed *Saccharomyces cerevisiae*. Appl Microbiol Biotechnol. 2010;87(4):1447-54.

52. Todeschini AL, Morillon A, Springer M, Lesage P. Severe adenine starvation activates Ty1 transcription and retrotransposition in *Saccharomyces cerevisiae*. Mol Cell Biol. 2005;25(17):7459-72.

53. Bradshaw VA, McEntee K. DNA damage activates transcription and transposition of yeast Ty retrotransposons. Mol Gen Genet. 1989;218(3):465-74.

54. Kawamata T, Horie T, Matsunami M, Sasaki M, Ohsumi Y. Zinc starvation induces autophagy in yeast. J Biol Chem. 2017;292(20):8520-30.

55. Bucci MD, Weisenhorn E, Haws S, Yao Z, Zimmerman G, Gannon M, et al. An autophagy-independent role for atg41 in sulfur metabolism during zinc deficiency. Genetics. 2018;208(3):1115-30.

56. Iwanyshyn WM, Han GS, Carman GM. Regulation of phospholipid synthesis in *Saccharomyces cerevisiae* by zinc. J Biol Chem. 2004;279(21):21976-83.

57. Breslow DK, Cameron DM, Collins SR, Schuldiner M, Stewart-Ornstein J, Newman HW, et al. A comprehensive strategy enabling high-resolution functional analysis of the yeast genome. Nat Meth. 2008;5(8):711-8.

58. Apuy JL, Busenlehner LS, Russell DH, Giedroc DP. Ratiometric pulsed alkylation mass spectrometry as a probe of thiolate reactivity in different metalloderivatives of *Staphylococcus aureus* pI258 CadC. Biochemistry. 2004;43(13):3824-34.

59. Apuy JL, Chen X, Russell DH, Baldwin TO, Giedroc DP. Ratiometric pulsed alkylation/mass spectrometry of the cysteine pairs in individual zinc fingers of MRE-binding transcription factor-1 (MTF-1) as a probe of zinc chelate stability. Biochemistry. 2001;40(50):15164-75.

60. Mendoza VL, Vachet RW. Probing protein structure by amino acid-specific covalent labeling and mass spectrometry. Mass Spectrom Rev. 2009;28(5):785-815.

61. Ubhi D, Kago G, Monzingo AF, Robertus JD. Structural analysis of a fungal methionine synthase with substrates and inhibitors. J Mol Biol. 2014;426(8):1839-47.

62. Ubhi D, Kavanagh KL, Monzingo AF, Robertus JD. Structure of *Candida albicans* methionine synthase determined by employing surface residue mutagenesis. Arch Biochem Biophys. 2011;513(1):19-26.

63. Prasannan P, Suliman HS, Robertus JD. Kinetic analysis of site-directed mutants of methionine synthase from *Candida albicans*. Biochem Biophys Res Comm. 2009;382(4):730-4.

64. Hara T, Takeda TA, Takagishi T, Fukue K, Kambe T, Fukada T. Physiological roles of zinc transporters: molecular and genetic importance in zinc homeostasis. J Phys Sci. 2017;67(2):283-301.

65. Que EL, Bleher R, Duncan FE, Kong BY, Gleber SC, Vogt S, et al. Quantitative mapping of zinc fluxes in the mammalian egg reveals the origin of fertilization-induced zinc sparks. Nat Chem. 2015;7(2):130-9.

66. Barnett JP, Millard A, Ksibe AZ, Scanlan DJ, Schmid R, Blindauer CA. Mining genomes of marine cyanobacteria for elements of zinc homeostasis. Front Microbiol. 2012;3:142.

67. Herzberg M, Dobritzsch D, Helm S, Baginsky S, Nies DH. The zinc repository of *Cupriavidus metallidurans*. Metallomics. 2014;6(11):2157-65.

68. Ehrensberger KM, Mason C, Corkins ME, Anderson C, Dutrow N, Cairns BR, et al. Zinc-dependent regulation of the Adh1 antisense transcript in fission yeast. J Biol Chem. 2013;288(2):759-69.

69. de la Cruz J, Gomez-Herreros F, Rodriguez-Galan O, Begley V, de la Cruz Munoz-Centeno M, Chavez S. Feedback regulation of ribosome assembly. Curr Gen. 2018;64(2):393-404.

70. Lempiainen H, Shore D. Growth control and ribosome biogenesis. Curr Opin Cell Biol. 2009;21(6):855-63.

71. Brandes N, Reichmann D, Tienson H, Leichert LI, Jakob U. Using quantitative redox proteomics to dissect the yeast redoxome. J Biol Chem. 2011;286(48):41893-903.

72. Gomes RA, Vicente Miranda H, Silva MS, Graca G, Coelho AV, Ferreira AE, et al. Yeast protein glycation in vivo by methylglyoxal. Molecular modification of glycolytic enzymes and heat shock proteins. FEBS J. 2006;273(23):5273-87.

73. Zhao H, Eide D. The yeast *ZRT1* gene encodes the zinc transporter protein of a high-affinity uptake system induced by zinc limitation. Proc Natl Acad Sci U S A. 1996;93(6):2454-8.

74. Valasatava Y, Rosato A, Banci L, Andreini C. MetalPredator: a web server to predict iron-sulfur cluster binding proteomes. Bioinformatics. 2016;32(18):2850-2.

75. Eddy SR. Profile hidden Markov models. Bioinformatics. 1998;14(9):755-63.

76. Finn RD, Bateman A, Clements J, Coggill P, Eberhardt RY, Eddy SR, et al. Pfam: the protein families database. Nucleic Acids Res. 2014;42(Database issue):D222-30.

77. Putignano V, Rosato A, Banci L, Andreini C. MetalPDB in 2018: a database of metal sites in biological macromolecular structures. Nucleic Acids Res. 2018;46(D1):D459-D64.

78. UniProt Consortium T. UniProt: the universal protein knowledgebase. Nucleic Acids Res. 2018;46(5):2699.

79. Tyanova S, Temu T, Sinitcyn P, Carlson A, Hein MY, Geiger T, et al. The Perseus computational platform for comprehensive analysis of (prote)omics data. Nat Meth. 2016;13(9):731-40.

80. Dennis G, Jr., Sherman BT, Hosack DA, Yang J, Gao W, Lane HC, et al. DAVID: database for annotation, visualization, and integrated discovery. Genome Biol. 2003;4(5):P3.

81. MacDiarmid CW, Taggart J, Jeong J, Kerdsomboon K, Eide DJ. Activation of the yeast UBI4 polyubiquitin gene by Zap1 via an intragenic promoter is critical for zinc-deficient growth. J Biol Chem. 2016;291:18880-96.

82. MacDiarmid CW, Taggart J, Kerdsomboon K, Kubisiak M, Panascharoen S, Schelble K, et al. Peroxiredoxin chaperone activity is critical for protein homeostasis in zinc-deficient yeast. J Biol Chem. 2013;288(43):31313-27.

83. Ciesla M, Mierzejewska J, Adamczyk M, Farrants AK, Boguta M. Fructose bisphosphate aldolase is involved in the control of RNA polymerase III-directed transcription. Biochim Biophys Acta. 2014;1843(6):1103-10.

84. Freire AP, Martins AM, Cordeiro C. An experiment illustrating metabolic regulation in situ using digitonin permeabilized yeast cells. Biochem Educ. 1998;26:161-3.

FIGURES

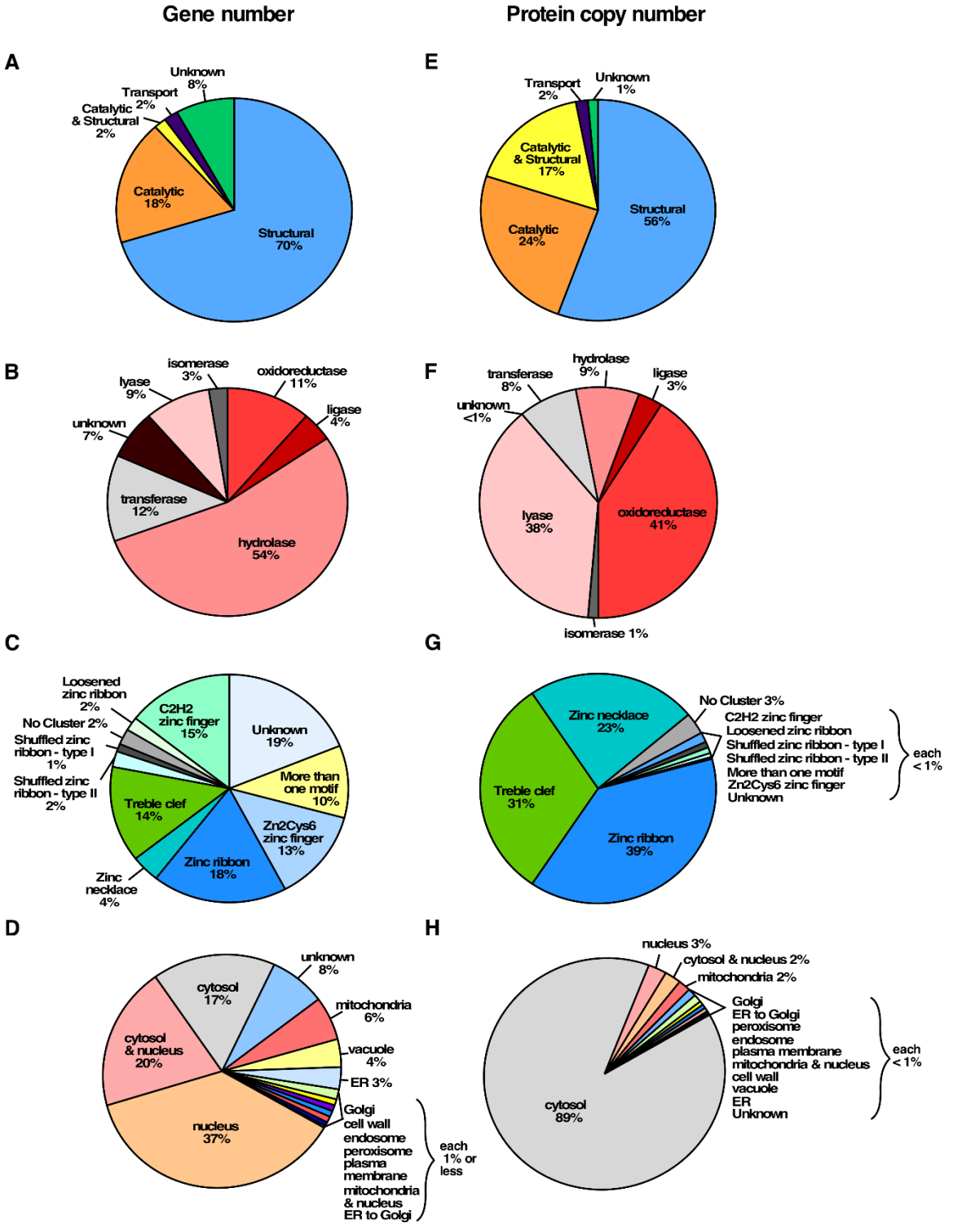
Gene number
Protein copy number
A
Unknown 8%
Transport 2%
Catalytic & Structural 2%
Catalytic 18%
Structural 70%
E
Transport 2%
Unknown 1%
Catalytic & Structural 17%
Structural 56%
Catalytic 24%
B
isomerase 3%
oxidoreductase 11%
lyase 9%
ligase 4%
unknown 7%
transferase 12%
hydrolase 54%
F
hydrolase 9%
transferase 8%
ligase 3%
unknown <1%
lyase 38%
oxidoreductase 41%
isomerase 1%
C
Loosened zinc ribbon 2%
C2H2 zinc finger 15%
Unknown 19%
No Cluster 2%
Shuffled zinc ribbon - type I 1%
More than one motif 10%
Shuffled zinc ribbon - type II 2%
Treble clef 14%
Zn2Cys6 zinc finger 13%
Zinc ribbon 18%
Zinc necklace 4%
G
No Cluster 3%
Zinc necklace 23%
C2H2 zinc finger
Loosened zinc ribbon
Shuffled zinc ribbon - type I
Shuffled zinc ribbon - type II
More than one motif
Zn2Cys6 zinc finger
Unknown
each < 1%
Treble clef 31%
Zinc ribbon 39%
D
unknown 8%
cytosol 17%
mitochondria 6%
cytosol & nucleus 20%
vacuole 4%
ER 3%
Golgi
cell wall
endosome
peroxisome
plasma membrane
mitochondria & nucleus
ER to Golgi
each 1% or less
nucleus 37%
H
nucleus 3%
cytosol & nucleus 2%
mitochondria 2%
Golgi
ER to Golgi
peroxisome
endosome
plasma membrane
mitochondria & nucleus
cell wall
vacuole
ER
Unknown
each < 1%
cytosol 89%

Figure 1. The zinc proteome of *S. cerevisiae*. The zinc proteome was classified based on general cofactor function (A, E), enzyme classification (B, F), structural zinc-binding site (C, G), and subcellular localization (D, H). In panels A-D, proportions were determined based on the number of genes encoding proteins in each group. In panels E-H, proportions were determined based on protein copy number in each group in replete cells.

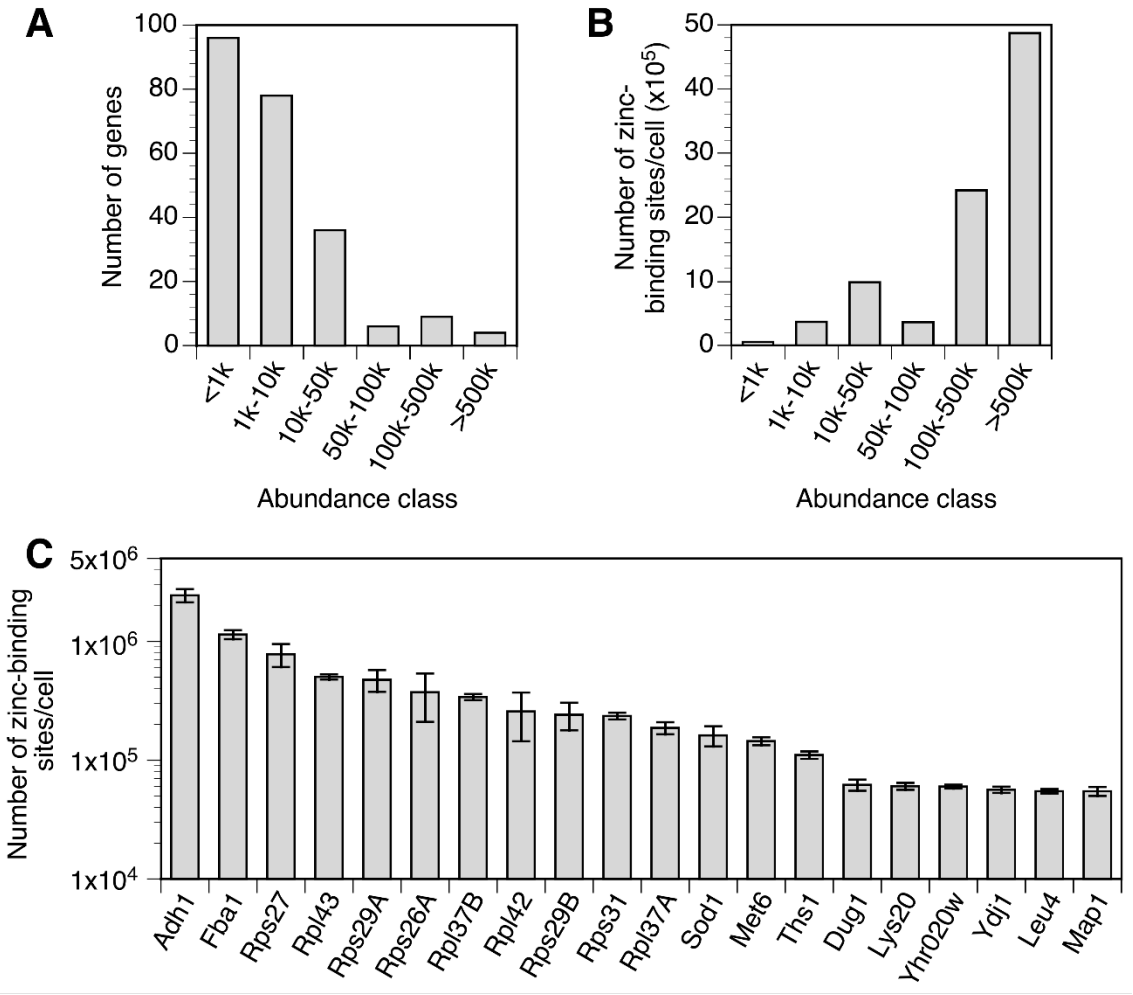

Figure 2. Abundance classes of the zinc proteome in replete cells. A) The number of genes encoding proteins in each abundance class is plotted. B) The number of predicted zinc atoms bound by proteins in each abundance class is plotted. C) The 20 proteins most abundant proteins in the zinc proteome are plotted with their predicted number of bound zinc atoms. Some ribosomal subunits are encoded by gene pairs, e.g. *RPS27A* and *RPS27B*, whose proteins are not distinguishable by mass spectrometry; these are labeled without specific reference to the paralogous genes. The error bars represent ± 1 S.D. calculated from 4 biological replicates

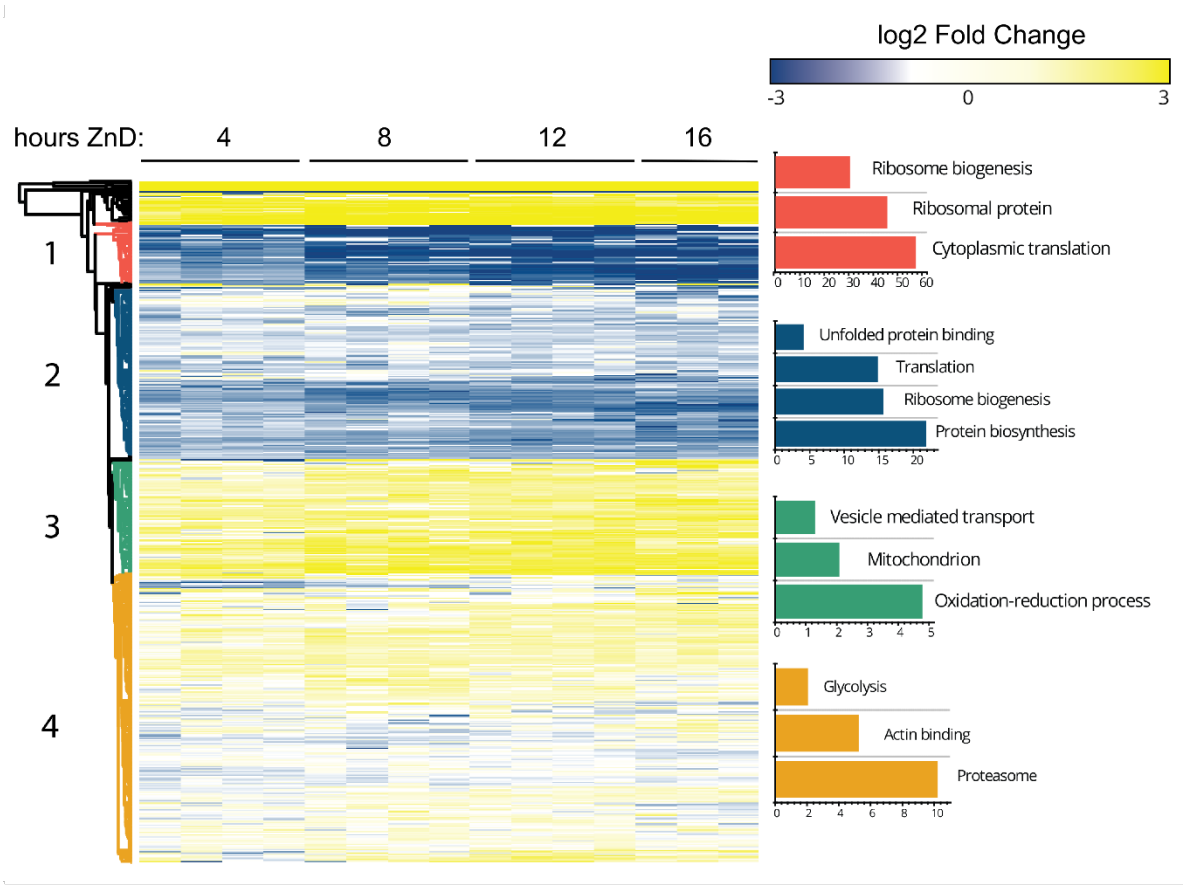

Figure 3. The response of the total proteome to the transition from zinc-replete to deficient conditions. Zinc-replete cells were transferred to a zinc-deficient medium and harvested for proteomics analysis after 4, 8, 12, and 16 h. The resulting changes in protein abundance relative to replete conditions for 2,119 proteins are plotted as a heat map. Cluster analysis was performed and four clusters (1-4) were identified. Gene ontology (GO) analysis of each cluster was then performed and significant terms observed are plotted with the -log of their p-values in each histogram color-coded for their corresponding cluster. Full GO results are provided **Table S4**.

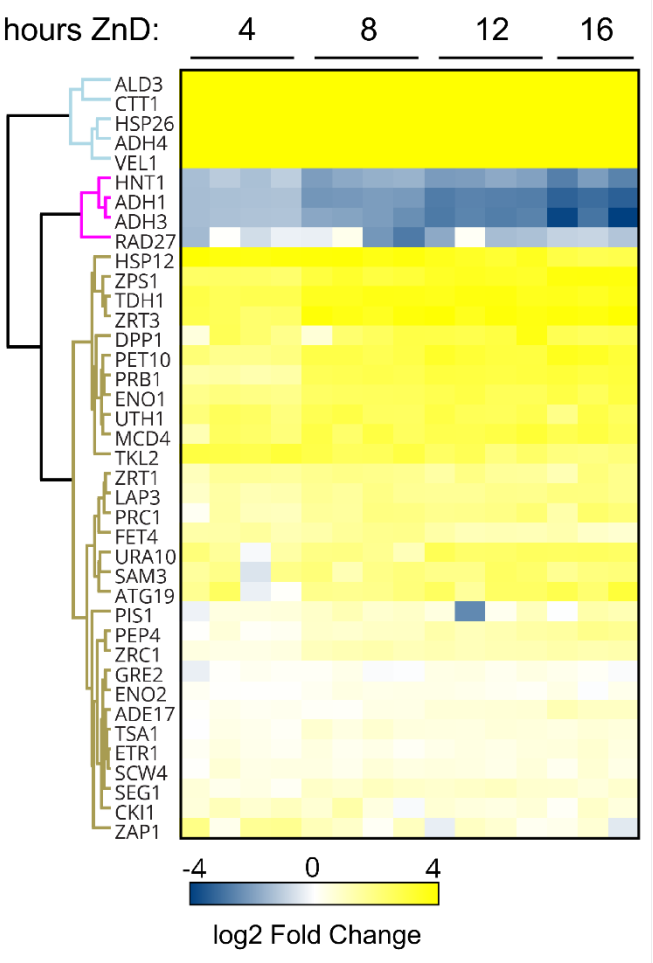

Figure 4. The response of proteins encoded by the Zap1 regulon to the transition from zinc-replete to deficient conditions. During the transition to zinc-deficient conditions, the resulting changes in protein abundance relative to replete conditions for 39 proteins are plotted as a heat map. Proteins affected similarly were identified by cluster analysis.

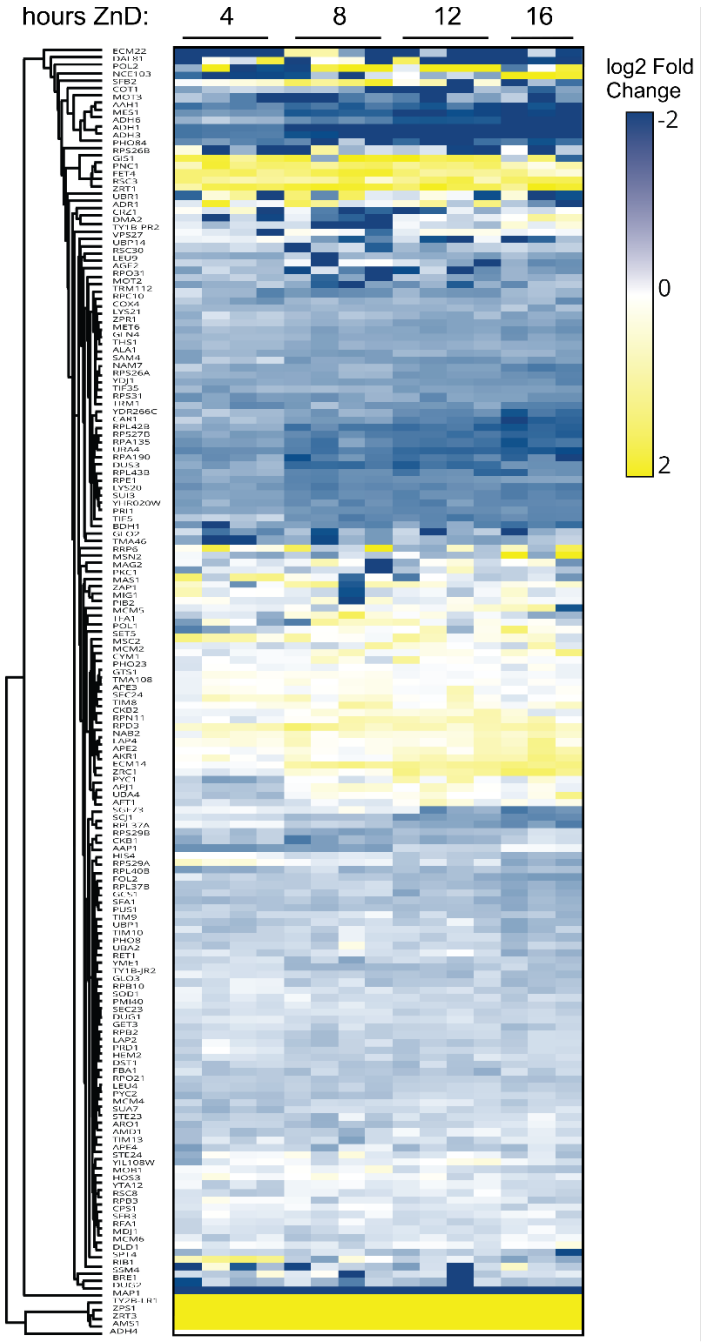

Figure 5. The response of proteins in the zinc proteome to the transition from zinc-replete to deficient conditions. During the transition to zinc-deficient conditions, the resulting changes in protein abundance relative to replete conditions for 159 proteins are plotted as a heat map. Proteins affected similarly were identified by cluster analysis.

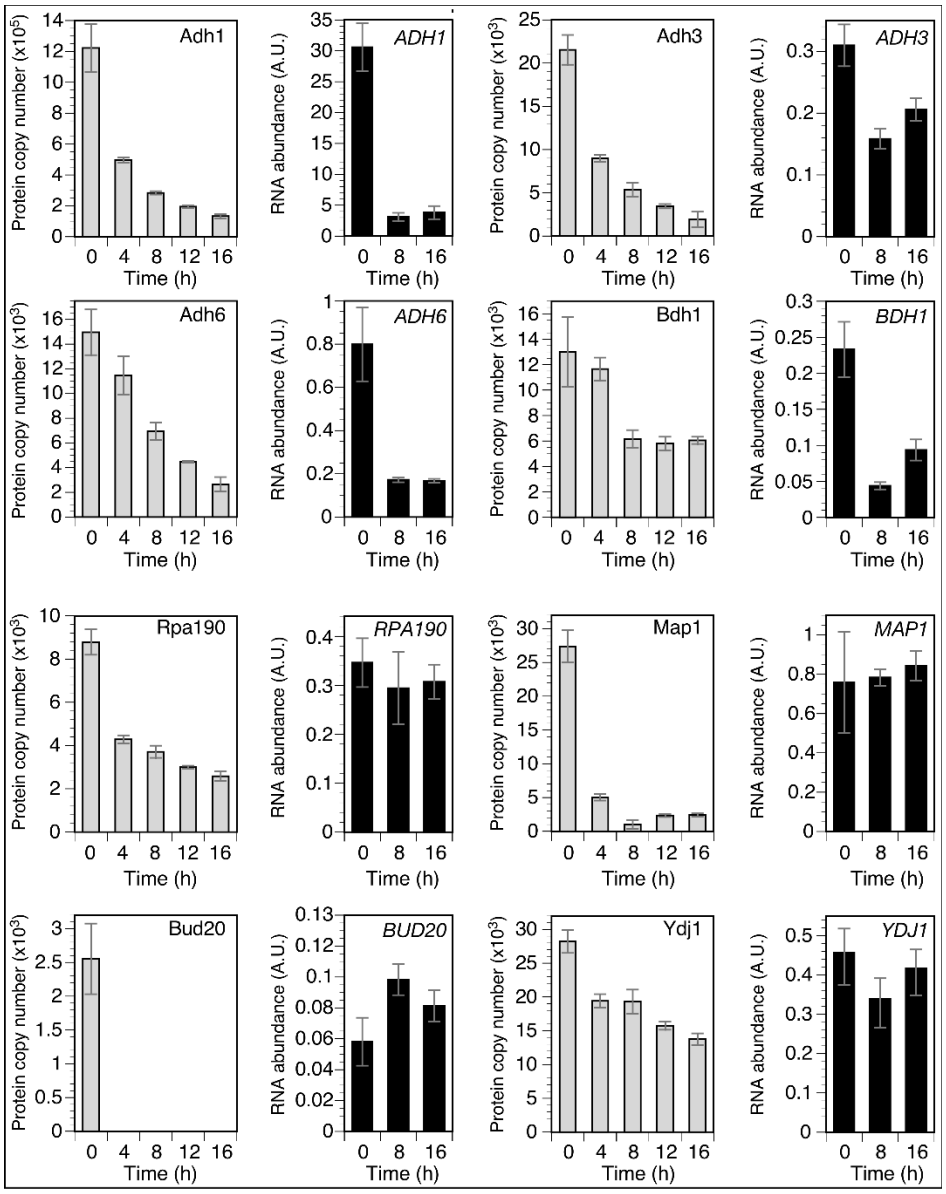

Figure 6. The effect of zinc deficiency on the abundance of example zinc proteins and their mRNA. For each, the effect on the transition from replete to deficient conditions is plotted relative to protein copy number (*left* panels, *gray* columns) and mRNA abundance (*right* panels, *filled* columns, A.U. = arbitrary units). Protein levels are from 3-4 replicates per timepoint and the mRNA levels were determined by quantitative RT-PCR (n = 3). The error bars indicate ± 1 S.D.

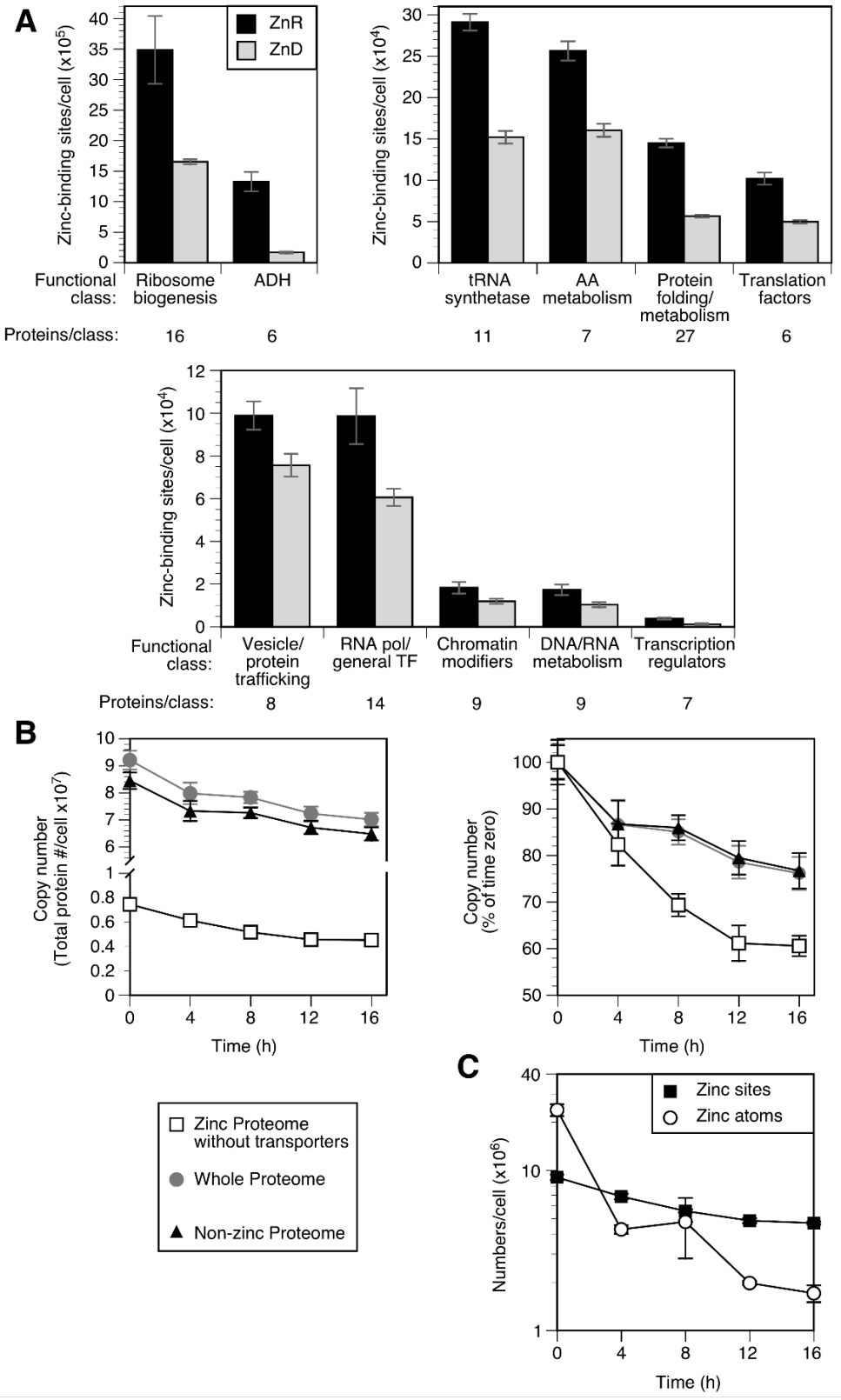
A
Zinc-binding sites/cell (x10^5)
ZnR
ZnD
Functional class:
Ribosome biogenesis
ADH
Proteins/class:
16
6
Zinc-binding sites/cell (x10^4)
tRNA synthetase
AA metabolism
Protein folding/ metabolism
Translation factors
11
7
27
6
Zinc-binding sites/cell (x10^4)
Functional class:
Vesicle/ protein trafficking
RNA pol/ general TF
Chromatin modifiers
DNA/RNA metabolism
Transcription regulators
Proteins/class:
8
14
9
9
7
B
Copy number (Total protein #/cell x10^7)
Time (h)
Copy number (% of time zero)
Time (h)
Zinc Proteome without transporters
Whole Proteome
Non-zinc Proteome
C
Zinc sites
Zinc atoms
Numbers/cell (x10^6)
Time (h)

Figure 7. Zinc sparing is widespread in the zinc proteome. A) 120 members of the zinc proteome that decrease during zinc deficiency were grouped by general function and plotted as the number of zinc-binding sites in each group under replete (*filled* columns) and deficient (i.e. 16 h) (*gray* columns) conditions. B) The effect of zinc deficiency on the copy number per cell of the total proteome (*circles*), the total proteome not including the zinc proteome (*triangles*), and the zinc proteome (*squares*) is plotted. C) The estimated number of zinc atoms bound by the zinc proteome (*squares*) is plotted relative to the number of zinc atoms per cell as determined by ICP-AES (*circles*). The error bars indicate ± 1 S.D calculated from 3-4 biological replicates.

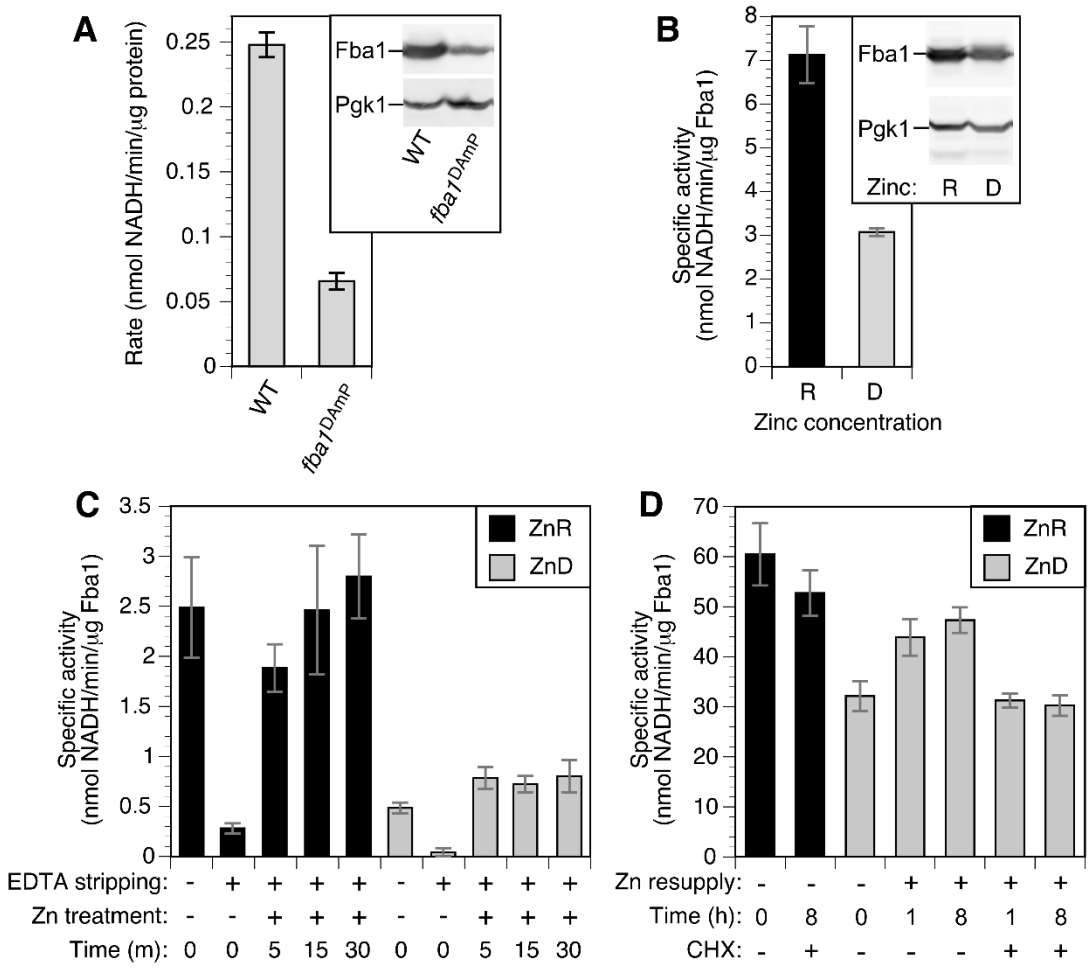

Figure 8. Effects of zinc status on Fba1 aldolase activity. A) Aldolase activity in wild-type (BY4741) and *fba1*^{DAmP} cells normalized to total protein. The inset shows an immunoblot of Fba1 protein level detected with anti-Fba1 and anti-Pgk1 in 20 µg of total protein. B) Aldolase specific activity in zinc-replete (R) and deficient (D) BY4741 cells normalized to Fba1 protein levels. The inset shows an immunoblot of Fba1 protein level detected as described for panel A. C) Aldolase specific activity in permeabilized replete (ZnR) and deficient (ZnD) cells before and after in vitro EDTA stripping and zinc resupply for the times indicated. D) Aldolase specific activity in zinc-replete and deficient cells following zinc resupply in vivo with and without cycloheximide treatment (100 µg/ml). The error bars indicate ± 1 S.D (n = 3).

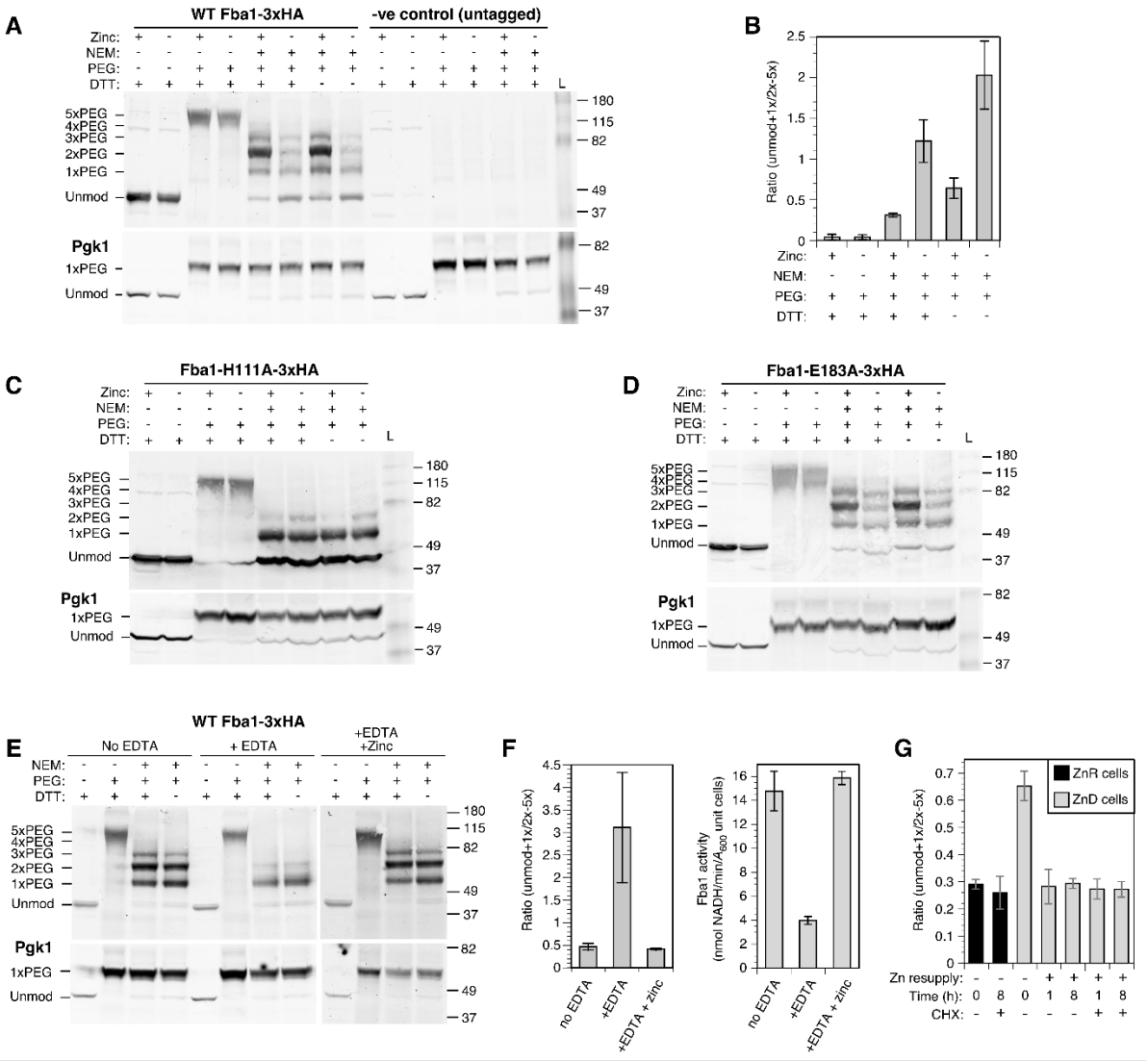

Figure 9. In vivo analysis of zinc binding by Fba1. A) NEM/PEG-maleimide analysis of wild-type (BY4742) cells expressing Fba1-3xHA or an untagged Fba1 allele. Zinc-replete (+) or deficient (-) cells were treated with and without NEM, proteins harvested, and then treated with or without DTT prior to PEG-maleimide treatment. The positions of molecular mass markers (kDa) and of unmodified and PEG-modified forms of Fba1-3xHA are indicated. Pgk1, which has a single cysteine that is insensitive to zinc supply, was used as a control for the efficiency of PEG labeling. B) Quantitation of the results in panel A. The ratios of unmodified + 1x PEG-modified to 2x-5x PEG-modified forms are shown and the error bars indicate ± 1 S.D (n = 3). C,D) NEM/PEG-

maleimide analysis of wild-type (BY4742) cells expressing Fba1-H111A-3xHA or Fba1-E183A-3xHA as described for panel A. E) NEM/PEG-maleimide analysis of permeabilized wild-type (BY4742) cells expressing Fba1-3xHA following stripping with EDTA and reloading with zinc. F) Quantitation of the results in panel E. The ratios of unmodified + 1x PEG-modified to 2x-5x PEG-modified forms are shown (*left* panel) is compared with Fba1 activity determined from the same samples (*right* panel). The error bars indicate ± 1 S.D (n = 3). G) NEM/PEG analysis of wild-type (BY4743) cells expressing Fba1-3xHA grown in zinc-replete (ZnR) or deficient (ZnD) and following resupply with zinc (100 μM in LZM) in vivo for 1 and 8 h, with and without cycloheximide treatment (100 μg/ml). The ratios of unmodified + 1x PEG-modified to 2x-5x PEG-modified forms are shown and the error bars indicate ± 1 S.D (n = 3).

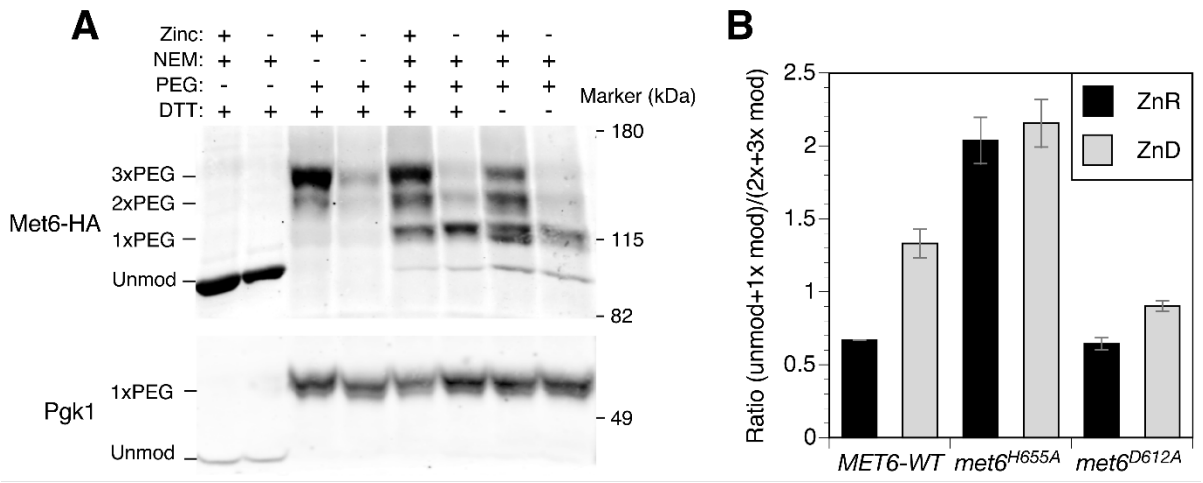

Figure 10. In vivo analysis of zinc binding by Met6. A) NEM/PEG-maleimide analysis of wild-type (BY4742) cells expressing Met6-HA. Zinc-replete (+) or deficient (-) cells were treated with and without NEM, proteins harvested, and then treated with and without DTT prior to PEG-maleimide treatment. The positions of molecular mass markers (kDa) and unmodified and PEG-modified forms of Met6-HA are shown. Pgk1 was detected as a control for PEG labeling efficiency. B) Quantification of NEM/PEG-maleimide analysis of wild-type (BY4742) cells expressing Met6-HA, Met6^{H655A}-HA or Met6^{D612A}-HA as described for panel A. The ratios of unmodified + 1 x PEG-modified to 2-3 x PEG-modified forms are shown and the error bars indicate ± 1 S.D (n = 3).

Table 1. Protein copy number and RNA abundance for example zinc proteome members under zinc-replete (0 h) and deficient (8 and 16 h) conditions. Protein copy numbers are from mass spectrometry analysis and mRNA abundance was determined by quantitative RT-PCR (n = 3). The ratios of levels at 16 h and 0 h are reported and the p-values were calculated using Student's t-test.

	Protein Copy Number (per cell)					RNA Level				
Protein/Gene	**0 h**	**8 h**	**16 h**	**Ratio of T16/T0**	**p-value**	**0 h**	**8 h**	**16 h**	**Ratio of T16/T0**	**p-value**
Zrt1	29467	104388	99222	3.36	0.001	1.444	7.064	11.028	7.64	0.00005
Zrt3	627	7351	8247	13.20	0.001	0.520	5.261	5.422	10.43	0.000009
Adh1	1222338	283955	132595	0.11	0.000006	30.58	3.11	3.81	0.12	0.04
Adh3	21531	5370	1905	0.09	0.00009	0.31	0.16	0.21	0.66	0.002
Adh5	2659	0	0	N/A	N/A	0.53	0.24	0.36	0.67	0.01
Adh6	14959	6939	2649	0.18	0.00005	0.80	0.17	0.17	0.21	0.0003
Bdh1	13002	6165	6047	0.47	0.01	0.23	0.04	0.09	0.40	0.0005
Aah1	3344	1206	801	0.24	0.01	0.29	0.29	0.23	0.77	0.09
Bud20	2552	0	0	N/A	N/A	0.06	0.10	0.08	1.40	0.05
Car1	12831	8155	4461	0.35	0.006	0.05	0.03	0.03	0.65	0.03
Dus3	3684	1471	1200	0.33	0.02	0.04	0.04	0.03	0.78	0.3
Fcy1	15308	0	0	N/A	N/A	0.83	0.38	0.52	0.63	0.02
Map1	27378	1034	2405	0.09	0.00007	0.76	0.78	0.84	1.11	0.6
Mes1	28274	8847	6347	0.22	0.001	0.59	0.12	0.14	0.23	0.002
Met6	144826	101595	86610	0.60	0.003	1.18	0.55	0.88	0.75	0.1
Nmd3	3559	1398	1720	0.48	0.01	0.51	0.25	0.26	0.50	0.003
Reh1	356	141	200	0.56	N/A	0.23	0.11	0.23	1.03	0.6
Rpa12	3567	0	0	N/A	N/A	0.72	0.28	0.36	0.51	0.001
Rpa135	5595	2543	1844	0.33	0.003	0.24	0.22	0.18	0.76	0.2
Rpa190	8784	3709	2580	0.29	0.0003	0.35	0.29	0.31	0.89	0.2
Rpe1	13710	6477	6076	0.44	0.01	0.14	0.12	0.12	0.81	0.06
Sui3	27585	12387	11510	0.42	0.009	1.26	0.38	0.51	0.40	0.0002
Ths1	55203	36381	31764	0.58	0.005	1.40	0.49	0.82	0.59	0.0001
Tif35	24715	14869	12549	0.51	0.006	3.65	1.34	1.76	0.48	0.0003
Tif5	35778	18271	17712	0.50	0.005	0.43	0.23	0.26	0.61	0.03
Ura4	23647	11292	8225	0.35	0.006	0.83	0.13	0.22	0.26	0.0007
Ycr087c-A	2431	0	0	N/A	N/A	0.30	0.15	0.12	0.40	0.000008
Ydj1	28211	19306	13749	0.49	0.002	0.46	0.34	0.42	0.91	0.3
Yhr020w	59964	29010	26517	0.44	0.002	0.36	0.22	0.29	0.80	0.2
Zpr1	5310	4095	3285	0.62	0.02	0.20	0.21	0.16	0.77	0.1

SUPPLEMENTAL FIGURES AND TABLES

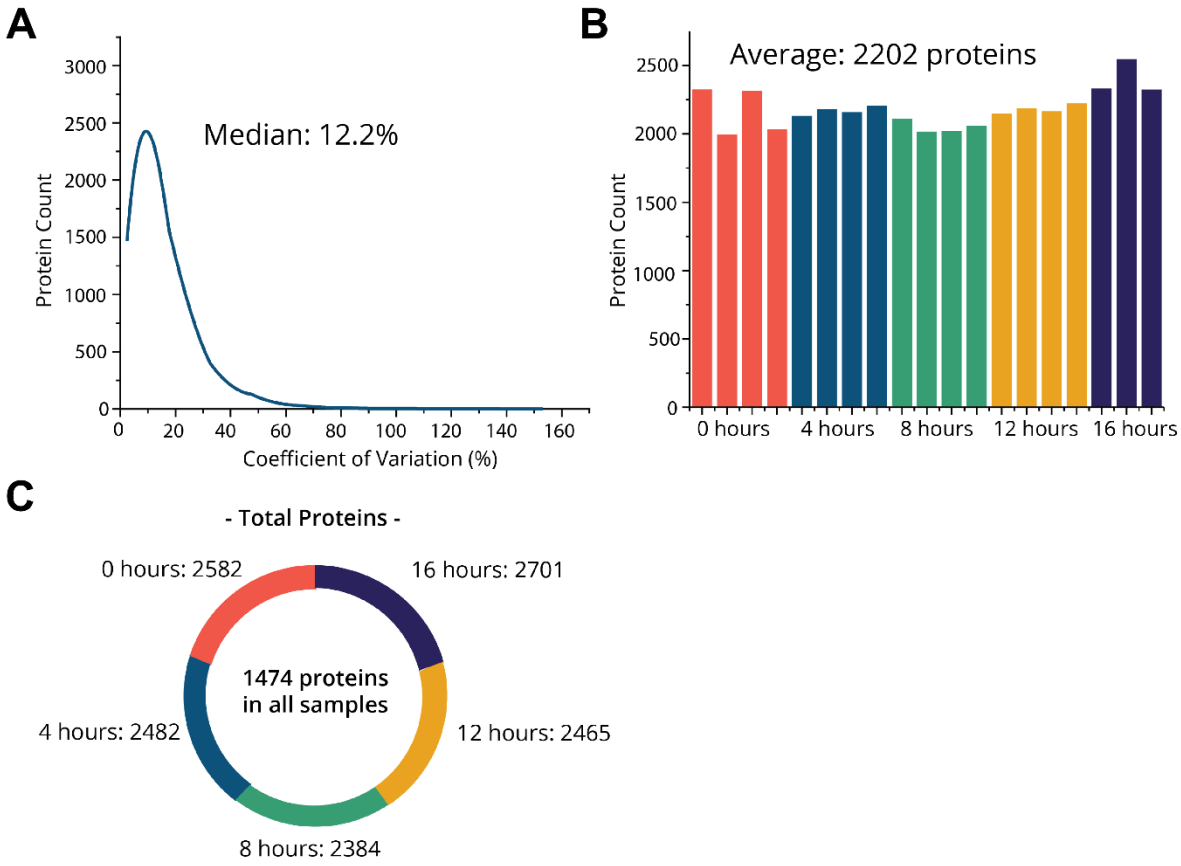

Figure S1. Evaluation of proteomics reproducibility. A) The median coefficient of variation within each time point was 12%. B) An average of 2,202 proteins were detected in each sample. C) Across all five time points, 1,474 proteins were detected in all samples.

Chapter 3: Exploring the *in vivo* interacting targets of 2-cys peroxiredoxin Tsa1 under zinc deficiency

ABSTRACT

Zinc is a critical structural and/or catalytic cofactor of many proteins. Zinc deficiency is a cellular stress that generates oxidative stress and induces the unfolded protein response. Zinc-deficient yeast cells have evolved mechanisms to overcome this stress such as inducing a zinc-responsive 2-cys peroxiredoxin Tsa1 that also functions as a chaperone. In this report, I confirmed that Rpd3, a class I histone deacetylase highly conserved from yeast to mammalian cells, has a small pool of apoprotein that lost its zinc cofactor in zinc-replete cells but a significantly larger pool in deficient cells. I also confirmed Rpd3 interacts with Tsa1 in both zinc-replete and deficient cells by using a proximity-based BioID essay and a pull-down analysis, thus confirming Rpd3 as a novel *in vivo* Tsa1 target.

INTRODUCTION

Zinc is a critical structural and/or catalytic cofactor of many proteins. One prominent class of zinc proteins is enzymes that modify histones, such as DNA methyltransferases, histone acetyltransferases, histone deacetylases and other histone modifiers. In yeast, zinc often serves as structural cofactor (e.g. Sir2, Hst1-4, Esa1, etc) or serve as both catalytic and structural cofactor (e.g. Rpd3, and Hos1-3) of these histone modifiers. Among these enzymes, Rpd3, a class I histone deacetylase has attracted much attention as it is highly conserved from yeast to mammalian cells (HDAC1,2,3, and 8) and has been shown to regulate transcription, cell cycle arrest adaptive response, replication origin firing, macro-autophagy and adaption to various stress[1–7]. In yeast, Rpd3 uses one zinc atom per monomer and accumulates to ~ 3000 copies in synthetic defined (SD)

media and ~ 4000 copies in zinc-replete cells. The expression of Rpd3 gradually increases to ~6000 copies in zinc-deficient cells based on our proteomics analysis from **Chapter 2**.

Recently, the involvement of Rpd3 complexes in diverse stress responses has been studied. Rpd3 is the catalytic core of HDAC complexes Rpd3L, Rpd3S and Rpd3μ and deacetylates the lysine residues of various proteins including the core histones (H2A, H2B, H3 and H4). The three Rpd3 complexes seem to regulate a diverse and yet distinct of cellular functions. For example, Rpd3L appears to localize more at the promoters to activate genes such as interacting with Hog1 to activate genes that respond to high osmolarity stress in yeast[6]. Rpd3L is also involved in regulating cells adaption to heat shock response[5]. Rpd3μ is a unique yeast Rpd3 complex that was characterized by Baker et al. It contains only three subunits including Rpd3, Snt2 and Ecm5. It was proposed to be a central complex that connects cell signaling and chromatin remodeling to respond to a variety of cellular stress such as oxidative stress. Cells lacking Snt2 or Rpd3 are resistant to hydrogen peroxide treatment, and Rpd3μ subunits seem to be enriched at promoters of H_2O_2-responsive genes[8]. Another interesting finding suggests that in response to starvation stress, *Drosophila* Rpd3 accumulates in the nucleolus and form foci in a dose-dependent manner, enriches at the rRNA promoters to activate rRNA synthesis and increases protein expression of autophagy-related proteins to resist starvation[9]. All these studies suggest a role of Rpd3 in yeast and other organisms in assisting cells to adapt to various stresses.

Although critical, little research has been done in directly connecting zinc loss of histone modifying enzymes such as Rpd3 to their protein-protein interactions, and/or other downstream effects during zinc deficiency. Zinc deficiency is a unique cellular stress that features oxidative

stress and unfolded protein response[10,11]. The zinc-responsive peroxiredoxin Tsa1 appears to be central to both stresses. Background knowledge of Tsa1 was introduced in **Chapter 2** so it will not be repeated here. It has been shown that Tsa1 has chaperone activity and foci co-localized with Hsp104-GFP disaggregase were observed in zinc-deficient cells lacking Tsa1[11,12]. However, the identity of these foci remained unknown. Results from **Chapter 2** of this thesis indicated the accumulation of apoproteins in zinc-deficient yeast cells. Therefore, I hypothesized that the Tsa1 protein chaperone is critical in preventing aggregation of unmetalated zinc apoproteins as zinc is important in protein folding. In this chapter, I aim to explore and identify novel *in vivo* targets of the Tsa1 chaperone.

RESULTS

The solubility of some zinc proteins depends on the Tsa1 protein.

To identify potential targets of the Tsa1 chaperone, we used fluorescence microscopy to screen GFP-tagged alleles of ~100 of the most abundant zinc proteins for those that form foci specifically in actively growing, zinc-deficient *tsa1*Δ cells. To obtain the list of zinc proteins that only aggregate due to zinc deficiency, we excluded several proteins that form foci in both zinc-deficient medium and in stationary phase where cells run out of glucose (data not shown). To validate that the zinc proteins aggregate on their own, rather than as an artifact caused by the presence of the C-terminal GFP tag, we also performed fluorescence microscopy on N-terminal RFP-tagged alleles of ~10 remaining zinc proteins. After excluding the proteins that only form foci with the GFP tag, we obtained a list of four zinc proteins that form bright foci, suggesting reduced protein solubility and increased aggregation, specifically in actively growing, zinc-deficient cells lacking

Tsa1 (**Fig. 1A**). These four proteins are Nce103, Car1, Bdh1, and Rpd3. Nce103 is a carbonic anhydrase that catalyzes the reversible reaction where CO_2 is converted to H_2CO_3. Nce103 uses one catalytic zinc per monomer and is thought to supply bicarbonate to key metabolic pathways in the yeast cell[13]. Car1 binds one zinc of unknown function and is an arginase that is involved in the first step of urea cycle where arginine is converted to ornithine[14]. Bdh1 is a highly abundant (R,R)-butanediol dehydrogenase that uses two zinc atoms functioning as both catalytic and structural cofactors of the enzyme[15]. Rpd3 is the catalytic core of HDAC complexes Rpd3L, Rpd3S and Rpd3μ in yeast. It uses one zinc per monomer and deacetylates the lysine residues of various proteins including the core histones (H2A, H2B, H3 and H4)[7].

To test whether these foci form from insoluble aggregated proteins, we used Hsp104-GFP, a heat shock protein that functions as a disaggregase that untangles aggregated proteins, as a marker to overlay with the RFP-tagged zinc proteins. Indeed, RFP-Nce103 and RFP-Car1 foci colocalized with Hsp104-GFP, suggesting that the foci formed by these zinc proteins are insoluble aggregates (**Fig. 1B**). Overall, the above results indicated that solubility of zinc proteins, Nce103, Car1, and possibly Bdh1 and Rpd3, depends on Tsa1. Prior to publication of this work, colocalization of Bdh1 and Rpd3 with Hsp104-GFP will be required to test this hypothesis of insolubility for those two proteins.

BioID analysis shows that Tsa1 interacts with Rpd3 in vivo.

To test the hypothesis that Tsa1 is preventing aggregation of unmetalated zinc apoproteins, potentially Nce103, Car1, Bdh1 and Rpd3, through its chaperone function, I investigated the protein-protein interaction (PPI) *in vivo* between Tsa1 and these four zinc proteins. Tsa1 was

proposed to act like small heat shock proteins as a "holdase"-type chaperone that keeps its unfolded target from further aggregating[12]. Therefore, the rationale behind establishing PPI is that Tsa1 has to physically interact with its zinc apoprotein target to prevent it from aggregating. To test for physical PPI *in vivo*, I used the proximity-based BioID assay which uses a mutant version of biotin ligase (BirA*) from *Escherichia coli* as "bait" to "fish out" interacting or neighboring proteins[16]. Fusing Tsa1 with BirA* enables the fusion protein to biotinylate potential Tsa1 interacting targets *in vivo*, which will be captured with a high-affinity streptavidin agarose resin and then be enriched by elution and analyzed by immunoblotting. To establish the experimental conditions that ensure successful elution of Tsa1 interacting targets, I titrated the optimal concentration of biotin to be supplemented to the growth media, tested different constructs of the fusion protein for their ability to biotinylate neighboring proteins(BirA*-Tsa1 vs Tsa1-BirA*), tested the protein abundance level of BirA* control and BirA*-Tsa1 fusion protein, and determined the optimal elution methods for BioID analysis in yeast cells (data not shown).

The results showed that among the four targets that formed foci in zinc-deficient *tsa1*Δ cells, only the class I histone deacetylase Rpd3 was confirmed as a potential interacting target of the Tsa1 chaperone as there is significantly higher abundance of biotinylated Rpd3 in *tsa1*Δ cells expressing BirA*-Tsa1, compared to the BirA* control alone (**Fig. 2A**, *lower panel, lane 3 and 7*). This result remained highly significant (**Fig. 2C**) after quantifying biotinylated Rpd3, normalizing with total biotinylated peptides (shown in *upper panel* of **Fig. 2A**), and then normalizing the ratio with Rpd3 protein abundance from zinc-replete and zinc-deficient cells, respectively (**Fig. 2B**). I also confirmed the results in various strains with different genetic backgrounds using a native Rpd3 antibody. To further investigate whether Tsa1 is directly interacting with Rpd3 per se, rather than

other proteins within Rpd3 complexes, I picked two shared subunits Ume1 and Sin3 of Rpd3L and Rpd3S[7]. As shown in **Figure 2D** (*lower panel*), neither Ume1-HA nor Sin3-HA showed significantly different biotinylated peptides between *tsa1*Δ cells expressing BirA*-Tsa1 and cells expressing BirA* control alone. This result suggests that Tsa1 specifically interacts with Rpd3 and not other proteins in the Rpd3-containing complexes.

Next, I sought to determine which function of Tsa1 is required to interact with Rpd3. Tsa1 has two critical cysteines Cys48 and Cys171. When Tsa1 functions as a classic peroxidase, H_2O_2 oxidizes the catalytic cysteine (or peroxidatic cysteine) Cys48 to sulfenic acid, then a second cysteine Cys171 from another Tsa1 monomer will resolve the sulfenic acid by forming a disulfide bond[17]. The chaperone function of Tsa1 requires hyperoxidization of Cys48 to sulfinic acid, which enables Tsa1 to oligomerize into a stacking "donut"-shaped higher molecular structure with enhanced chaperone activity[18]. Newer research also indicates that in addition to the active peroxidatic active site, a YF motif located at the C-terminus of Tsa1 is important to sense the peroxide level in the cellular environment[19,20]. Tsa1 alleles lacking the YF motif are resistant to hyperoxidation and therefore lack chaperone function[21].

I fused five mutant alleles of Tsa1 on the N-terminus of BirA*. Based on the current literature, C48D and C48E are two mutants that can mimic Tsa1 with enhanced chaperone activity[17], the C171S mutant that mimics Tsa1 with no peroxidatic activity, the C48S mutant abolishes both chaperone and peroxidase activities of Tsa1[11], and the ΔYF mutant is correlated with reduced chaperone activity[22]. The results showed that mutating the key sites and regions of Tsa1 reduces the abundance of biotinylated Rpd3, compared to the wild-type of Tsa1 (**Fig. 2E and 2G**). There

was no significant level of detectable biotinylated Rpd3 from zinc-replete cells expressing these different Tsa1 mutants (data not shown). In zinc-deficient cells, biotinylated Rpd3 from all six mutants can be clearly observed in the Anti-Rpd3 blot (**Fig.2E** *lower panel*), quantification of these biotinylated Rpd3 were shown in **Fig. 2G**. An interesting observation is that although ΔYF mutant has less protein abundance (data not shown), it biotinylates relatively more total peptides (**Fig. 2E**, *lane 6*). Whether these observations suggest that there is less interaction between Rpd3 and the C48D and C48E, more interaction between ΔYF mutant allele of Tsa1 is unknown by BioID analysis alone. Further experiments, such as pulldown analysis using these different mutants, and experiments that differentiating Tsa1 functions are needed to confirm the results from Figure 2E and 2G.

Overall, although it remains unclear whether Tsa1 prevents the aggregation of the target proteins through its chaperone function, the BioID analysis (**Fig. 2**) supports the hypothesis that Tsa1 is physically interacting with Rpd3, rather than other Rpd3 complex proteins *in vivo*.

Pull-down analysis confirms that Tsa1 interacts with Rpd3 in both zinc-replete and zinc-deficient cells in vivo.

To further test whether Tsa1 interacts with Rpd3, I performed a pull-down analysis. I fused the maltose-binding protein (MBP) to the C-terminus of wild-type Tsa1 and its C171S mutant, used amylose resin to capture any proteins that interact with Tsa1-MBP (or MBP alone), and a maltose-containing elution buffer to obtain eluates that were analyzed by immunoblotting. Based on the results, it appears that the interaction between Tsa1 and Rpd3 is not extensive and could very likely be a transient interaction (data not shown). By fusing MBP with C171S mutant in this experiment,

it allowed me to create a "trap" that can capture transient PPI between Tsa1 and Rpd3 as C171S mutant cannot resolve the oxidized Cys48 so it forces Tsa1 to form disulfide bond with other proteins[23].

Figure 3A showed that I detected high molecular weight proteins (above 120 kDa) forming only in *tsa1*Δ cells expressing Tsa1-MBP C171S and not in the wild-type cells expressing MBP control (**Fig. 3A**, *upper left panel*). Adding 100 μM hydrogen peroxide seemed to create more cross-linked species with even higher molecular weight that run above the blotted area of the gel. These high molecular weight proteins disappeared after treating the same eluates with DTT, indicating they are oxidatively linked species. The results also showed that cross-linked proteins were detected in both zinc-replete and zinc-deficient cells, with more intense bands showing in zinc-replete cells (**Fig. 3A**, *upper left panel, first 4 lanes*). This is partially consistent with the observation where I was not able to detect Rpd3 at its regular molecular weight (~49 kDa) in zinc-deficient cell lysates in this experiment (**Fig. 3A**, *lower left panel, last four lanes*) and therefore was unable to visualize the cross-linked proteins in zinc-deficient eluates as clear as in zinc-replete cells. Another key observation is that there is higher amount of regular-sized Rpd3 in *tsa1*Δ cells expressing Tsa1-MBP C171S, despite the protein expression level of Rpd3 being the same (**Fig. 3A**, *lower left panel, first four lanes*) and the pull-down efficiency remains similar (**Fig. 3A**, *upper right panel*). Due to the constraints of the blot size and due to the unknown nature of the molecular weight of the cross-linked species, I was not able to quantify their relative abundance. I was also unable to normalize the increased Rpd3 in eluates to its abundance after reducing the eluates with DTT as I could not accurately quantify total Rpd3 protein abundance in zinc-deficient cell lysates.

To test whether the cross-linked species are indeed Rpd3-Tsa1 complexes, I performed another experiment including *rpd3*Δ cells expressing Tsa1-MBP C171S as a negative control. While the cross-linked species were not visible on the eluate blot in this experiment due to not enough total protein obtained from the lysates (**Fig. 3B**, *upper left panel*), there was a significant difference in reduced eluates (**Fig. 3B**, *upper right panel*) in both zinc-replete and zinc-deficient cells. With *rpd3*Δ cells expressing Tsa1-MBP C171S as a negative control, we confirmed that these bands are indeed Rpd3 protein. After normalizing the abundance of reduced Rpd3 to its protein abundance (**Fig. 3B**, *lower left panel*), including the ones dissociated from the cross-linked species from DTT treatment, I observed a ~5.5 fold increase of eluted Rpd3 in *tsa1*Δ cells expressing Tsa1-MBP C171S validating that Tsa1 is interacting with Rpd3 in zinc-replete cells. However, I was still unable to detect any expression of Rpd3 at its native size in zinc-deficient cells (**Fig. 3B**, *lower left panel*) therefore unable to get a quantification from zinc-deficient cells. Judged by the band intensity comparison between lane 4 and lane 5 in **Figure 3B** (*upper right panel*), I infer that there is also an increase of eluted Rpd3 in zinc-deficient *tsa1*Δ cells expressing Tsa1-MBP C171S.

Overall, the MBP pull-down analysis demonstrated that Tsa1 interacts with Rpd3 in both zinc-replete and zinc-deficient yeast cells. However, whether there is more Tsa1-Rpd3 interaction in zinc-replete or zinc-deficient cells remains unknown.

In vivo NEM/PEG-maleimide analysis shows that Rpd3 apoprotein is present in zinc-replete cells but accumulate significantly more in zinc-deficient cells.

To test the hypothesis that the Tsa1 chaperone is critical in preventing aggregation of unmetalated zinc apoproteins, I sought to assess the zinc metalation status of Rpd3 *in vivo* in zinc-replete and

zinc-deficient yeast cells. The technique of NEM/PEG-maleimide analysis was the same as discussed in **Chapter 2**. Rpd3 is a class I histone deacetylase that is highly conserved from yeast to mammalian cells. It contains 10 cysteines. Although none of the cysteines are directly involved in zinc binding, there are two cysteine residues that are located close to the zinc site and thus their accessibility to NEM modification could be changed by zinc metalation status. Without NEM or PEG modifications, Rpd3 from either zinc-replete or deficient cells was detected just above ~49 kDa on immunoblots (**Fig. 4A**, *lane 1 and 2*). With denaturation and PEG-maleimide treatment, Rpd3 proteins migrate at ~100 kDa, which corresponds to the addition of five PEG moieties (**Fig. 4A**, *lane 3 and 4*). There is higher expression of Rpd3 in zinc-deficient cells, an observation supported by previous immunoblotting and proteomics data from **Chapter 2**, which explains why the bands in lanes *2 and 4* are more intense than bands in lanes *1 and 3* from zinc-replete cells (**Fig. 4A**). When cells were transferred from zinc-replete to zinc-deficient media for 4, 8, and 14 hours, they were treated with NEM *in vivo* prior to PEG-maleimide treatment *in vitro* at each time point. The results showed changing sensitivity to NEM when cells were transferred from zinc-replete to zinc-deficient media, detectable primarily by the intensity change in unmodified and 1x PEG modified bands (**Fig. 4A**, *lane 5-8*). This indicates that as cells become more zinc deficient, there is increased sensitivity to NEM. However, different from Fba1 aldolase (**Chapter 2)**, there is no dramatic decrease of fully PEG modified Rpd3 (5x PEG in **Fig. 4A**). The background band (indicated by the * in **Fig. 4A**) further complicated the interpretation of Rpd3 apoprotein bands versus fully-metalated bands. Overall, the quantified time-course NEM/PEG-maleimide analysis of Rpd3 showed that there are some Rpd3 apoproteins with changed conformation present even in zinc-replete cells, while there is at least 2-fold more Rpd3 apoproteins accumulating in cells after 8 hours in zinc deficiency.

To further assess whether the conformation change observed for the wild-type Rpd3 was due to change of zinc binding *in vivo*, a mutant with histidine zinc ligand at position 188 mutated to alanine (H188A) was generated. This mutant has been shown to be unable to bind zinc and has little to no deacetylase activity[24]. This H188A mutant showed no significant change in sensitivity to NEM as the bands showed no intensity changes as cells became increasingly zinc deficient (**Fig. 4C**, *lane 5-8*). There were also very little 4xPEG and 5xPEG shown on the immunoblot, indicating there were no conformation changes when cells expressing Rpd3-H188A transferred from zinc-replete to zinc-deficient medium. These results suggest that loss of zinc binding was the cause behind the conformation changes observed in **Figure 4A**.

Rpd3 apoprotein stability may be partially dependent on Tsa1 in zinc-deficient cells.

To explore the downstream consequence(s) of Tsa1-Rpd3 interaction, Rpd3 protein accumulation with or without Tsa1 were investigated. The hypothesis being addressed was that if Tsa1 is interacting with Rpd3 as a chaperone, the abundance of Rpd3 might decrease in a *tsa1Δ* mutant as a result of protein degradation. Likewise, the H188A ligand mutant would accumulate to lower levels than the wild-type protein and be more sensitive to the absence of Tsa1. *rpd3*Δ and *rpd3Δtsa1Δ* cells were transformed with plasmids expressing wild-type Rpd3, H188A mutant allele of Rpd3, or an empty vector (pFL38). Cells were grown in either zinc-replete or deficient medium for at least four generations, harvested and protein extracted with the TCA method. The same amounts of total protein (100 μg) were loaded and Rpd3 (wild type or H188A) abundance was analyzed using the native Rpd3 antibody and quantified (**Figure 5**). The results showed that there was at least 3-fold less H188A mutant protein expressed (**Fig. 5A**, *lane 3-4, and 9-10*)

compared to wild-type Rpd3 (**Fig. 5A**, *lane 1-2, and 7-8*) regardless of zinc-status and the presence of Tsa1. Furthermore, there is no significant difference in H188A mutant level in zinc-replete cells with or without Tsa1. This indicates that the decreased expression of H188A mutant is mostly due to the fact that H188A cannot bind zinc and zinc is critical to its stability. However, the presence of Tsa1 might play a small, but significant, role in stabilizing Rpd3 apoproteins in zinc deficiency specifically as H188A mutant showed a further 2-fold less expressed in zinc-deficient *tsa1Δ* cells (**Figure 5B**).

DISCUSSION AND FUTURE DIRECTIONS

In this chapter, I tested the hypothesis that the Tsa1 chaperone is critical in preventing aggregation of unmetalated zinc apoproteins. Our lab first performed a genetic screen with fluorescence microscopy of GFP-tagged alleles of ~100 most abundant zinc proteins to see which proteins form insoluble aggregate foci without Tsa1 specifically in actively growing, zinc-deficient yeast cells. Contrary to expectations, we found very few zinc proteins that formed aggregates in zinc-deficient cells. The four proteins that did aggregate were Nce103 (carbonic anhydrase), Bdh1((R,R)-butanediol dehydrogenase), Car1 (arginase) and Rpd3 (histone deacetylase) (**Figure 1**). It is worth noting that the formation of insoluble aggregate foci without Tsa1 is not direct evidence to establish Nce103, Bdh1, Car1 and Rpd3 are Tsa1 chaperone targets as there are many other factors, such as oxidative stress, factors that disrupt protein translation/folding, that might influence the formation of insoluble aggregate foci[25]. For example, the absence of Tsa1 could further disrupt the redox environment of zinc-deficient yeast cells, thus affecting the expression, activities or locations of other heat shock proteins that potentially function as direct chaperones of zinc proteins induce or prevent them from forming insoluble aggregates. Therefore, it was important to test whether the four zinc proteins physically interact with Tsa1 to be its chaperone targets.

I next assessed the protein-protein interaction (PPI) between Tsa1 and the four zinc proteins (Nce103, Bdh1, Car1 and Rpd3) using an *in vivo* proximity-based protein-protein interaction analysis, BioID[16]. BioID analysis uses a mutant version of *Escherichia coli* biotin ligase BirA. Mutated BirA* (R188G) biotinylates specific lysine residues of any proteins that come within the proximity of BirA* (i.e. ~10 nm) and thus can be used as an *in vivo* tool for labeling interacting proteins. By fusing BirA* to the N-terminus of Tsa1, proteins that interact with Tsa1 will be

biotinylated, captured by the high-capacity streptavidin resin and eluted with a biotin-containing elution buffer. Although the inventors of BioID cautioned that BioID alone cannot determine whether a protein is definitely interacting with the "bait" without other methods (e.g. yeast two hybrid, or pull-down assays) to confirm its results, there are many benefits of BioID. BioID creates a covalent bond between biotin and the target protein *in vivo*, so it could capture the weak transient PPI and could endure the downstream purification process which makes BioID a very sensitive *in vivo* PPI screening tool. Critics of BioID also argue that if a specific protein X showed changed biotinylation level in zinc-replete or zinc-deficient cells, it could either mean that protein X has changed interaction with Tsa1 or it could also mean that protein X has undergone a conformation change leading to different number of lysine residues being exposed to and modified by BirA*. While this is a legitimate concern in interpreting data, we can rule out the second possibility, i.e. conformation change induced biotinylation change, by including a BirA*-only control in the experiment. If there is significant increased biotinylated protein X in cells expressing BirA*-Tsa1, but not in cells expressing BirA* only, it can be concluded that protein X is specifically interacting with Tsa1. The influence of protein conformation changes on biotinylation of protein X should only be considered when we are comparing biotinylated protein abundance between zinc-replete and zinc-deficient cells. For example, two Tsa1 target candidates, Car1 and Bdh1, were not considered interacting with Tsa1 as there were similar number of biotinylated peptides (biotinylated Car1-GFP, and Bdh1-GFP) in eluates from *tsa1*Δ cells expressing BirA*-Tsa1 and its wild-type control expressing BirA* only (data not shown). GFP tag alone was shown to be significantly more biotinylated in zinc-deficient *tsa1*Δ cells. FLAG-, RFP-, HA- tagged Nce103 were also tested by BioID analysis but neither FLAG-Nce103, RFP-Nce103, nor Nce103-HA showed changed biotinylation level (data not shown). Therefore, Nce103-GFP was also ruled out

as interacting with Tsa1 by BioID analysis (data not shown). Rpd3 was the only one among the four zinc proteins that showed to be specifically interacting with Tsa1, as Rpd3 is highly biotinylated only in *tsa1*Δ cells expressing BirA*-Tsa1 (**Fig. 2A-C**).

Next, I confirmed the Tsa1-Rpd3 interaction with a classic pull-down analysis (**Fig. 3A-B**). By fusing maltose-binding protein to the C-terminus of Tsa1 and by using the C171S mutant allele of Tsa1, I was able to create a "trap" that captures the transient interaction between Tsa1 and Rpd3 in both zinc-replete and zinc-deficient cells. There were visible high molecular weight cross-linked species, that disappear after DTT treatment, in *tsa1*Δ cells expressing Tsa1-MBP C171S but not in wild-type cells expressing MBP control (**Fig. 3A**). There were less cross-linked species in zinc-deficient cells expressing Tsa1-MBP C171S. That was partially due to there was very little detectable Rpd3 in the crude lysate samples, which was aliquoted from the total protein lysate loaded onto the amylose resin. This suggests that the degree of enrichment of Rpd3 from lysate to eluate could be significantly higher in zinc-deficient cells, considering that I did observe Rpd3 in reduced eluates (**Fig. 3B**, *upper right panel, lane 4 and 5*). It remains unknown why I did not detect Rpd3 in zinc-deficient cell lysates, as previous immunoblots from protein extracted using TCA method and data from proteomic analysis in **Chapter 2** all show that Rpd3 is 1.5-fold more abundant in zinc-deficient cells compare to in zinc-replete cells. One problem that remains to be solved is whether Tsa1 is directly interacting with Rpd3 or indirectly interacting with Rpd3 due to interaction with other subunits in Rpd3 complexes. There are three characterized Rpd3 complexes: Rpd3L, Rpd3S and the Rpd3μ[8,26]. While all three Rpd3 complexes play critical roles in the cell such as heat stress, transcriptional regulation, and mediating oxidative stress etc, they each have a set of subunits[7]. Rpd3L and Rpd3S both include many distinctive subunits but they share two

subunits, Ume1 and Sin3. I performed BioID using cells simultaneously expressing Ume1-HA or Sin3-HA and BirA*-Tsa1/ BirA* alone. The results showed no difference between biotinylated Ume1-HA or biotinylated Sin3-HA between cells expressing BirA*-Tsa1 or BirA* alone, suggesting that there is no specific interaction between Sin3 and Tsa1 or Ume1 and Tsa1 (**Fig. 2D**). Because I did not confirm these results using MBP pull-down assay, I am unable to rule out the possibility of Tsa1 interacting with either Rpd3L or Rpd3S. It is also possible that Tsa1 is interacting with a subunit from Rpd3μ. Rpd3μ complex only has two subunits, Snt2 and Ecm5 whose protein expression is relatively low (~ 1000 copy per cell in rich medium) – our proteomics data was not able to detect either of them. For any readers who are interested in investigating the interaction between other Rpd3 complex subunit with Tsa1, Snt2 would be a great candidate for future studies. Snt2 is a zinc protein that binds six zinc atoms per monomer, and its structural zinc sites use cysteine as exclusive ligands. It could be very likely that Tsa1 is interacting with Snt2, and Rpd3μ complex, to mediate oxidative stress or oxidative signal in zinc-deficient yeast cells.

To test whether Rpd3 is an apoprotein in zinc-deficient cells, I used NEM/PEG-maleimide analysis. The quantified time-course NEM/PEG-maleimide analysis of Rpd3 showed that there is a small pool of Rpd3 apoproteins with changed conformation present even in zinc-replete cells, while there is at least 2-fold more Rpd3 apoproteins accumulating in cells after 8 hours in zinc deficiency. Although I observed increased reactivity with NEM in cells at 4, 8, and 14 hour of zinc deficiency marked by increased intensity of unmodified or 1xPEG modified bands, there is little change of the fully PEG modified (4xPEG and 5x PEG) Rpd3 bands (**Fig. 4A**). This does not necessarily suggest that majority of Rpd3 is not in apo form. There might be other reasons that need to be explored to explain why there was little change in 4xPEG and 5xPEG bands in **Figure 4A**. Some

preliminary data have shown that it is very likely the Rpd3 apoproteins in zinc-deficient cells were oxidized (**Figure S1**). When treated with or without DTT, the fully PEG modified (5xPEG) bands, especially from zinc-deficient cells, migrated down and created a smear on the immunoblot (**Fig. S1**, *lane 8 of left panel and lane 4, 8 of right panel*). Exactly which cysteines of Rpd3 were being oxidized that caused such differences (± DTT) is unknown. Future experiments that couple Rpd3 activity assay, zinc binding status and cysteine mutation could be useful to provide a whole picture of the oxidation status of Rpd3 or Rpd3 apoproteins. One question arises from the time-course NEM/PEG-maleimide analysis is that why is there Rpd3 apoprotein in zinc-replete cells? This echoes back to the question I raised in the introduction chapter (**Chapter 1**): what signal induces apoprotein? Apparently, zinc loss caused by insufficient supply of zinc atoms in the cells is not the only reason that induces apoprotein formation, at least not in the case of Rpd3. A time-course NEM/PEG-maleimide analysis coupled with proteomics could offer an insight to see the scale of apoproteins in zinc-replete cells but it is worth noting that each protein has a different sensitivity to NEM (concentration and treatment time) which can further complicate the experimental design. One possible explanation for Rpd3 apoprotein accumulation is that important zinc proteins, such as transcription factor p53 in mammalian cells, are constantly cycling between apo- and metalated-form, or cells keep a small pool of apoprotein at all times. Once zinc deficiency stress increases, more zinc proteins are trapped in the apo-form and thus serve as signaling cue for cells to adopt other ways to adapt to different level of zinc deficiency. This small pool of apoproteins could also be a way cells take as a precaution to "sense" rapid change of zinc levels in the environment so they can react rapidly. Another explanation is that during zinc-replete conditions, cells use this pool of apoproteins as a "fine-tuning" tool to regulate gene expressions and other critical cellular functions. When zinc becomes scarce, other transcriptional regulation mechanisms are activated

to work together with the accumulation of apoproteins to control the downstream cellular pathways. This idea can be supported by the evidence that Rpd3 regulates *ZRT1* transcription alongside Zap1 transcription factor[27].

The next question is what is the purpose of Tsa1-Rpd3 interaction? The interaction between Tsa1-Rpd3 could have an immediate effect on the protein abundance of Rpd3, as well as modulating Rpd3 and/or Tsa1 activity. I tested the indirect effect of Tsa1 on the protein abundance of Rpd3 and its apoproteins in zinc-replete and zinc-deficient cells (**Fig. 5**). The results show that there is a small but significant effect of Tsa1 on the protein abundance of both wild-type Rpd3 and the apoproteins (H188A ligand mutant of Rpd3) in zinc-deficient cells not in zinc-replete cells. This result can be explained through the small % of Tsa1-Rpd3 interaction. Considering the results from the pull-down analysis (**Fig. 3A**, *upper left panel*), most of Rpd3 being pulled down is at its native size (~ 49kDa) with few bands showing cross-linked high molecular weight. This seems to suggest that Tsa1 is only interacting with a small pool of Rpd3, which is consistent with the small but significant effect on Rpd3 protein abundance here. For readers who are interested in exploring the other immediate consequences of Tsa1-Rpd3 interaction, measuring Rpd3 activity with an activity assay will be an interesting experiment to do. There was some evidence that HDAC8 (an Rpd3-like class I HDAC) enzyme activity can be modulated by a redox-switch that oxidizes two key cysteines *in vitro*[28]. Based on the preliminary data that Rpd3 is more oxidized in zinc-replete cells, it could be possible that the oxidation is regulating Rpd3 activity through the Tsa1-Rpd3 interaction. To test this possibility, one must establish that (1) Rpd3 is indeed oxidized, and there is a difference in Rpd3 oxidation in zinc-replete and deficient cells, (2) identifying the cysteines being oxidized could also help design mutation experiments to further demonstrate that Tsa1 is the

protein that is directly oxidizing Rpd3, and (3) there is a change in Rpd3 activity between zinc-replete and deficient cells. On the other hand, the interaction between Tsa1 and Rpd3 could potentially affect acetylation status of Tsa1 as well. In a cell culture study using human cell lines, absence of HDAC6 (a class I HDAC) was shown to increase the abundance of acetylated PrxI and PrxII[29]. Both Prx I and Prx II are a 2-cys peroxiredoxins but PrxI is an ortholog of Tsa1. The increase of acetylated PrxI allows cells to resist higher level of H_2O_2 treatment as well as allowing PrxI to resist hyperoxidation therefore resisting to oligomerize[29]. Changing the acetylation status of PrxI has been associated with several neurodegenerative diseases that feature protein aggregation, but the location and molecular functional consequence of lysine acetylation needs to be considered[30]. However, more work needs to be done to test this hypothesis of acetylation regulating peroxiredoxin functions.

The downstream functional effects of Rpd3-Tsa1 interaction could be multiple as both histone deacetylases and peroxiredoxins have been recognized as critical hubs of cellular activities. Specifically related to zinc biology, the potential downstream effect of Rpd3-Tsa1 interaction is to "fine-tuning" *ZRT1* gene expression. *ZRT1* encodes the high affinity zinc uptake transporter and is highly induced in zinc-deficient cells[31,32]. Zrt1 expression is regulated transcriptionally by Zap1. Under zinc deficiency, the Zap1 transcription factor binds to the zinc-responsive elements (ZREs) located in the promoter of *ZRT1* to activate its transcription so cells can take up zinc efficiently[31]. However, it has been shown in a genome-wide study that Rpd3 represses *ZRT1* transcription: deletion of Rpd3 led to a 9-fold increase of *ZRT1* mRNA in rich media[33]. The mechanism of how Rpd3 repress *ZRT1* transcription has also been discovered; Rpd3 activates long cryptic unstable transcripts that prevent Zap1 binding to ZREs and thus efficiently shuts down *ZRT1* transcription

in zinc-replete cells[27]. It will be interesting to see how Rpd3 apoproteins and the H188A ligand mutant affect *ZRT1* transcript level using Northern blotting.

Another critical question that remains to be solved is that what role does Tsa1 play in interacting with Rpd3? Results from the BioID analysis seem to suggest that there are no significant differences of Tsa1-Rpd3 interaction between different Tsa1 mutants, i.e. C48D, C48E, C171S, ΔYF, or C48S, of Tsa1 (Figure 2E and 2G). Given the limitations of the BioID analysis, an MBP pull-down analysis with these Tsa1 mutant alleles may help provide insight to this question. In Figure 3, C171S mutant was used to create a "trap" to capture the transient interaction between Tsa1 and Rpd3, and the results indeed showed that there were cross-linked species forming between Tsa1 and Rpd3 in both zinc-replete and zinc-deficient cells expressing Tsa1-MBP C171S plasmid (Figure 3). Unfortunately, the other mutants of Tsa1 were not used in this experiment due to limited time and capacity to grow large cultures in the same experiment. Another possible explanation to my observations is that when and how does Tsa1 switch between its functions under different physiological states remains unclear. For example, whether Tsa1 requires oligomerization to function as a molecular chaperone is still being investigated. Since the publication from Jang et al (2004), there has been a body of evidence showing that cysteine hyperoxidation is required for Tsa1 to oligomerize and to switch molecular chaperone function. However, this study was *in vitro* with citrate synthase as an artificial chaperone substrate[12]. It has been challenged by Teixeira et al. that a reduced, decameric 2-cys peroxiredoxin in a parasite Leishmania infantum works as an efficient chaperone both *in vitro* and *in vivo*[34]. It has also been shown that phosphorylation, besides cysteine hyperoxidation, can shift 2-cys peroxiredoxins from a peroxidase to a molecular chaperone[35]. More evidence will be needed to determine what structure

Tsa1 adopts as a chaperone and that could help us to understand the nature of the Tsa1-Rpd3 interaction.

To summarize, in this chapter, we first obtained evidence that Rpd3 forms insoluble protein aggregates specifically in zinc-deficient *tsa1*Δ cells. Then I confirmed Tsa1 is physically interacting with Rpd3 in both zinc-replete and deficient cells, with possibly more Rpd3 in zinc-deficient cells. This interaction is consistent with the observation that Rpd3 has a small pool of apoproteins in zinc-replete cells but has significantly more apoproteins accumulating in zinc-deficient cells. Although not being able to directly pinpoint chaperone role of Tsa1 to the interaction between Tsa1 and Rpd3, the work from this chapter adds a new *in vivo* interacting target of Tsa1 for future study.

EXPERIMENTAL METHODS

Strains and growth conditions- Yeast were grown in synthetic defined (SD), or low zinc medium (LZM), as previously described31. LZM contains 20 mM citrate and 1 mM EDTA to buffer pH and zinc availability. Glucose (2%) was the carbon source for all experiments. LZM + 0.3 μM ZnCl2 was routinely used as the zinc-deficient condition in this chapter, and LZM + 100 μM ZnCl2 as the replete condition. The yeast strains used in this work were BY4742 (MATa his3 leu2 ura3 lys2), tsa1Δ (MATα tsa1::LEU2 his3 leu2 ura3 lys2), rpd3Δ (MATα tsa1::KanMX4 his3 leu2 ura3 lys2), rpd3Δtsa1(MATα rpd3::KanMX4 tsa1::LEU2 his3 ura3 lys2).

Protein extraction and immunoblotting- Yeast protein extracts were prepared for immunoblotting with a TCA extraction protocol as previously described11. SDS-PAGE and immunoblotting was conducted using a Li-Cor Odyssey infrared dye detection system as previously described11. Antibodies used were anti-Rpd3 (C-4, Santa Cruz Biotechnology, product# sc-398880), and anti-Pgk1 (Abcam product 22C5D8, lot # GR166098). IR 680 dye-labeled secondary anti-mouse antibody (product 680LT, lot # C30605-02), and IR 800 dye-labeled secondary anti-rabbit antibody (product 800CW, lot # C50512-05) was obtained from Li-Cor.

Plasmid constructions- All plasmids were constructed by homologous recombination in yeast. Plasmids expressing Tsa1 and its mutant (C48S, C171S, C48D, ΔYF), Rpd3-H188A mutant were constructed based on previous published work. Plasmids expressing Sin3 or Ume1 with a triple repeat of the hemagglutinin antigen (HA) epitope fused to the C-terminus were constructed by PCR-amplification of the Ume1 (or Sin3) coding DNA sequence fused to the HA tags and terminator of the low copy episomal plasmid YCp-ZRC1-HA digested with HpaI and EcoRI. The

Ume1 fragment was amplified with oligonucleotides (5'-CACGACGTTGTAAAACGACGGCCAGTGAATTCCATGAGGTATGCACGAAGTGG-3') and (5'-TAGCCCGCATAGTCAGGAACATCGTATGGGTAACTTTTGGCAGCTCCAACC-3'). The Sin3 fragment was amplified with oligonucleotides (5'-CACGACGTTGTAAAACGACGGCCAGTGAATTCAGGTTTCCCAACGTGTGGTC-3') and (5'-TAGCCCGCATAGTCAGGAACATCGTATGGGTATTGAATCTTAGCCCCCTTGTCT-3').

BioID analysis- To identify the in vivo targets of Tsa1, BioID analysis developed by Roux et al (Roux et al 2013). 30 mL cultures of yeast were grown in biotin-free zinc-replete (LZM + 100 µM ZnCl2) or zinc-deficient (LZM + 0.3 µM ZnCl2) condition supplemented with a final concentration of 10 ug/L biotin in the growing cultures. After harvest, cells were centrifuged immediately and equal volume (0.5 mL) of ice-cold 20% TCA were added, centrifuged again to remove supernatant and pellets stored at -80 °C for further processing. Protein was extracted using a TCA extraction protocol and redissolved in buffer A (200 mM Tris base, 1% SDS, 1 mM EDTA). Equal quantity of proteins (2mg total) were prepared using a SB buffer (50 mM Tris-Cl pH, 100 mM NaCl, 0.1% Tween 20, 0.1% SDS, 1 mM EDTA, and 1mM DTT). High-capacity streptavidin-agarose beads (Thermo Fisher Scientific, product #20357) were aliquoted to 75 uL beads/1mg total protein onto a column (Thermo Scientific, Pierce Centrifuge Column, 0.5mL, product# 89868) and washed using the SB buffer. Protein samples were loaded on the column, samples were incubated at room temperature for 1-2 hours. After incubation, each column capturing biotinylated proteins were washed with SB buffer twice, and eluates extracted by adding 75 uL Extraction Buffer (1X SDS-PAGE buffer + 5 mM biotin +BME), heated at 102°C for 15 minutes and repeat

the same elution process again for maximum elution efficiency. Eluates were analyzed by immunoblotting with different antibodies indicated above.

Pull-down analysis- To confirm the interacting targets of Tsa1, maltose-binding protein (MBP) pulldown analysis was performed. 150 to 200 mL cultures of yeast were grown n zinc-replete (LZM + 100 μM ZnCl2) or deficient (LZM + 0.3 μM ZnCl2) medium to log phase (A595 0.3-0.4) and harvested by centrifugation. Cells were washed with ice cold water + 1 mM EDTA. Pellets could be frozen at -80 °C for further processing. Pellets (fresh or frozen) were resuspended with 0.5 mL ice cold zinc-free lysis buffer containing 20 mM Tris-Cl pH 7.5, 200 mM NaCl, 5% Glycerol, 1% Triton X-100, 1 mM PMSF, 10 mM NEM in 100% ethanol, 5 μM MG132 and 1X yeast protease inhibitor cocktail in DMSO solution (Sigma-Aldrich, product #P8215). Cells were vortexed for 10 minutes at 4 °C, and then spun at top speed (14k rpm) at 4 °C for 10 minutes. Supernatant were transferred to a new tube as lysate. Lysate were normalized to the same protein concentration (~ 10 ug/uL) and an aliquot was taken for Rpd3 protein abundance analysis. Amylose resin were prepared and washed five times using a wash buffer containing 20 mM Tris-Cl pH 7.5, 200 mM NaCl, 5% Glycerol, 1% Triton X-100, 1 mM PMSF, 1 mM NEM in 100% ethanol, 2.5 μM MG132 and 1X yeast protease inhibitor cocktail in DMSO solution. A total of 10-14 mg of lysate were loaded to the column (Bio-Rad Bio-spin disposable chromatography column, product #732-6008) and the columns were inserted into collection tubes (Falcon 8 mL round bottom tube, product #35-2027). Lysates were incubated for 5 minutes at 4 °C and then spin down at 250 X g (~ 750 rpm). Columns capturing MBP interacting proteins were washed 10 times with wash buffer to reduce the background proteins. Flowthroughs were collected for troubleshooting. After sufficient washes, 120 uL of elution buffer (wash buffer + 10 mM maltose) were added to

the column and eluates obtained. 4X Protein Sample Loading Buffer (Li-Cor, product # 928-40004) were added to the eluates ¼ volume, and proteins denatured at 37 °C for an hour. Eluates were analyzed by immunoblotting with different antibodies indicated above.

NEM/PEG maleimide analysis- To identify cysteine residues showing zinc-dependent reactivity with N-ethylmaleimide (NEM) in vivo, 5 ml cultures of yeast were grown in zinc-replete (LZM + 100 μM ZnCl2) or deficient (LZM + 0.3 μM ZnCl2) medium to log phase (A595 0.3-0.4) and harvested by centrifugation. Cells were washed twice with ice-cold 1 x PBS + 1 mM EDTA and resuspended in 5 ml PBS + 1 mM EDTA. A solution of 1 mM NEM (specifically tested to optimally react with Rpd3) in 100% ethanol was added to 5 ml of cells to give a final concentration of 0.05 mM NEM. For a negative control, the same volume of 100% ethanol was added to an identical aliquot of cells. After 10, 20, or 30 min incubation at 30° with shaking, the cultures were harvested by centrifugation and washed twice with 1 x PBS. Protein was extracted using the TCA method11 and redissolved in buffer A (200 mM Tris base, 1% SDS, 1 mM EDTA). After measurement of protein concentration (DC protein assay, Bio-Rad), aliquots of protein were processed to modify cysteines with mPEG-2kDa (Sigma) as previously described11. Briefly, aliquots of 500 μg protein were treated with 20 mM DTT for 10 min at 65°C to reduce disulfide bonds, then reprecipitated by adding 1/10 volume 100% TCA. Precipitated samples were centrifuged and washed twice with acetone to remove TCA, then redissolved in buffer B (100 mM Tris-Cl pH 7.4, 2% SDS, 1 mM EDTA) + 5 mM PEG-maleimide (mPEG). After overnight incubation at 30°C, 10-30 μg of each protein sample was analyzed by SDS-PAGE and immunoblotting to determine the degree of mPEG modification of cysteine residues. To determine

the degree to which cysteines were normally oxidized in vivo (and thus unavailable for reaction with NEM), some control samples were not treated with DTT prior to mPEG treatment.

REFERENCES

1. Yeheskely-Hayon D, Kotler A, Stark M, Hashimshony T, Sagee S, Kassir Y. The roles of the catalytic and noncatalytic activities of Rpd3L and Rpd3S in the regulation of gene transcription in yeast. *PLoS One*. 2013;8(12):1-16. doi:10.1371/journal.pone.0085088
2. Knott SRV, Viggiani CJ, Tavaré S, Aparicio OM. Genome-wide replication profiles indicate an expansive role for Rpd3L in regulating replication initiation timing or efficiency, and reveal genomic loci of Rpd3 function in Saccharomyces cerevisiae. *Genes Dev*. 2009;23(9):1077-1090. doi:10.1101/gad.1784309
3. Backues SK, Lynch-Day MA, Klionsky DJ. The Ume6-Sin3-Rpd3 complex regulates ATG8 transcription to control autophagosome size. *Autophagy*. 2012;8:1835-1836. doi:10.4161/auto.21845
4. Carrozza MJ, Li B, Florens L, et al. Histone H3 methylation by Set2 directs deacetylation of coding regions by Rpd3S to suppress spurious intragenic transcription. *Cell*. 2005;123(4):581-592. doi:10.1016/j.cell.2005.10.023
5. Ruiz-Roig C, Viéitez C, Posas F, De Nadal E. The Rpd3L HDAC complex is essential for the heat stress response in yeast. *Mol Microbiol*. 2010;76(4):1049-1062. doi:10.1111/j.1365-2958.2010.07167.x
6. De Nadal E, Zapater M, Alepuz PM, Sumoy L, Mas G, Posas F. The MAPK Hog1 recruits Rpd3 histone deacetylase to activate osmoresponsive genes. *Nature*. 2004;427(6972):370-374. doi:10.1038/nature02258
7. McDaniel SL, Strahl BD. Stress-Free with Rpd3: a Unique Chromatin Complex Mediates the Response to Oxidative Stress. *Mol Cell Biol*. 2013;33(19):3726-3727. doi:10.1128/mcb.01000-13
8. Baker LA, Ueberheide BM, Dewell S, Chait BT, Zheng D, Allis CD. The Yeast Snt2

Protein Coordinates the Transcriptional Response to Hydrogen Peroxide-Mediated Oxidative Stress. *Mol Cell Biol*. 2013;33(19):3735-3748. doi:10.1128/mcb.00025-13

9. Nakajima E, Shimaji K, Umegawachi T, et al. The histone deacetylase gene Rpd3 is required for starvation stress resistance. *PLoS One*. 2016;11(12):1-17. doi:10.1371/journal.pone.0167554
10. Eide DJ. The oxidative stress of zinc deficiency. *Metallomics*. 2011;3(11):1124-1129. doi:10.1039/c1mt00064k
11. Macdiarmid CW, Taggart J, Kerdsomboon K, et al. Peroxiredoxin chaperone activity is critical for protein homeostasis in zinc-deficient yeast. *J Biol Chem*. 2013;288(43):31313-31327. doi:10.1074/jbc.M113.512384
12. Jang HH, Lee KO, Chi YH, et al. Two enzymes in one: Two yeast peroxiredoxins display oxidative stress-dependent switching from a peroxidase to a molecular chaperone function. *Cell*. 2004;117(5):625-635. doi:10.1016/j.cell.2004.05.002
13. Aguilera J, Van Dijken JP, De Winde JH, Pronk JT. Carbonic anhydrase (Nce103p): An essential biosynthetic enzyme for growth of Saccharomyces cerevisiae at atmospheric carbon dioxide pressure. *Biochem J*. 2005;391(2):311-316. doi:10.1042/BJ20050556
14. Smart WC, Coffman JA, Cooper TG. Combinatorial regulation of the Saccharomyces cerevisiae CAR1 (arginase) promoter in response to multiple environmental signals. *Mol Cell Biol*. 1996;16(10):5876-5887. doi:10.1128/mcb.16.10.5876
15. Gonzalez E, Fernandez MR, Larroy C, et al. Characterization of a (2R,3R)-2,3-butanediol dehydrogenase as the Saccharomyces cerevisiae YAL060W gene product: Disruption and induction of the gene. *J Biol Chem*. 2000;275(46):35876-35885. doi:10.1074/jbc.M003035200

16. Roux KJ, Kim DI, Raida M, Burke B. A promiscuous biotin ligase fusion protein identifies proximal and interacting proteins in mammalian cells. *J Cell Biol*. 2012;196(6):801-810. doi:10.1083/jcb.201112098

17. Irokawa H, Tachibana T, Watanabe T, et al. Redox-dependent Regulation of Gluconeogenesis by a Novel Mechanism Mediated by a Peroxidatic Cysteine of Peroxiredoxin. *Sci Rep*. 2016;6(January):1-16. doi:10.1038/srep33536

18. Troussicot L, Burmann BM, Molin M. Structural determinants of multimerization and dissociation in 2-Cys peroxiredoxin chaperone function. *Structure*. 2021;29(7):640-654. doi:10.1016/j.str.2021.04.007

19. Wood ZA, Poole LB, Karplus PA. Peroxiredoxin evolution and the regulation of hydrogen peroxide signaling. *Science (80-)*. 2003;300(April):650-653. doi:10.1126/science.1080405

20. Hall A, Karplus PA, Poole LB. Typical 2-Cys peroxiredoxins - Structures, mechanisms and functions. *FEBS J*. 2009;276(9):2469-2477. doi:10.1111/j.1742-4658.2009.06985.x

21. Sayed AA, Williams DL. Biochemical characterization of 2-cys peroxiredoxins from Schistosoma mansoni. *J Biol Chem*. 2004;279(25):26159-26166. doi:10.1074/jbc.M401748200

22. Hanzén S, Vielfort K, Yang J, et al. Lifespan Control by Redox-Dependent Recruitment of Chaperones to Misfolded Proteins. *Cell*. 2016;166(1):140-151. doi:10.1016/j.cell.2016.05.006

23. Roger F, Picazo C, Asami C, et al. Peroxiredoxin promotes longevity and H 2 O 2 - resistance in yeast through redox- modification of PKA. 2019.

24. Kadosh D, Struhl K. Histone deacetylase activity of Rpd3 is important for transcriptional

repression in vivo. *Genes Dev*. 1998;12(6):797-805. doi:10.1101/gad.12.6.797

25. Weids AJ, Ibstedt S, Tamás MJ, Grant CM. Distinct stress conditions result in aggregation of proteins with similar properties. *Sci Rep*. 2016;6(February):1-12. doi:10.1038/srep24554

26. Biswas D, Takahata S, Stillman DJ. Different Genetic Functions for the Rpd3(L) and Rpd3(S) Complexes Suggest Competition between NuA4 and Rpd3(S). *Mol Cell Biol*. 2008;28(14):4445-4458. doi:10.1128/mcb.00164-08

27. Toesca I, Nery CR, Fernandez CF, Sayani S, Chanfreau GF. Cryptic transcription mediates repression of subtelomeric metal homeostasis genes. *PLoS Genet*. 2011;7(6). doi:10.1371/journal.pgen.1002163

28. Jänsch N, Meyners C, Muth M, et al. The enzyme activity of histone deacetylase 8 is modulated by a redox-switch. *Redox Biol*. 2019;20(September 2018):60-67. doi:10.1016/j.redox.2018.09.013

29. Parmigiani RB, Xu WS, Venta-Perez G, et al. HDAC6 is a specific deacetylase of peroxiredoxins and is involved in redox regulation. *Proc Natl Acad Sci U S A*. 2008;105(28):9633-9638. doi:10.1073/pnas.0803749105

30. Rhee SG, Woo HA, Kil IS, Bae SH. Peroxiredoxin functions as a peroxidase and a regulator and sensor of local peroxides. *J Biol Chem*. 2012;287(7):4403-4410. doi:10.1074/jbc.R111.283432

31. Zhao H, Eide D. The yeast ZRT1 gene encodes the zinc transporter protein of a high-affinity uptake system induced by zinc limitation. *Proc Natl Acad Sci U S A*. 1996;93(6):2454-2458. doi:10.1073/pnas.93.6.2454

32. Eide DJ. Zinc transporters and the cellular trafficking of zinc. *Biochim Biophys Acta - Mol*

Cell Res. 2006;1763(7):711-722. doi:10.1016/j.bbamcr.2006.03.005

33. Bernstein BE, Tong JK, Schreiber SL. Genomewide studies of histone deacetylase function in yeast. *Proc Natl Acad Sci U S A*. 2000;97(25):13708-13713. doi:10.1073/pnas.250477697

34. Teixeira F, Tse E, Castro H, et al. Chaperone activation and client binding of a 2-cysteine peroxiredoxin. *Nat Commun*. 2019;10(1):1-14. doi:10.1038/s41467-019-08565-8

35. Jang HH, Kim SY, Park SK, et al. Phosphorylation and concomitant structural changes in human 2-Cys peroxiredoxin isotype I differentially regulate its peroxidase and molecular chaperone functions. *FEBS Lett*. 2006;580(1):351-355. doi:10.1016/j.febslet.2005.12.030

FIGURES

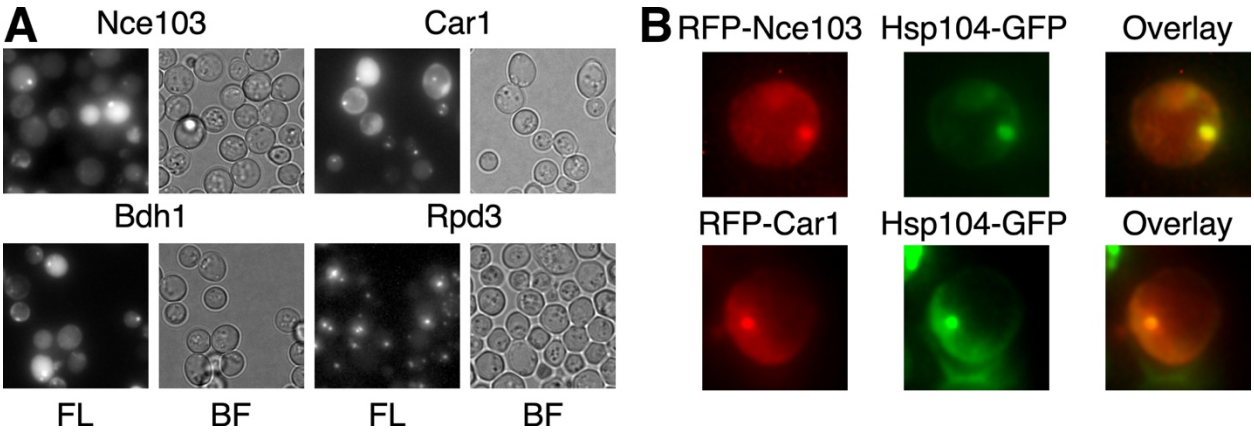

Figure 1. Microscopy screening reveals foci of proteins in zinc-deficient *tsa1*Δ mutant cells. A) *tsa1*Δ cells expressing Nce103-GFP, Car1-GFP, Bdh1-GFP, and Rpd3-GFP were grown in zinc-deficient media for at least four generations, harvested at cell density around 0.4 A_{595}, and formation of foci captured by fluorescence (GFP) microscopy (FL= fluorescence lighting, BF= blank field) B) zinc-deficient *tsa1*Δ cells expressing RFP-Nce103, RFP-Car1 were shown to harbor foci that co-localize with Hsp104-GFP disaggregase, a marker for insoluble protein aggregates. This suggests that RFP-Nce103 and RFP-Car1 have decreased protein solubility in zinc-deficient *tsa1*Δ cells that are actively growing.

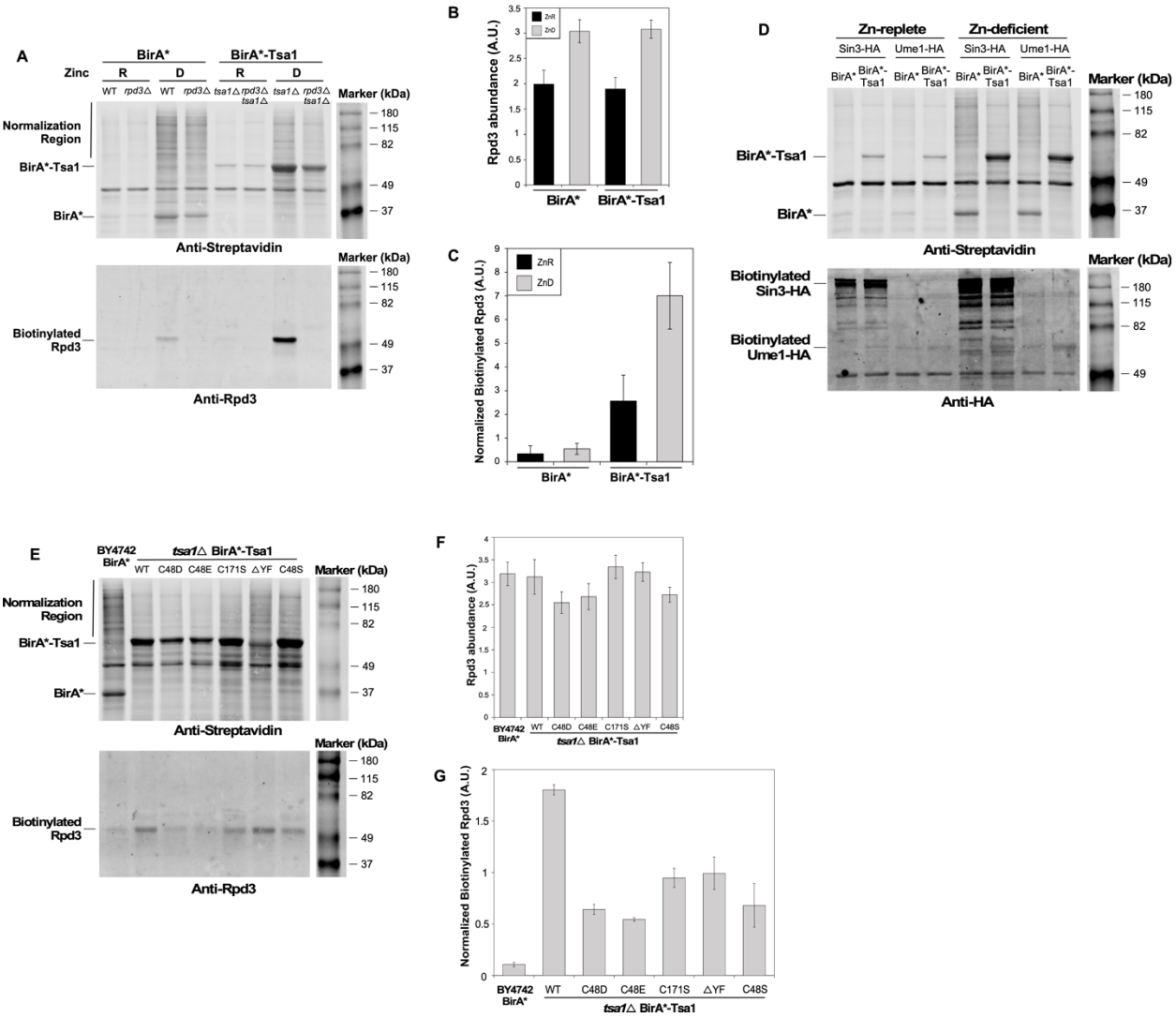

Figure 2. Rpd3 interacts with Tsa1 *in vivo*. A) BioID proximity-based protein-protein interaction analysis of cells of the indicated genotype expressing BirA*, a mutant form of biotin ligase that biotinylates proteins that come into its proximity), and BirA*-Tsa1. Zinc-replete (R) or zinc-deficient (D) cells were harvested at cell density around 0.4 A_{595}, proteins extracted by the TCA method and incubated with high-capacity streptavidin agarose beads, eluted with 5 mM biotin containing elution buffer and analyzed by immunoblotting with different antibodies. Total biotinylated peptides, and biotinylated Rpd3 detected by streptavidin (*upper* panel) and a native

Rpd3 antibody (*lower* panel), respectively. B) Protein abundance of Rpd3 quantified by immunoblotting. Left two bars are wild-type (BY4742) expressing BirA* and right two bars are *tsa1*Δ cells expressing BirA*-Tsa1, grown respectively in zinc-replete (ZnR) or zinc-deficient (ZnD) for at least four generations. The error bars indicate ± 1 S.D (n = 3). C) Normalized biotinylated Rpd3 abundance is a ratio calculated by dividing the intensity of biotinylated Rpd3 in panel A (*lower* panel) with total biotinylated peptide (noted as "Normalization Region" in panel A, *upper* panel), and then normalized with Rpd3 protein abundance to get the final normalized biotinylated Rpd3. The error bars indicate ± 1 S.D (n = 3). D) Wild-type (BY4742) cells expressing BirA* and *tsa1*Δ cells expressing BirA*-Tsa1were transformed with either Sin3-HA or Ume1-HA plasmids. Cells were grown, harvested, and lysates processed the same method as in panel A. Biotinylated Sin3-HA and Ume1-HA were detected by anti-HA antibody (*lower* panel). E) Wild-type (BY4742) cells expressing BirA* and *tsa1*Δ cells expressing BirA*-Tsa1were transformed with vector alone, or with plasmids that express WT, C48D, C48E, C171S, ΔYF, and C48S mutant alleles of BirA*-Tsa1. Cells were grown, harvested and lysates processed using the same method as in panel A. Shown in the graph are only data from zinc-deficient cells. Biotinylated Rpd3 detected respectively by a native Rpd3 antibody (*lower* panel). F, G) were quantified and normalized the same way as panels B and C.

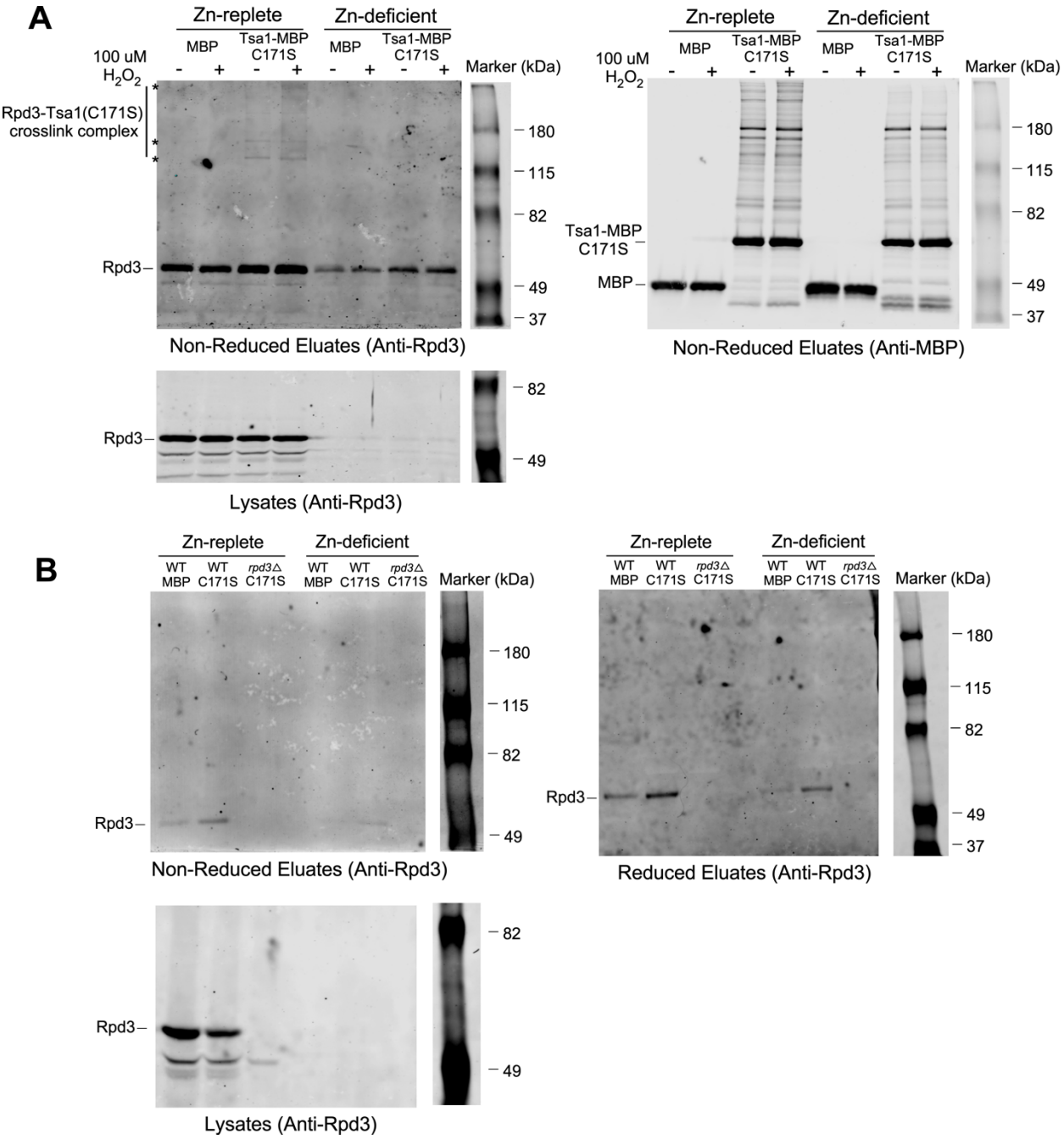

Figure 3. Pull-down assay suggests that Rpd3 interacts with Tsa1 in both zinc-replete and zinc-deficient cells. A) Wild-type (BY4742) expressing Maltose-Binding Protein (MBP) and *tsa1*Δ cells expressing Tsa1-MBP C171S mutant were grown in zinc-replete or zinc-deficient media for at least four generations. Cells were harvested at cell density around 0.4 A_{595} and treated with or without 100 μM H_2O_2 for 5 minutes, lysed, and the same amount of total lysate proteins

loaded on amylose resin and eluted with 10 mM maltose containing elution buffer. Cross-linked products between Tsa1 and Rpd3 were analyzed in non-reduced eluates by immunoblotting with a native Rpd3 antibody (*upper left* panel). Total non-reduced eluates were analyzed with an MBP antibody (*upper right* panel) and total protein abundance of Rpd3 was analyzed in reduced lysates (*lower left* panel). B) Wild-type (BY4742) expressing MBP, *tsa1*Δ cells expressing Tsa1-MBP C171S, and *tsa1*Δ *rpd3*Δ cells expressing Tsa1-MBP C171S were grown in zinc-replete or zinc-deficient medium. Cells were harvested at cell density around 0.4 A_{595} lysed, peptides captured by amylose resin and eluted with maltose-containing elution buffer. Lysates and eluates were analyzed in the same way as discussed in panel A.

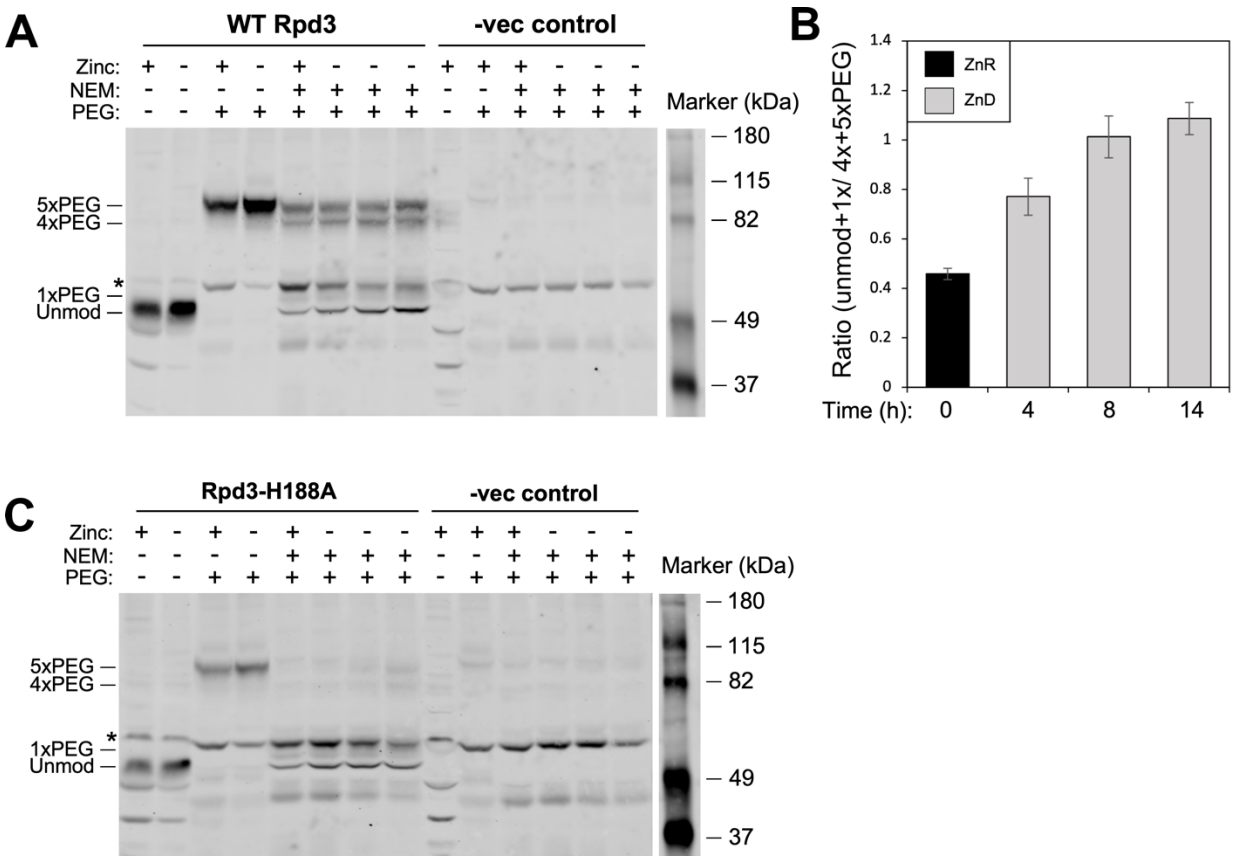

Figure 4. *In vivo* time-course analysis of zinc binding status by Rpd3. A) NEM/PEG-maleimide analysis of *rpd3*Δ cells expressing WT Rpd3 or an empty vector (-vec, pFL38). Zinc-replete (+, or ZnR) or zinc-deficient (-, or ZnD) cells were treated with and without NEM, lysed, proteins harvested, and then treated with or without PEG-maleimide. Unmodified and modified (1xPEG to 5xPEG-modified) forms of Rpd3 are indicated. The * denotes a background band detected by the antibody. B) Quantification of the results in panel A (left 8 lanes). The ratios of unmodified + 1x PEG-modified to 4x and 5x PEG-modified forms are shown and the error bars indicate ± 1 S.D (n = 3). C) NEM/PEG-maleimide analysis of *rpd3*Δ cells expressing H188A mutant allele of Rpd3 or an empty vector (-vec, pFL38). Cells were treated and samples analyzed as described in panel A.

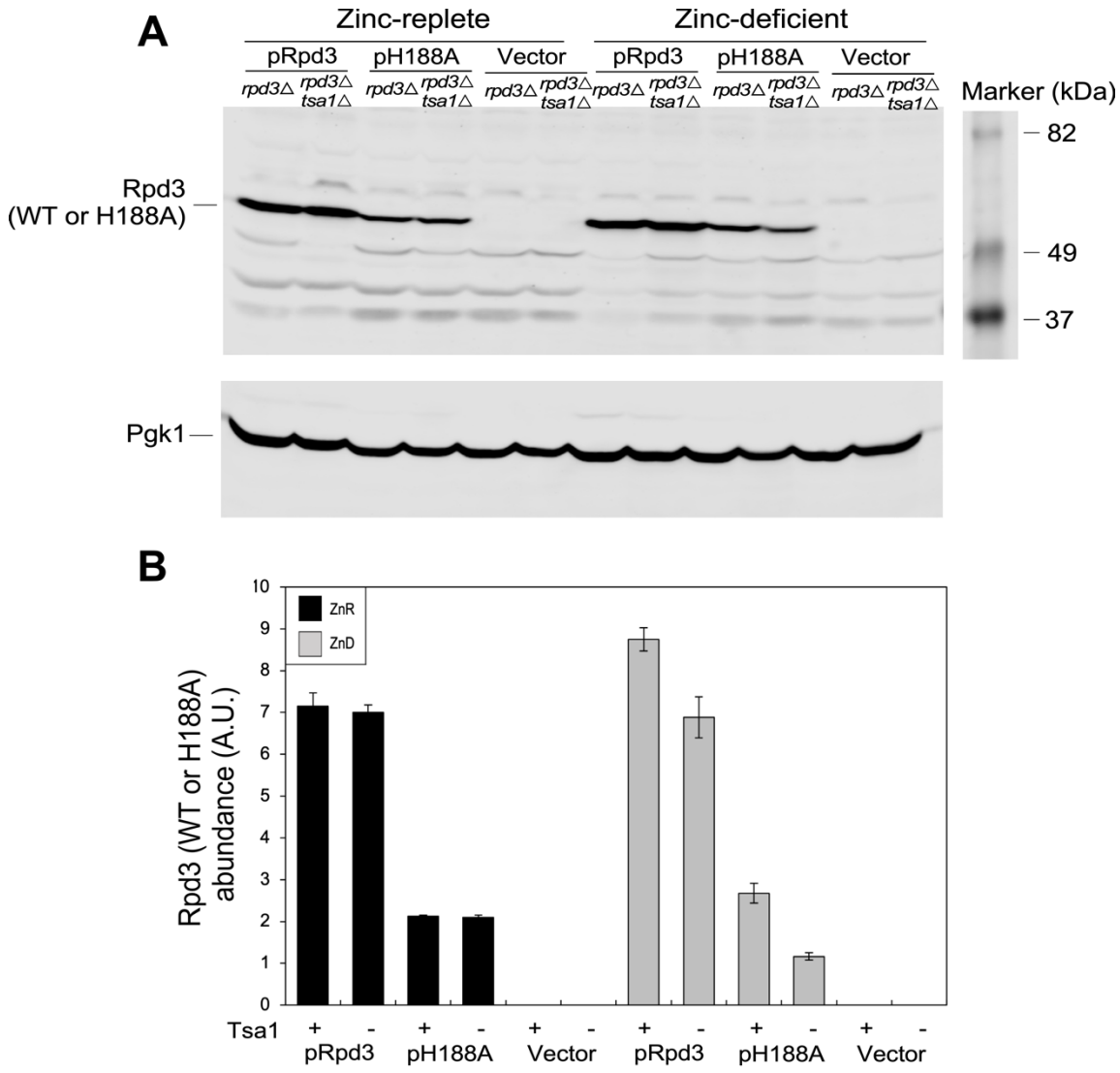

Figure 5. Rpd3 apoprotein stability may be partially dependent on Tsa1 in zinc-deficient cells. A) *rpd3*Δ cells, or *rpd3*Δtsa1Δ cells expressing WT Rpd3, H118A Rpd3 or an empty vector (pFL38) were grown in zinc-replete (ZnR) or zinc-deficient (ZnD) medium for at least four generations. Cells were harvested at cell density around 0.4 A_{595}, protein extracted and same amount (100μg) of total protein loaded for immunoblotting analysis. Protein abundance of WT or H188A form of Rpd3 was analyzed using a native Rpd3 antibody. Pgk1 was used as a control. B) Quantification of the results in panel A. Error bars indicate ± 1 S.D (n = 3).

SUPPLEMENTAL FIGURES

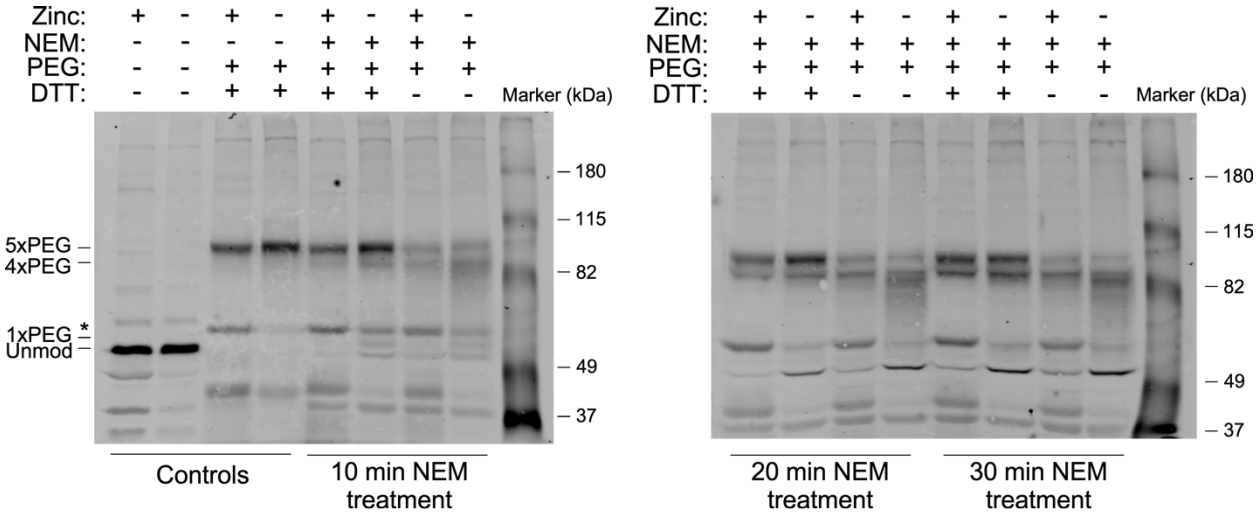

Figure S1. Rpd3 shows signs of oxidation in zinc-deficient cells. Wild-type (BY4742) cells were cultured in zinc-replete or zinc-deficient medium. Cells were aliquoted and treated without or with NEM for 10, 20 or 30 minutes, proteins extracted with TCA method, and then treated with or without DTT prior to PEG-maleimide treatment. Unmodified and modified (1xPEG to 5xPEG-modified) forms of Rpd3 are indicated. The * denotes a background band detected by the antibody. Oxidized Rpd3 were shown as a smear in *lane 8* in the left panel, and *lane 4 and 8* in the right panel.